Theses and Dissertations | 1. Thesis and Dissertation Collection, all items

1993-12

Interaction effects of a lower heated tube on pool boiling of R-124 from an upper horizontal tube

Yusician, Joseph E.

Monterey, California. Naval Postgraduate School

http://hdl.handle.net/10945/26595

Interaction Effects of a Lower Heated Tube on
Pool Boiling of R-124 from an Upper Horizontal Tube

by

Joseph E. Yusician, Jr.
Lieutenant, United States Navy
B.S.M.E., Drexel University, 1984

Submitted in partial fulfillment
of the requirements for the degree of

MASTER OF SCIENCE IN MECHANCIAL ENGINEERING

from the

NAVAL POSTGRADUATE SCHOOL
December 1993

Department of Mechanical Engineering

REPORT DOCUMENTATION PAGE

Report Security Classification: Unclassified		1b Restrictive Markings			
Security Classification Authority		3 Distribution/Availability of Report Approved for public release; distribution is unlimited.			
Declassification/Downgrading Schedule					
Performing Organization Report Number(s)		5 Monitoring Organization Report Number(s)			
Name of Performing Organization aval Postgraduate School	6b Office Symbol 34	7a Name of Monitoring Organization Naval Postgraduate School			
Address *(city, state, and ZIP code)* onterey CA 93943-5000		7b Address *(city, state, and ZIP code)* Monterey CA 93943-5000			
Name of Funding/Sponsoring Organization aval Surface Warfare Center	6b Office Symbol 2272	9 Procurement Instrument Identification Number			
dress *(city, state, and ZIP code)* nnapolis, MD 21402-5067		10 Source of Funding Numbers			
		Program Element No	Project No	Task No	Work Unit Accession No

Title *(include security classification)* INTERACTION EFFECTS OF A LOWER HEATED TUBE ON POOL BOILING OF R-124 FROM AN UPPER ORIZONTAL TUBE (UNCLASSIFIED)

Personal Author(s) Joseph E. Yusician, Jr.

a Type of Report aster's Thesis	13b Time Covered From To	14 Date of Report *(year, month, day)* December 1993	15 Page Count 192

Supplementary Notation The views expressed in this thesis are those of the author and do not reflect the fficial policy or position of the Department of Defense or the U.S. Government.

Cosati Codes			18 Subject Terms *(continue on reverse if necessary and identify by block number)* HEAT TRANSFER, INTERACTION EFFECTS OF A LOWER HEATED TUBE ON POOL BOILING FROM AN UPPER TUBE, R-124 REFRIGERANT
eld	Group	Subgroup	

Abstract *(continue on reverse if necessary and identify by block number)*

An investigation of the interaction effects of a lower heated tube on pool boiling of pure R-124 from an upper horizontal tube as conducted at a saturation temperature of 2.2 °C. The test tubes used were: (1) smooth tubes and (2) deformed surface TURBO-B) enhanced tubes. The effects of tube spacing/configuration and lower tube heat flux on the heat transfer performance the upper tube were investigated.

For both tube arrays, the enhancing effect of bubbles from a lower tube was dramatic. This enhancement increased as lower be heat flux increased. However, when upper tube heat fluxes were greater than 20 kW/m^2, all enhancement disappeared.

For a smooth tube array in natural convection, the effect of a lower heated tube on the heat transfer from an upper tube was all. In nucleate boiling, a P/D of 1.8 gave the best upper tube heat transfer performance and a vigorously nucleating lower be eliminated upper tube hysteresis. With the lower tube unheated and an upper tube heat flux of greater than 3 kW/m^2, the rformance using R-124 was generally better than for R-114. With a nucleating lower tube (at 10 kW/m^2), again the rformance of R-124 was better, but only for upper tube heat fluxes of greater than 40 kW/m^2.

For a TURBO-B tube array, a 30 degree offset of the upper tube reduced the upper tube heat transfer performance (compared the in-line configurations). This may indicate bubbles depart TURBO-B tubes differently than smooth tubes.

Distribution/Availability of Abstract X unclassified/unlimited ___ same as report ___ DTIC users	21 Abstract Security Classification Unclassified	
a Name of Responsible Individual Paul J. Marto	22b Telephone *(include Area Code)* 408-656-2989	22c Office Symbol ME/Mx

FORM 1473,84 MAR   83 APR edition may be used until exhausted   security classification of this pag

ABSTRACT

An investigation of the interaction effects of a lower heated tube on pool boiling of pure R-124 from an upper horizontal tube was conducted at a saturation temperature of 2.2 °C. The test tubes used were: (1) smooth tubes and (2) deformed surface (TURBO-B) enhanced tubes. The effects of tube spacing/configuration and lower tube heat flux on the heat transfer performance of the upper tube were investigated.

For both tube arrays, the enhancing effect of bubbles from a lower tube was dramatic. This enhancement increased as lower tube heat flux increased. However, when upper tube heat fluxes were greater than 20 kW/m^2, all enhancement disappeared.

For a smooth tube array in natural convection, the effect of a lower heated tube on the heat transfer from an upper tube was small. In nucleate boiling, a P/D of 1.8 gave the best upper tube heat transfer performance and a vigorously nucleating lower tube eliminated upper tube hysteresis. With the lower tube unheated and an upper tube heat flux of greater than 3 kW/m^2, the performance using R-124 was generally better than for R-114. With a nucleating lower tube (at 10 kW/m^2), again the performance of R-124 was better, but only for upper tube heat fluxes of greater than 40 kW/m^2.

For a TURBO-B tube array, a 30 degree offset of the upper tube reduced the upper tube heat transfer performance (compared to the in-line configurations). This may indicate bubbles depart TURBO-B tubes differently than smooth tubes.

iii

TABLE OF CONTENTS

LIST OF TABLES

LIST OF FIGURES

xii

NOMENCLATURE

This nomenclature reflects that which is found within programs SETUPJY (Appendix A) and DRPJY (Appendix B). Note that the upper and lower test tube dimensions are the same since like test tubes are used.

SYMBOL	UNITS	NAME/DESCRIPTION
A	m^2	Area
Ab	m^2	Tube active boiling surface area
Ac	m^2	Tube cross-sectional area
Cp	$J/kg \cdot K$	Specific heat of upper tube
ACp	$J/kg \cdot K$	Specific heat of lower tube
D	m	Diameter
Do	m	Tube outside diameter
Di	m	Tube inside diameter
D1	m	Tube diameter at thermocouple positions
D2	m	Tube diameter at active boiling section
g	m/s^2	Gravitational acceleration
h	$W/m^2 \cdot K$	Heat transfer coefficient of upper tube
Ah	$W/m^2 \cdot K$	Heat transfer coefficient of lower tube
I	A	Upper tube current
AI	A	Lower tube current
Ir	A	Upper tube current from AC current sensor
AIr	A	Lower tube current from AC current sensor

k	W/m·K	Thermal conductivity associated with the upper tube
Ak	W/m·K	Thermal conductivity associated with the lower tube
kc	W/m·K	Copper thermal conductivity
L	m	Tube active boiling length
Lu	m	Tube non-boiling length
Nu		Nusselt number
P	m	Tube outside surface perimeter
Pr		Prandtl number associated with the upper tube
APr		Prandtl number associated with the lower tube
Pg	Pa	Gas pressure
Psat	Pa	Saturation pressure
Q	W	Upper tube boiling surface heat transfer rate
AQ	W	Lower tube boiling surface heat transfer rate
Qf	W	Upper tube heat transfer rate through one non-boiling end
AQf	W	Lower tube heat transfer rate through one non-boiling end
Qh	W	Upper tube cartridge heater heat transfer rate
AQh	W	Lower tube cartridge heater heat transfer rate
q"	W/m²	Upper tube heat flux
Aq"	W/m²	Lower tube heat flux
Ra		Rayleigh number
T	°C	Temperature

Tavg	°C	Upper tube average wall temperature at a thermocouple location
ATavg	°C	Lower tube average wall temperature at a thermocouple location
Tc	°C	Critical temperature
Tf	°C	Upper tube film temperature
ATf	°C	Lower tube film temperature
Tn	°C	Temperature at the nth thermocouple location
Tsat	°C	Saturation temperature
Two	°C	Upper tube outer wall temperature
ATwo	°C	Lower tube outer wall temperature
V	V	Upper tube cartridge heater voltage
AV	V	Lower tube cartridge heater voltage
Vr	V	Upper tube AC-DC true RMS converter output voltage
AVr	V	Lower tube AC-DC true RMS converter output voltage
α	m²/s	Thermal diffusivity associated with the upper tube
Aα	m²/s	Thermal diffusivity associated with the lower tube
β	1/K	Upper tube volumetric thermal expansion coefficient
Aβ	1/K	Lower tube volumetric thermal expansion coefficient
δ		Uncertainty in measurement
θb	K	Upper tube wall superheat (Two - Tsat)
Aθb	K	Lower tube wall superheat (Two - Tsat)
μ	kg/m·s	Dynamic viscosity associated with the upper tube

Aμ	kg/m·s	Dynamic viscosity associated with the lower tube
υ	m²/s	Kinematic viscosity associated with the upper tube
Aυ	m²/s	Kinematic viscosity associated with the lower tube
ρ	kg/m³	Density associated with the upper tube
Aρ	kg/m³	Density associated with the lower tube

ACKNOWLEDGMENTS

I would like to dedicate this work to my wife, Theresa, for her patience, tolerance, reassurance and everlasting support throughout my tour at the Naval Postgraduate School.

I. INTRODUCTION

The United States Navy intends to eliminate its dependence on chlorofluorocarbons (CFC's) as soon as feasible. Currently, the Navy is using CFC-114 (Refrigerant or R-114) in most of it's chilled water air conditioning (AC) plants. These shipboard AC plants provide the chilled cooling water to cool the vital weapons systems and electronic components besides providing habitability comfort for the crew.

The Navy has identified a hydrochlorofluorocarbon, HCFC-124 or R-124, as a possible mid-term replacement for R-114 in naval shipboard AC systems. With an ozone depletion potential (ODP) of only 2% compared to 70% for R-114, R-124 is a much more tolerable fluid to use until an acceptable alternative refrigerant can be found that has zero ODP.

Although both refrigerants operate near the same evaporating temperature (2.2 °C), the characteristics of R-124 under similar conditions as R-114 are quite different. For example, the refrigeration components (i.e., heat exchangers, piping, etc.) must be able to withstand: (1) the higher operating pressures of R-124 (11 psig at 2.2 °C compared to 0 psig for R-114) and (2) the higher vapor pressure after the system is secured (in a main engineering space at 100 °F, R-124 would reach 66 psig compared to 31 psig for R-114). Given the system components can operate safely at these higher

1

pressures of R-124, then the hardware modifications to the system should be limited to:

1. Modifying the compressor to maintain rated capacity and use a miscible alkylbenzene oil for lubrication.

2. Reset/replace the system safety devices to account for the higher pressures of R-124.

3. Replace the system seals with neoprene seals, which resist deterioration when in contact with R-124, to maintain leak tight integrity.

Besides hardware modifications, another main concern is how does the heat transfer characteristics of R-124 compare to R-114. Table 1, from Bertsch [Ref. 1], provides

TABLE 1. R-114/R-124 PHYSICAL PROPERTIES AT 2.2 °C

Property	R-114	R-124
Psat (kPa)	96	177
ρ(liq) (kg/m^2)	1526	1429
ρ(vapor) (kg/m^2)	7.5	11.3
Cp(liq) (J/kg·K)	932	1060
h_{fg} (kJ/kg)	134.7	158.9
k(liq) (W/m·K)	0.0701	0.0744
μ(liq) (g/m·s)	0.4449	0.3375
σ (N/m)	0.0136	0.0129

the physical properties of R-114 and R-124 at a saturation temperature of 2.2 °C. As seen from Table 1, R-124 has higher latent heat of vaporization, vapor density and

thermal conductivity than R-114 at 2.2 °C and a considerably lower liquid viscosity. Therefore, it is reasonable for one to assume that R-124 would have better heat transfer performance at 2.2 °C than R-114. Bertsch [Ref. 1] evaluated and compared the heat transfer performance of R-114 and R-124 for a single horizontal smooth tube and various enhanced tubes using pure refrigerant and refrigerant/oil mixtures. One of his conclusions was:

> For smooth and finned tubes, significant improvements in heat transfer (>50%) were obtained in pure R-124 compared with pure R-114 at the same saturation temperature. This was attributed to the higher saturation pressure of R-124 activating more nucleation sites and the higher latent heat of vaporization, vapor density and thermal conductivity of R-124 over R-114.

Perry [Ref. 2] investigated the effect of oil, pressurization and subcooling on the onset of nucleate boiling of R-124 from a single horizontal tube. When Perry [Ref. 2] compared his results to Bertsch [Ref. 1] for pure R-124, he found a larger incipient wall superheat was being obtained, but almost identical data trends were observed at high heat fluxes and decreasing heat fluxes. He attributed the larger incipience to his degassing procedure of the refrigerent system after reassembly.

Now, what if multiple tubes are arranged in a bundle configuration? How do the lower tubes influence the heat transfer performance of the upper tubes? Lake [Ref. 3] in search of an answer to these questions, used a configuration

3

of two horizontal tubes (smooth and enhanced tubes) in vertical alignment, submerged in a pool of R-114, separated by a pitch-to-diameter (P/D) ratio. After using various combinations of P/D ratios and lower tube heat fluxes, Lake [Ref. 3] found that a nucleating lower tube significantly enhanced the heat transfer performance of an upper tube, particularly at low heat fluxes. Also, a P/D ratio of 1.8 gave the best heat transfer performance for smooth tubes at high heat fluxes (no P/D effect was found using the enhanced tubes).

To fully understand the nucleate pool boiling characteristics of R-124 and to directly compare the heat transfer performance of R-124 to R-114, multiple tube pool boiling data for R-124 is needed. Therefore, the following thesis objectives were established:

1. Collect natural convection and pool boiling heat transfer data of pure R-124 using a single smooth and enhanced tube and check the repeatability with the existing R-124 data of Bertsch [Ref. 1] and Perry [Ref. 2].

2. Collect natural convection and pool boiling heat transfer data of R-124 over a range of increasing and decreasing heat fluxes using two tubes while varying the spacing between the tubes and the heat flux on the lower tube.

3. Compare the R-124 data to the R-114 data obtained by Lake [Ref. 3].

4

II.   LITERATURE SURVEY

A.   POOL BOILING

Pool boiling occurs when a heated surface is submerged below the free surface of a liquid pool, at a temperature sufficiently above the local saturation temperature to cause bubbles to form from the surface. Figure 2.1, from Bar-Cohen [Ref. 4], is a pool boiling curve for a highly wetting liquid with several regimes displayed. Only the natural convection (or single phase convection), boiling incipience and nucleate boiling regimes are discussed.

1. Natural Convection

The regime (a-b) in Figure 2.1, is where heat transfer occurs because of the liquid flow caused by buoyancy forces due to density differences in the liquid pool.   In this regime, the heat flux from the heated surface is proportional to some power of wall superheat (i.e., $q'' \propto \Delta T_w^{1.25}$ or $\Delta T_w^{1.33}$). This proportionality remains valid until the wall superheat reaches a value where vapor bubbles first form on the heated surface.

2. Boiling Incipience

The onset of nucleate boiling (ONB) or incipient boiling is a random phenomenon (You et al. [Ref. 5]) which
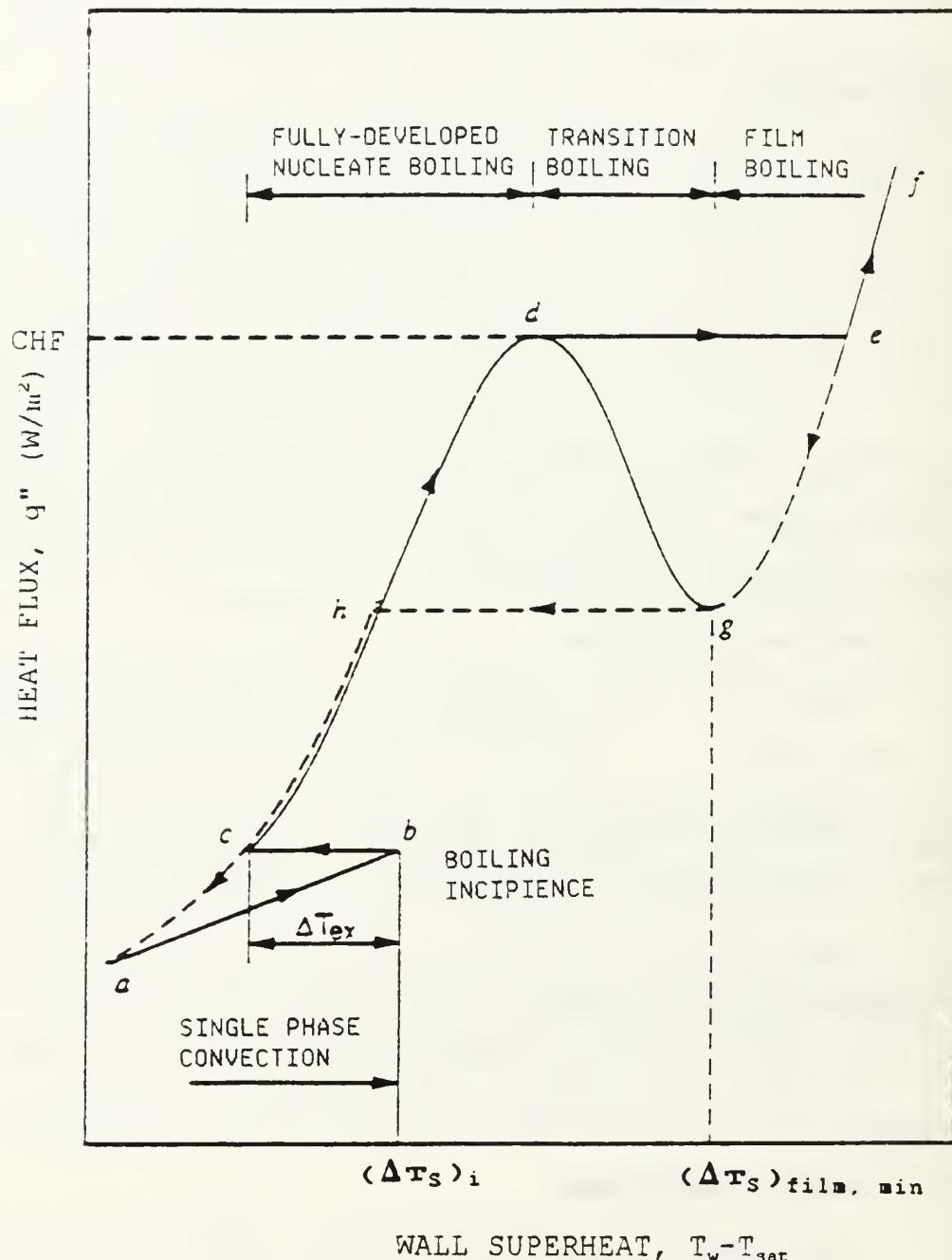
Figure 2.1   Pool Boiling Curve

is influenced by factors such as surface condition of the heated surface, liquid properties and dissolved gases in the liquid pool. Bar-Cohen and Simon [Ref. 6] and Tong et al. [Ref. 7] investigated boiling incipience of highly-wetting liquids using refrigerants and dielectrics. They found that these liquids effectively flood the micro-cavities on a tube surface, causing fewer active embryos (micro-cavities containing trapped vapor). Ultimately, these highly-wetting liquids require larger wall superheats to initialize bubble growth in the flooded micro-cavities. As a result of the larger wall superheats (up to 100 °C, Bar-Cohen and Simon [Ref. 6]), nucleation at (b), in Figure 2.1, occurs in an explosive manner. This explosive boiling from the active micro-cavities causes the larger inactive cavities to activate, rapidly decreasing the required wall superheat to sustain boiling, noted as ΔT_{ex} in Figure 2.1. This drift from (b) to (c) only occurs during increasing heat flux and is referred to as thermal overshoot or superheat excursion.

3. Nucleate Boiling

The regime (c-d) in Figure 2.1 is the fully developed nucleate boiling region. At (c), small isolated bubbles are leaving the heated surface at low heat fluxes. As the heat flux is increased, these small bubbles become more numerous as more active sites are created. At high heat fluxes, these bubbles begin to coalesce, forming slugs of vapor, which grow

and depart from the surface. According to Thome [Ref. 8], in this regime, heat removal is accomplished by sensible heat in the form of superheated liquid or as latent heat in vapor bubbles. Also, the principal mechanisms of heat transfer are: (1) liquid-phase convection, enhanced by the stripping of the thermal boundary layer by the departing vapor bubbles, and (2) evaporation of the thin liquid micro-layer trapped between a growing vapor bubble and the heated surface.

B. SINGLE TUBE HEAT TRANSFER EXPERIMENTS WITH R-124 AT NAVAL POSTGRADUATE SCHOOL

Bertsch [Ref. 1] and Perry [Ref. 2] independently studied the heat transfer performance of single smooth and enhanced tubes submerged in a liquid pool of R-124 at 2.2 °C. Perry [Ref. 2] determined that in natural convection the experimentally based correlation, equation (1), developed by Churchill and Chu [Ref. 9] fairly well predicted the heat transfer performance of a smooth tube.

$$Nu = \left[0.6 + 0.387 \left(\frac{Ra}{(1 + (0.559/Pr)^{9/16})^{16/9}} \right)^{1/6} \right]^2 \quad (1)$$

where   Nu = Nusselt number = hDo/k

Ra = Rayleigh number = $(g \cdot \beta \cdot \{Twall - Tsat\} \cdot Do^3)/(\upsilon \cdot \alpha)$

During nucleate boiling, most correlations available to predict the heat transfer performance of a smooth tube are expressed as heat flux as a function of tube wall superheat. Bertsch [Ref. 1] used a best fit correlation through his experimental nucleate boiling data to express the heat flux from a smooth single tube in pure R-124 as:

$$q'' = (17.0)\Delta T_w^3 \quad (W/m^2) \qquad (2)$$

In the above equation, the wall superheat ΔT_W is expressed in degrees Celsius.

For a single enhanced tube, Bertsch [Ref. 1] concluded that nucleate pool boiling enhancement (i.e., improvements in heat transfer compared to a single smooth tube) were as much as 6.2 times for re-entrant cavity surfaces (TURBO-B and HIGH FLUX). Thome [Ref. 10] attributes these enhancements to the numerous re-entrant cavities that trap vapor, which create a large boiling site density, reducing the wall superheat required to sustain nucleation.

C. SMALL TUBE ARRAY HEAT TRANSFER PERFORMANCE

The effect of a lower tube on the heat transfer performance of an upper tube is very important when designing flooded evaporators. It is essential to understand the mechanisms that affect the heat transfer performance in small

9

tube arrays in natural convection and nucleate boiling for both smooth and enhanced surfaces.

1. Natural Convection

In natural convection, the interaction effects of a lower heated tube on the heat transfer performance of an upper tube are the result of two offsetting mechanisms. With a lower tube heated, a rising heated buoyant plume impinges on and flows around an upper tube, which subjects the upper tube to local forced convection effects. This forced convection increases the local fluid velocity around the upper tube and raises the upper tube heat transfer coefficient. Additionally, the heated plume from the lower tube increases the local ambient temperature of the fluid impinging on the upper tube. This reduces the natural convection buoyancy driving force for this tube, decreasing the upper tube heat transfer coefficient. Therefore, the presence of a lower heated tube has opposing influences on the heat transfer performance of an upper tube. Which of these influences is dominant depends on the tube spacing, local heat flux and the thermophysical properties of the fluid.

Sparrow and Niethammer [Ref. 11] studied the effect of vertical separation between two horizontal cylinders on the heat transfer performance of an upper cylinder in natural convection using air. It was discovered that heat transfer

10

enhancement[1] increased as the distance between the tubes increased with a maximum enhancement of approximately 1.3 for $7 < P/D < 9$. Also, for a $P/D < 3$, the enhancement decreases below 1.0. Al-Alusi and Bushnell [Ref. 12] and Tokura et al. [Ref. 13] also working with a small array of horizontal smooth cylinders in air, found generally the same results. As the distance between the cylinders increased, the heat transfer enhancement increased, reaching a maximum, then returning to a lower value of enhancement.

Sparrow and Boessneck [Ref. 14] investigated the effect of transverse misalignment of a lower cylinder on the heat transfer performance of an upper cylinder, for $2 \leq P/D \leq 9$, using air. For the perfectly aligned upper and lower cylinders, the heat transfer enhancement of the upper cylinder increased as the P/D ratio increased. Again, the largest enhancement was found with a P/D of 9 and the P/D of 2 produced the lowest enhancment. As misalignment was increased, the enhancement began to merge to a common value of about 1.03 at sufficiently large offsets (about 2.5 cylinder diameters). Sparrow and Boessneck concluded that this behavior is caused by the rising plume from the lower cylinder presenting a pre-heated quasi-forced-convection flow to the

---

[1]Enhancement is defined for a small tube array as the upper cylinder heat transfer coefficient when both cylinders are heated divided by the upper cylinder heat transfer coefficient when the lower tube is unheated.

upper cylinder. At smaller P/D ratios, the increased local ambient temperatures of the fluid impinging on the upper cylinder dominates and decreases the upper cylinder heat transfer performance. At larger P/D ratios, the forced convection effects are more dominant and increase the heat transfer from the upper cylinder.

Inagaki and Komori [Ref. 15] studied natural convection heat transfer from two vertically aligned horizontal cylinders in water. As discovered with air, a decrease in enhancement which falls below 1.0, is found for P/D < 1.0. A maximum enhancement of 1.25 occurs between 2.5 ≤ P/D ≤ 3.0 and at larger P/D ratios, the enhancement decreases to 1.0. Inagaki and Komori attribute this behavior to the same two opposing influences discussed previously.

2. Nucleate Boiling

For small tube arrays in nucleate boiling, the most significant mechanism of enhancement within the array, is the well documented bundle effect[2]. Cornwell and associates [Refs. 16-19] studied fluid flow in tube bundles and found significiant enhancements in heat transfer in the upper portions of the bundles, concluding that forced convection and bubbly flow from the lower tubes, creating sliding bubbles

---

[2]Bundle effect is the enhancement of an upper tube due to the activation (i.e., the nucleation of bubbles) of lower tubes within the bundle.

12

around the upper tube, cause significant enhancement at low heat flux conditions.

Fujita et al. [Ref. 20] conducted tests with an array of three horizontal smooth tubes in R-113 at 0.1 MPa. For heat fluxes < 20 kW/m^2, the bundle effect enhanced the upper tube heat transfer performance. Fujita et al. [Ref. 20] also used an array of two smooth tubes, where the lower tube heat flux was held constant and the upper tube heat flux was decreased uniformly. The upper tube enhancement increased as the lower tube heat flux was raised. Lake [Ref. 3] investigated the effect of P/D ratio and lower tube heat flux on the heat transfer performance of an upper tube, using an array of two smooth tubes in R-114 at 1 atmosphere. For these tests, the bottom tube heat flux was held constant and the upper tube heat flux was raised and lowered steadily. Lake found that for an upper tube heat flux of < 20 kW/m^2, the enhancement of the upper tube was due to a bundle effect and the amount of enhancement increased with increased lower tube heat flux, which is consistent with Fujita et al. [Ref. 20]. Also, Lake found that for upper tube heat fluxes of > 20 kW/m^2, all bundle effects faded and that the P/D ratio of 1.8 provided the best upper tube heat transfer performance.

For a small array of enhanced tubes, several authors report findings similar to those found for the smooth tube arrays. Stephan and Mitrovic [Ref. 21], using a small array of three horizontal T-shaped finned tubes in R-114 at 0.2 MPa

and R-12 at 0.15 MPa, found bundle effects present at heat fluxes < 20 kW/m^2, with these effects disappearing as the heat flux was raised. Hahne and associates [Refs. 22-24], using two different fin arrays in R-11 at 0.1 MPa, also found significant bundle effects for heat fluxes of < 20 kW/m^2, which subside at higher heat fluxes. Hahne et al. [Ref. 24] also investigated the influence of P/D ratio on upper tube heat transfer. For heat fluxes < 20 kW/m^2, the maximum P/D ratio tested (P/D of 3.0) produced the best heat transfer performance for both finned arrays. Above 20 kW/m^2, neither P/D ratio nor tube fin pitch affected the upper tube heat transfer. Lake [Ref. 3], in conjunction with his testing of smooth tube performance above, found no effect of P/D ratio on HIGH FLUX tube (porous coated tube) performance at any heat flux and that there was no effect from a lower heated tube on the heat transfer performance of a nucleating upper HIGH FLUX tube. Fujita et al. [Ref. 20], like Lake, also tested porous coated tubes using the same testing conditions as for the smooth tubes and he concluded that the lower tube heat flux setting had no influence on the heat transfer coefficient of the upper tube, which agrees with the conclusions of Lake [Ref. 3].

III.   EXPERIMENTAL APPARATUS

A.   SYSTEM DESCRIPTION

A schematic diagram of the experimental apparatus is shown in Figure 3.1. Details of the apparatus design, construction and calibration are discussed by Karasabun [Ref. 25], Reilley [Ref. 26] and Sugiyama [Ref. 27]. The apparatus is very similar to the one used by Lake [Ref. 3] to conduct pool boiling of pure R-114 with a two tube configuration. The only major change being the replacement of the Pyrex-glass Tees used as the condenser and evaporator. Bertsch [Ref. 1] replaced the Pyrex-glass Tees with fiberglass reinforced Pyrex-glass Tees enabling the system to withstand the increased operating pressure of R-124.

As shown in Figure 3.1, the present system contains the following components: (1) a reinforced Pyrex-glass Tee, used as the evaporator to boil the refrigerant; (2) a reinforced Pyrex-glass Tee, used as the condenser to condense the refrigerant vapor; (3) a liquid refrigerant storage reservoir; (4) an oil storage and mixing subsystem (not used); (5) a vacuum pump; (6) an ethylene-glycol/water mixture cooling subsystem; (7) a condenser pump; (8) aluminum framework with plexiglass siding which houses

15
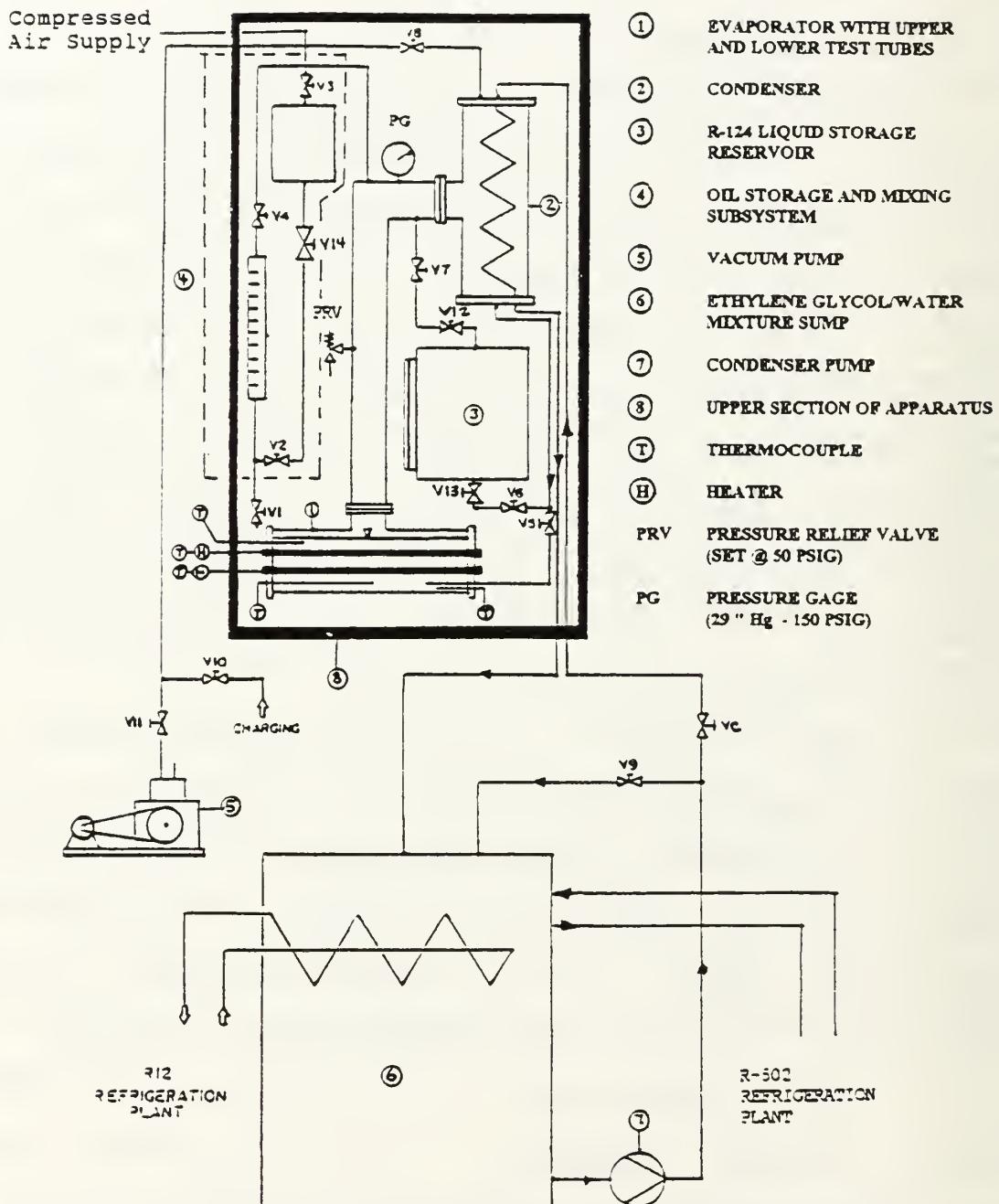
Figure 3.1   Schematic of Experimental Apparatus

16

components (1) through (4); and (9) a data acquisition and instrumentation system (not shown in Figure 3.1).

The system operates in a closed loop with vapor being generated by the heated tubes submerged in the R-124 liquid pool in the evaporator. The vapor travels to the condenser, via a two inch diameter aluminum L-shaped pipe, where it's condensed on a copper coil cooled by the chilled ethylene-glycol/water mixture. The condensed liquid refrigerant is gravity fed back to the evaporator via the return line.

B. BOILING TEST SECTION

1. Evaporator

The evaporator is a Corning Pyrex-glass Tee section (three inch nominal inner diameter) coated with a continuous winding of fiberglass impregnated filaments bonded with a modified epoxy resin. It was installed horizontally with the side-arm of the Tee vertical and hydrostatically safety tested to 75 psig by Bertsch [Ref. 1]. Aluminum endplates, 210 mm diameter and 12.7 mm thick, house the thermocouple wells, an oil entry fitting (not used) and the Teflon inserts, which hold the test tubes in position. The endplates are mated to the evaporator using cast-iron flanges. At the very bottom of the evaporator sits the refrigerant liquid return line from the condenser. A copper deflector plate was installed just above the return line to prevent any vapor bubbles that might

rise off the return line from impinging on the test tubes. The liquid refrigerant level in the evaporator is approximately 10 mm below the top of the evaporator and approximately 10 mm above the top of the upper tube. Figure 3.2 is a sketch of the evaporator and a cast-iron flange.

2. Evaporator Tubes

Figure 3.3 is a schematic of a boiling tube. Two different tube types were used in this study: a smooth tube and a TURBO-B enhanced surface tube. Table 2 provides the dimensions of each tube type while Figure 3.4 shows an

TABLE 2. DIMENSIONS OF TEST TUBES

Tube	D1 mm	D2 mm	Di mm	Do mm	L mm	Lu mm	kc W/m·K
smooth	12.4	15.9	12.7	15.9	203.2	76.2	344
TURBO-B	11.6	13.8	11.8	15.9	203.2	76.2	398

expanded view of the enhanced surface of the TURBO-B tube. Each tube is heated by a 1 kW, 240 volt stainless-steel cartridge heater. The heater measures 6.35 mm outside diameter, 203.2 mm overall length with a heated length of 190 mm and is centered inside the test tube. The tubes are instrumented with eight thermocouples at various locations to
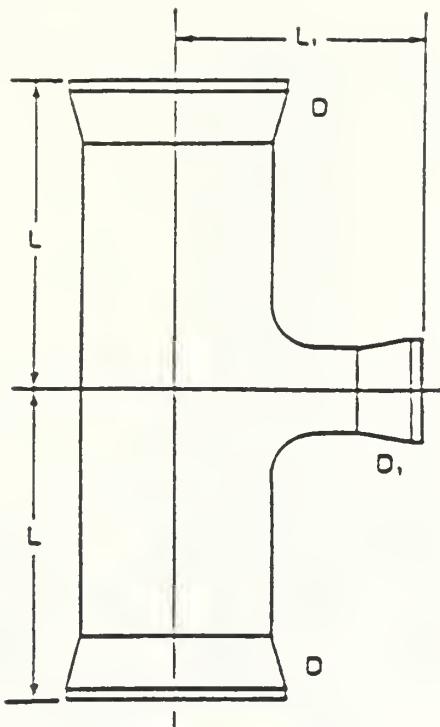
Corning Pyrex Glass Evaporator (D x D_1 = 402x51 mm, L = 178 mm, L_1 = 127 mm)
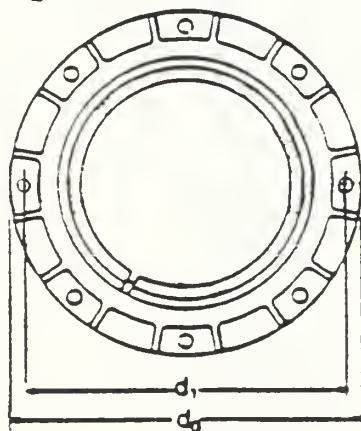
Cast Iron Flange (d_i = 190 mm, d_o = 210 mm)

Figure 3.2   Sketch of Pyrex Glass Evaporator
and Cast-Iron Flange
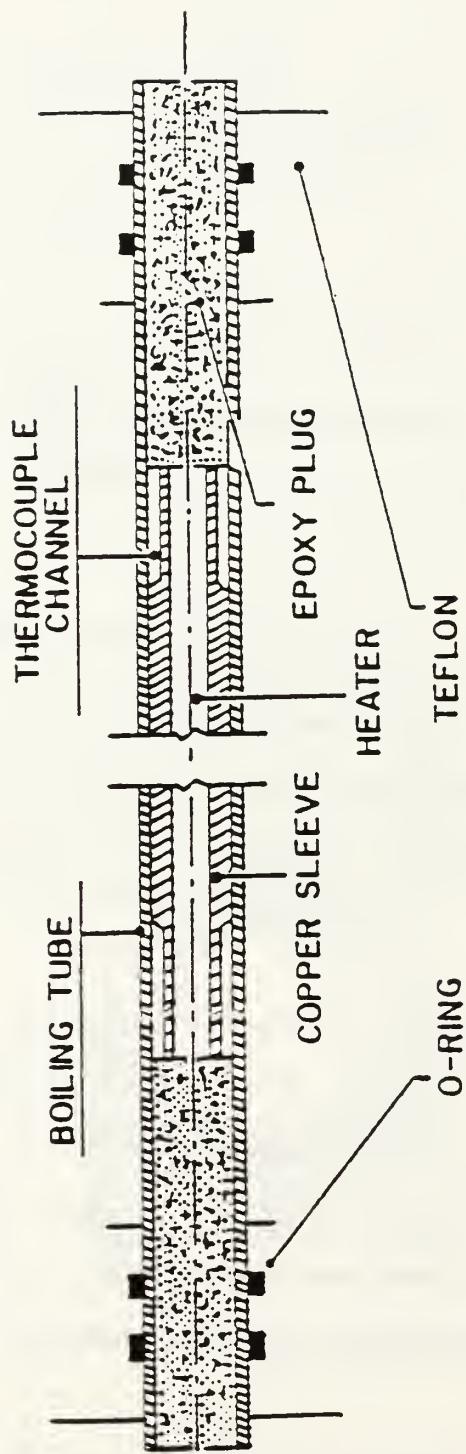
Figure 3.3 Schematic of a Test Tube

20
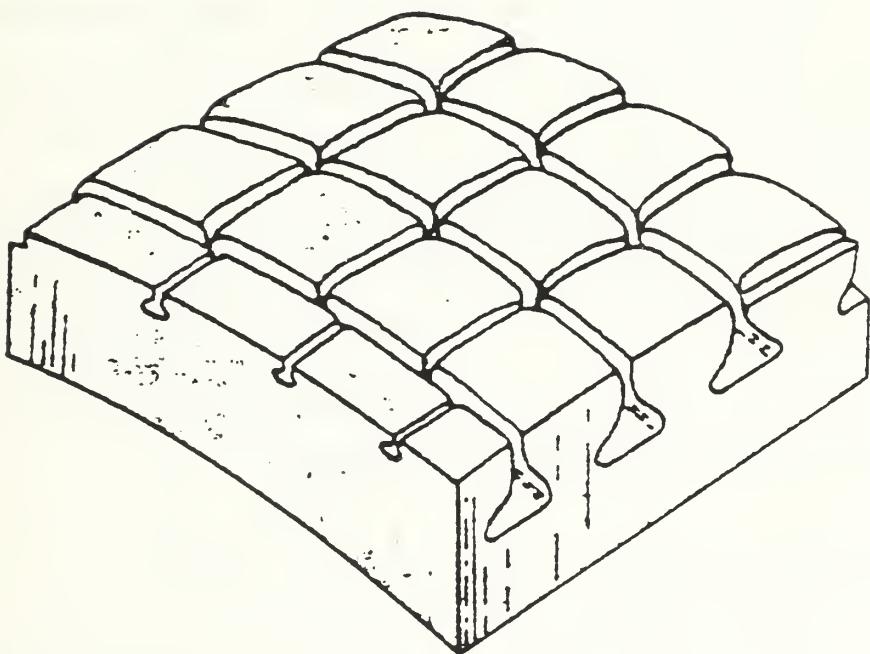
Figure 3.4   Surface Profile of Enhanced (TURBO-B) Tube

21

monitor the tube wall temperatures. Bertsch [Ref. 1] provides a detailed assembly procedure for the manufacturing and instrumentation of a test tube.

The test tubes are secured in the evaporator by Teflon inserts and sealed with o-rings (Figure 3.5). Strong-backs, shown in Figure 3.6, are used to anchor the Teflon inserts in the endplates.

3. Tube Configurations

Figure 3.7 shows the six tube configurations that were used. Configuration C0 is the single tube configuration used by Bertsch [Ref. 1] and Perry [Ref. 2]. In configurations C1 through C4, the top tube is fixed relative to the evaporator while the lower tube position is varied. Configuration C5 consists of rotating the Teflon insert used for C4 through an angle of 30°. Note that when rotation is completed, the upper tube position has moved off the evaporator centerline and the lower tube position remains unchanged.

C. CONDENSER SECTION

The condenser is also a fiberglass-epoxy coated Corning Pyrex-glass Tee section identical in size, shape and substance to the evaporator shown in Figure 3.2. It is mounted vertically (see Figure 3.1) with aluminum endplates bolted to cast-iron flanges, similar to the evaporator arrangement. The
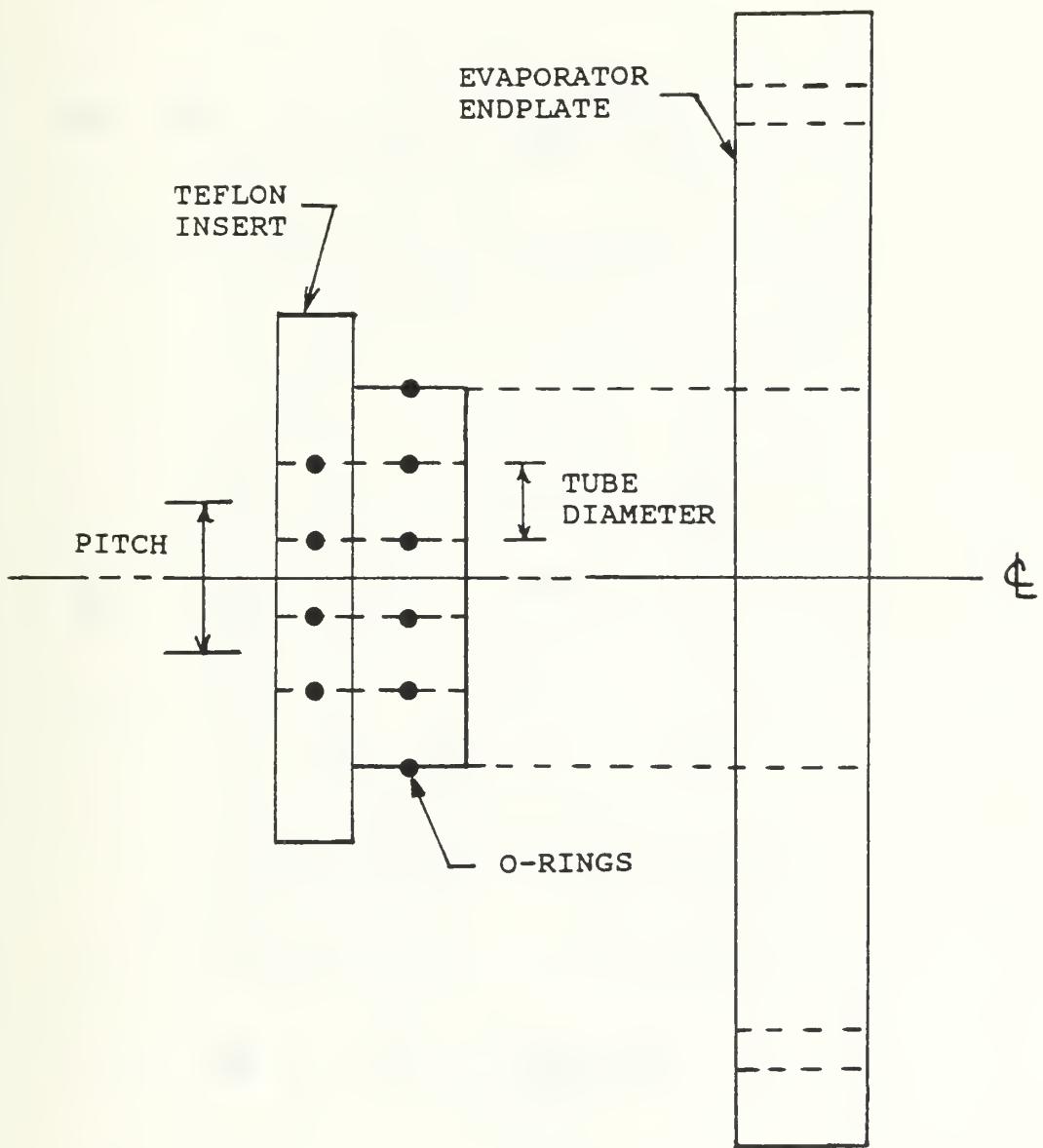
Figure 3.5 Sketch of an Endplate and Teflon Insert
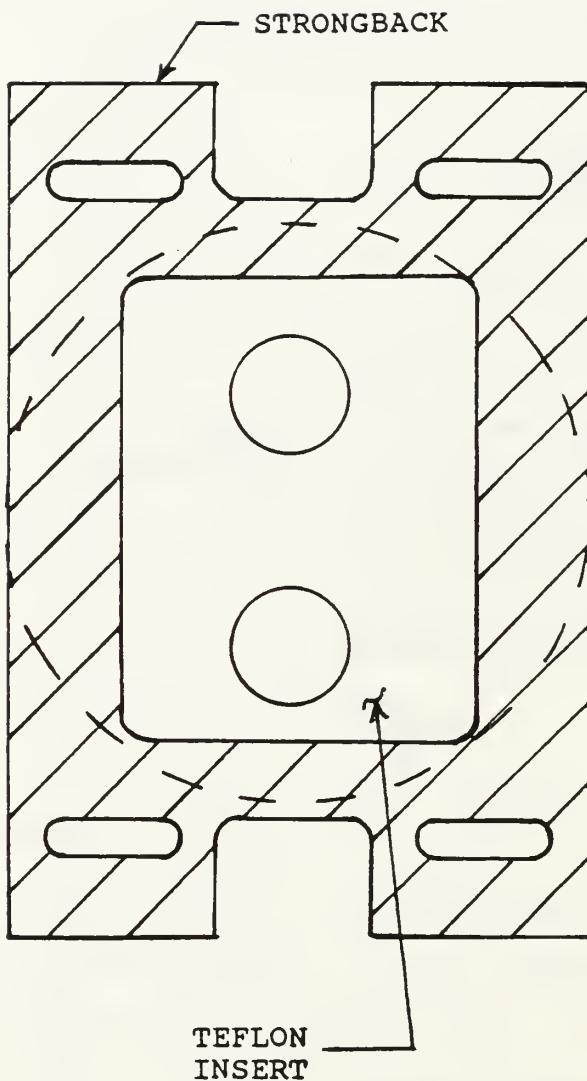
Figure 3.6   Sketch of a Strongback

24
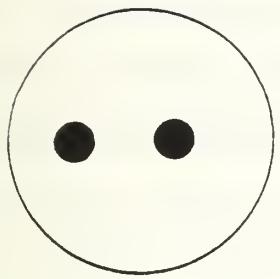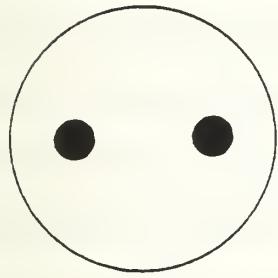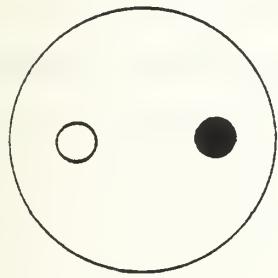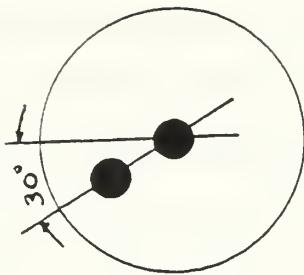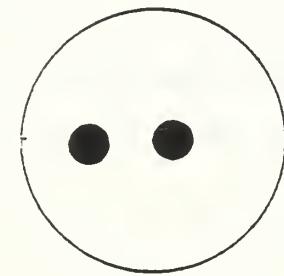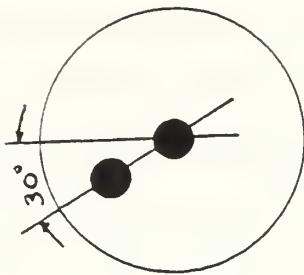
KEY ● - TUBE; O - NO TUBE (PLUGGED)

Figure 3.7 Tube Configurations

25

top endplate is fitted with connections for refrigerant charging/vacuum operations and the ethylene-glycol/water coolant inlet tube. The bottom endplate is fitted with connections for the gravity feed return line to the evaporator and the ethylene-glycol/water coolant outlet tube. The refrigerant vapor rises from the evaporator, passing through the L-shaped aluminum pipe and enters the condenser where it is condensed on a 3/8 inch outside diameter copper tube which is helically coiled inside the condenser.

D. REFRIGERANT STORAGE RESERVOIR

The refrigerant storage reservoir is an aluminum cylinder, 230 mm in diameter and 254 mm in height. It is located within the apparatus enclosure above the evaporator and below the condenser (see Figure 3.1). The reservoir enables the operator to store the liquid R-124 instead of releasing it into the atmosphere, prior to changing out the test tubes. The installed sight glass allows monitoring of the liquid level during replenishing from an outside source (i.e., 145 lb. storage cylinder) or refilling the evaporator after a test tube changeout. The reservoir is isolated from or aligned to the system by means of valves V6, V7, V12 and V13.

E. OIL SUBSECTION

This study was devoted to pure R-124. In order to ensure that no oil contaminated the system, the oil line from the oil cylinder to the evaporator was removed (see Figure 3.1) and the access on the evaporator endplate was capped. Perry [Ref. 2] describes the oil subsection components and the oil addition procedure for a refrigerant/oil mixture study.

F. COOLING SUBSYSTEM

1. Ethylene-Glycol/Water Coolant Sump

At the base of the apparatus sits a 0.15 cubic meter plexiglass tank containing approximately 30 gallons of ethylene-glycol/water mixture producing a freezing point of -25 °C. The sump rests on a wood platform and is wrapped with 22 mm thick foam rubber sheet for insulation. Supply and discharge connections for the condenser and sump pump as well as a thermocouple to monitor the sump temperature are installed.

2. Refrigeration Plants

A 1/2 ton R-502 and 1/4 ton R-12 refrigeration plants are used simultaneously to maintain the ethylene-glycol/water coolant temperature at about -15° C. Both plants are located close to the sump and contain the following components: (1) hermetically sealed compressor assembly; (2) air-cooled condenser; (3) receiver; (4) filter-dryer; (5) pressure

27

regulator;   (6) temperature control switch;   and (7) thermostatic expansion valve. The R-502 plant (Figure 3.8) uses a counter flow heat exchanger as the system evaporator while the R-12 plant uses a 9.5 mm diameter coiled copper tubing submerged in the sump tank as the system evaporator (Figure 3.1).

3. Pumps and Control Valve (VC)

A positive displacement sump pump, rated at 8 gpm, is connected to the discharge connection of the coolant sump with a one inch diameter PVC pipe. It circulates coolant from the sump through the R-502 evaporator and back to the sump. A similar pump, called the condenser pump, circulates coolant from the sump to the condenser, via the control valve VC, and back to the sump (see Figure 3.1). Valve VC is used by the operator to control the refrigerant pool saturation temperature. A manually operated bypass valve (V9, Figure 3.1) is installed upstream of valve VC to prevent overloading the condenser pump when valve VC is closed.

G. APPARATUS ENCLOSURE

A welded aluminum frame measuring 214 cm high, 61 cm wide and 51 cm deep is used to contain most of the system components.   The upper half of the frame contains the evaporator, condenser, oil subsystem, and refrigerant storage reservoir (see Figure 3.1). The lower half of the frame
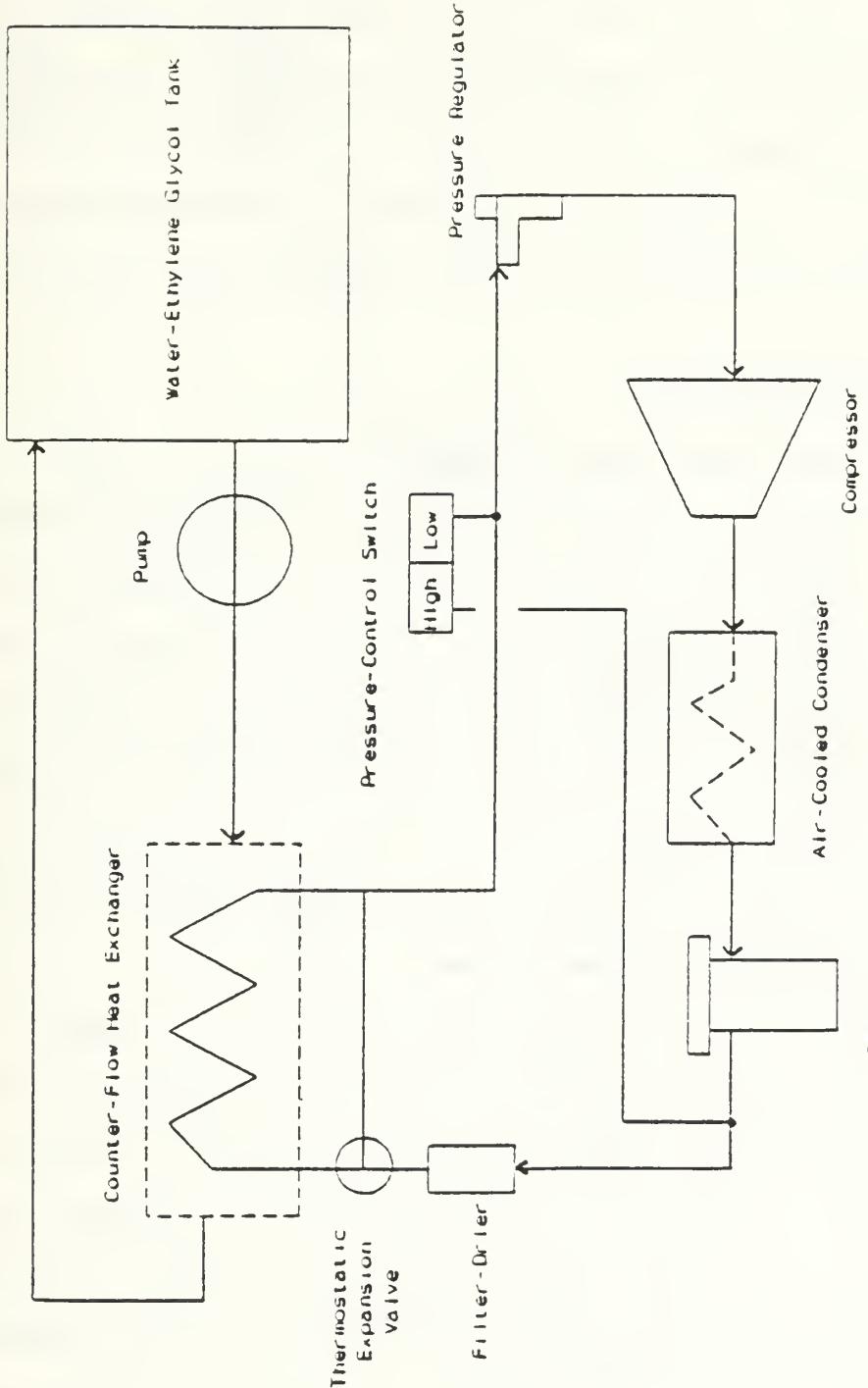
Figure 3.8   Schematic of R-502 Refrigeration System

29

contains the coolant sump tank. For operator safety and to reduce heat leakage into the evaporator and condenser, all sides of the upper half of the frame are covered with 13 mm thick plexiglass, hinged on both sides to allow access to the system components. Holes in the front plexiglass cover allow operation of valves V1 through V8 while maintaining the integrity of the enclosed upper frame.

H. INSTRUMENTATION

1. Power Measurement System

Figure 3.9 is a schematic of the power measurement system. Each boiling tube heater is powered by a 240 volt AC source controlled by a variac. The variac output ranges from 0-220 volt and 0-5 amp, adjustable by the operator to obtain the desired heat flux at the tube surface. The current and voltage sensors convert the AC input signal into DC voltages which are used as input by the Data Acquisition Unit.

2. Temperature Measurement

Temperatures are measured using 30 gauge (0.25 mm diameter) copper-constantan (type T) thermocouples. For each test tube, eight thermocouples are spaced over the heater sleeve, as shown in Figure 3.10, to measure the wall temperatures. Three thermocouples are inserted into housings that penetrate the evaporator endplate and are submerged in

30
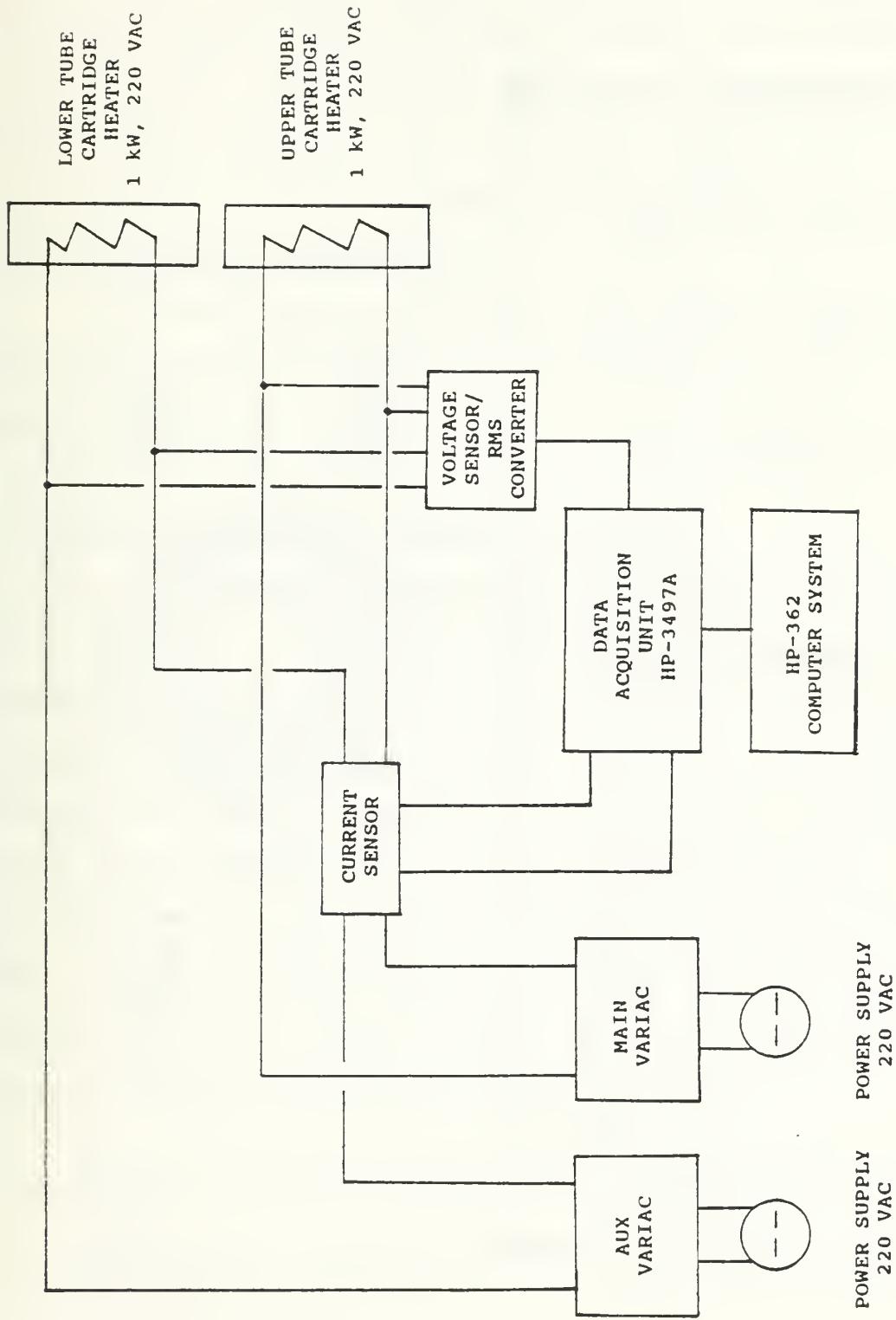
Figure 3.9 Schematic of the Power Measurement System

31

SECTION A-A (DIMENSIONS IN MM)
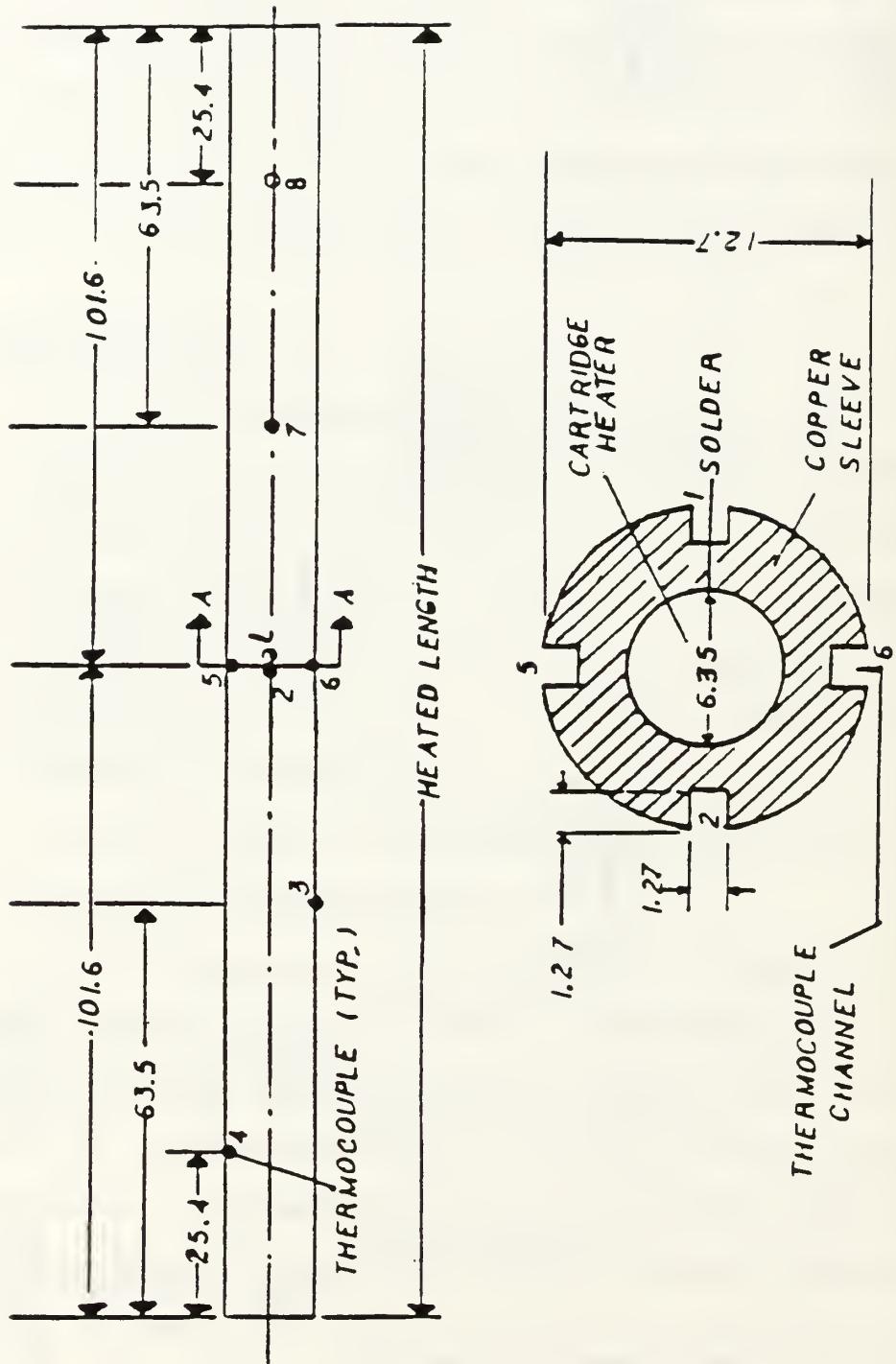
Figure 3.10 Thermocouple Positions

32

the refrigerant liquid pool at different locations (see Figure 3.1). Each housing is constructed of a low conductivity stainless steel body and a high conductivity copper tip (Figure 3.11). This minimizes the errors in pool temperature measurements caused by heat conduction through the housing. A single thermocouple is located in the coolant sump tank to measure the sump temperature.

Thermocouples were read by the a Hewlett-Packard (HP) 3497A Data Acquisition Unit which is controlled by an HP 326 Computer System.

I. DATA ACQUISITION AND REDUCTION PROGRAM

Data acquisition and reduction program DRP72, used by Lake [Ref. 3], was modified to incorporate the thermophysical properties of saturated R-124. Bertsch [Ref. 1] discusses the generation of the equations used in the program calculations. The modified DRP72 program was renamed DRPJY. Appendix B contains the program DRPJY. The program DRPJY directs the HP 362 Computer System and the HP 3497A Data Acquisition Unit to read and process all thermocouple, current and R.M.S. voltage readings. Using this information, DRPJY performs the following calculations (from Bertsch [Ref. 1]):

1. Converts voltage readings into tube temperatures and power.
2. Computes heat transfer rate from cartridge heaters.

33
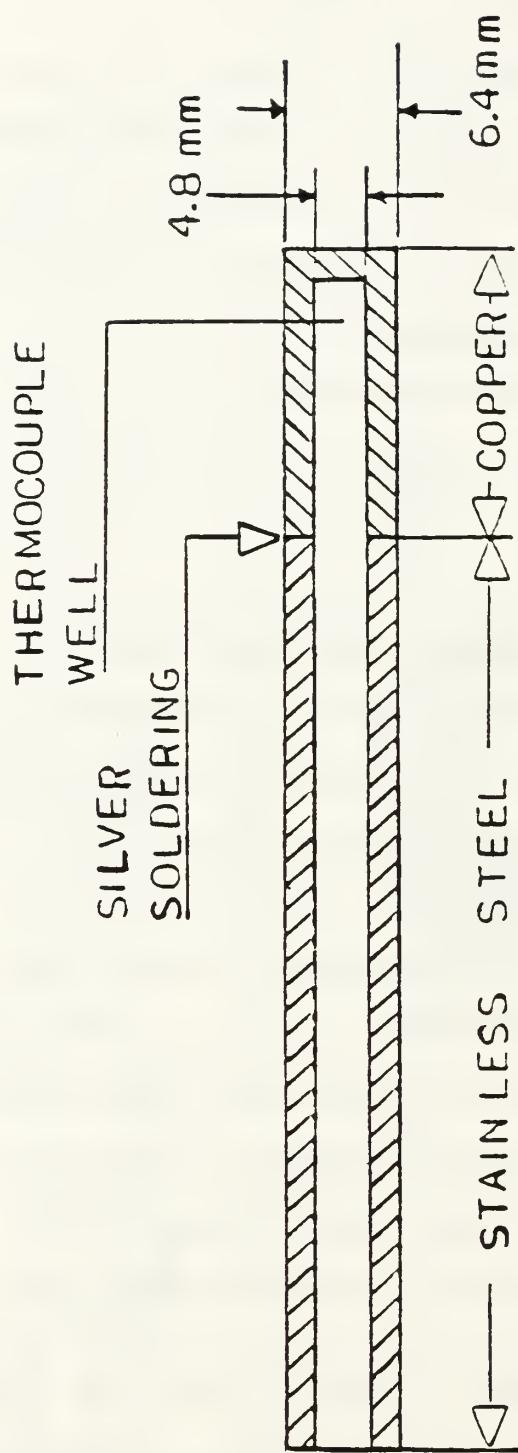
Figure 3.11 Sketch of Thermocouple Housing

3. Computes average test tube wall temperatures and wall superheat (Twall - Tsat).

4. Computes physical properties of R-124 using property correlations from RefProp [Ref. 28] at the film temperature (Twall + Tsat)/2.

5. Computes heat transfer coefficient of R-124 from the unheated ends and heated length of the test tubes.

6. Computes heat losses from the unheated ends of the test tubes.

7. Computes heat flux from heated length of test tubes.

The processed output data was printed by an HP Inkjet printer and stored on the computer hard drive. As a precaution, each output data file was copied to a 3.5 inch floppy disk in the event the computer hard drive becomes unreadable. Table 3 lists the channel assignments that are sensor inputs to the Data Acquisition Unit.

TABLE 3. HP-3497A CHANNEL ASSIGNMENTS

Channel	Channel Assignments
00-07	Upper test tube wall temperature (T1-T8)
08-15	Lower test tube wall temperature (T9-T16)
16	Liquid pool thermocouple (Tld1)
17	Liquid pool thermocouple (Tld2)
18	Liquid pool thermocouple (Tv)
19	Sump coolant temperature
20	R.M.S. voltage of tube heaters
21	Upper tube current sensor
22	Lower tube current sensor

IV. EXPERIMENTAL PROCEDURE

A. EVAPORATOR DISASSEMBLY PROCEDURE

The following procedure is used to transfer the liquid refrigerant from the evaporator to the reservoir to facilitate test tube changeouts:

1. Operate both R-502 and R-12 refrigeration systems to cool the sump tank temperature to approximately -15 °C.

2. Start the condenser pump and using control valve VC, adjust the coolant supply pressure to 1 psig.

3. Close valve V5 to isolate the evaporator from the condensing refrigerant vapor (see Figure 3.1).

4. Align the refrigerant storage reservoir to the system by opening valves V6, V7, V12 and V13.

5. Position and energize the high volume air dryer (set for high heat) so the heated air stream is blowing on the center of the evaporator. Adjust valve VC to ensure the refrigerant vapor is condensing.

6. After 1-2 hours, the evaporator should be dry with the liquid refrigerant in the reservoir and a small amount in the return line.

7. Close valves V6, V7, V12 and V13, isolating the reservoir from the system.

8. Secure and remove the air dryer.

9. Stop the condenser pump.

10. Open valves V8 and V10 to reduce to system pressure to atmospheric. Close valve V8 and V10 when the system pressure reads 0 psig on the system pressure gage.

11. Disconnect the test tube heater and thermocouple leads.

12. Remove strongbacks.

13. Remove Teflon inserts and test tubes.

B. EVAPORATOR ASSEMBLY PROCEDURE

1. Evaporator Assembly

Before installing smooth test tubes, rinse with acetone then wipe clean with lint-free wipes or if installing TURBO-B test tubes, brush the enhanced surfaces with a soft bristle brush (i.e., toothbrush) using ethyl alcohol then repeat the brushing using acetone and let the tubes air dry. Check the Teflon insert o-rings for damage and replace as necessary. Before installing the test tubes, wipe the evaporator interior clean with lint-free wipes. Install the test tubes in the evaporator using the Teflon inserts to secure the tubes in place. Snug the strongbacks up to the Teflon inserts and connect the thermocouple leads. Prior to connecting the heater leads, check the resistance between the heater leads and the outer tube wall using a multimeter. One megohm resistance or greater is satisfactory.

2. Leak Test

After assembling the evaporator and before charging the system with refrigerant, perform a vacuum test to verify the integrity of the system. Evacuate the system by starting the vacuum pump and opening valves V11 and V8 (see Figure 3.1). After evacuating the system to approximately 29

in. Hg, close valves V11 and V8, then stop the vacuum pump. If no drop in vacuum is detected (i.e., no leak) within 30 minutes, charge the system with R-124.

If a leak is detected, open valves V8 and V11 and pressurize the system with air to 20 psig. Apply a soap/water solution to the system sealing surfaces to identify the leak location (bubbles will be seen from the leak source). After identifying and repairing the leak, retest the system for leaks.

3. Charging System with Refrigerant

Once the system integrity is assured, fill the evaporator with R-124, using one of the following procedures, to a level *just below the top of the evaporator* (<u>NOTE</u>: some refrigerant will be lost during the degas procedure, therefore, it is important to fill the evaporator above the level needed to conduct data runs):

a. From Storage Reservoir

Open valves V12 and V7 to equalize the pressure between the storage reservoir and the system. Open valves V13, V6 and V5 to gravity fill the evaporator with liquid refrigerant. When the evaporator is filled to the proper level, close valves V6, V13, V7 and V12 to isolate the storage reservoir from the system.

b. *From Refrigerant Cylinder*

Connect the cylinder to valve V10 using the charging hose (Figure 3.1). Open valves V5, V8 and V10 and then open the cylinder liquid valve to release the refrigerant from the cylinder into the system. Close valves V8, V10 and the cylinder liquid valve when the evaporator is filled to the proper level. Disconnect the charging hose from valve V10 and stow the cylinder.

4. Degassing Procedure

This degas procedure is similar to Perry's [Ref. 3] degassing procedure B. Degas the system by boiling the refrigerant, using a upper test tube heat flux of 85 KW/m^2 and a lower test tube heat flux of 20 KW/m^2, for 30 minutes. Ensure the condenser pump is running and control valve VC is open to prevent overpressurizing the system. During the boiling process, air and non-condensible gases rise in the system and collect in the condenser. After the 30 minute boiling time has elapsed, secure the heat flux to the test tubes and stop the condenser pump. Let the system set for 30 minutes allowing the condensed refrigerant to drain to the evaporator. After the 30 minute set time has elapsed, start the vacuum pump and open valve V11, then open valve V8 for 20 seconds to remove the accumulated air and non-condensible gases. After closing valve V8, stop the vacuum pump and close valve V11.

5. **Data Acquisition Channel Check**

After all evaporator thermocouples (test tubes and pool) are connected, load and run program SETUPJY to verify the output of each thermocouple is correct. Any output that is inconsistent or suspect is either fixed or noted and later excluded from the calculations in program DRPJY.

C. STANDARD OPERATING PROCEDURE

The following procedure is used to conduct each data collection run:

1. Operate the R-502 and R-12 refrigeration systems to cool the sump to approximately -15 °C.

2. Energize the HP-362 Computer System, Data Acquisition Unit and the variac control panel.

3. Load and run program SETUPJY. Verify the thermocouple outputs are consistent.

4. Verify control valve VC is closed, then start the condenser pump.

5. Slowly open valve VC until the coolant pressure gage reads 1/8 psig. This pressure setting will ensure that the refrigerant pool will be slowly cooled.

6. Monitor the thermocouple outputs with SETUPJY until confident the thermocouples are operating properly. Note which thermocouples are inconsistent and must be excluded from program DRPJY.

7. When the refrigerant pool temperature is approaching 5 °C, load and run program DRPJY. Select 'TAKE DATA' option.

8. At the prompt, enter the filename that the data is to be stored under (page 38 explains the file naming scheme used).

41

9. At the prompt, enter the number of defective upper tube thermocouples that were identified by SETUPJY.

10. At the prompt, enter the defective upper tube thermocouple locations that were identified by SETUPJY.

11. At the prompt, enter the number of defective lower tube thermocouples that were identified by SETUPJY.

12. At the prompt, enter the defective lower tube thermocouple locations that were identified by SETUPJY.

13. Select the type of test tubes installed.

14. From the main menu, select 'SET Tsat'. Monitor the pool thermocouples and, if required, adjusted valve VC to maintain the desired pool saturation temperature of 2.22 ± 0.1 °C.

15. From the main menu, select 'SET UPPER TUBE HEAT FLUX', then adjust the main variac to the desired heat flux. Initial heat flux setting is 500-600 KW/m^2.

16. Press the keyboard button f1 to return to the main menu and select 'SET LOWER TUBE HEAT FLUX'. Adjust the aux variac to the desired heat flux.

17. From the main menu, select 'SET Tsat'. Adjust valve VC to maintain the desired pool saturation temperature while monitoring the pool thermocouples.

18. Once the pool saturation temperature is stable, return to the main menu and select 'TAKE DATA'.

19. For each heat flux setting steps 15-18 are repeated.

D. DATA FILES

Data were filed using the following convention:

Example (D0904ASC1):

1. First letter D indicates the file is a data file.

2. The following four characters indicate the date; in this example September 04, 1993.

42

3. The next letter indicates the order in which the data run was completed on that day; no letter - 1st run, A - 2nd run, B - 3rd run, etc.

4. The next one or two letters indicate the tubes used; S - smooth, TB - TURBO-B.

5. The last letter and number combination represent the tube configuration used.

Table 4 is a summarized list of the data runs completed.

TABLE 4. LIST OF DATA RUNS

Data File	Tube Type	Purpose
D0728ASC0	Smooth	Repeatability; single tube
D0804ASC0	Smooth	Repeatability; single tube
D0816SC0	Smooth	Repeatability; single tube
D0520SC1	Smooth	Repeatability; P/D = 2.0; no power on lower tube
D0714SC1	Smooth	Repeatability; P/D = 2.0; no power on lower tube
D0831SC1	Smooth	Data; repeatability; P/D = 2.0; no power on lower tube
D0901SC1	Smooth	Data; P/D = 2.0; 1 kW/m^2 on lower tube
D0902SC1	Smooth	Data; P/D = 2.0; 5 kW/m^2 on lower tube
D0902BSC1	Smooth	Data; P/D = 2.0; 20 kW/m^2 on lower tube
D0903SC1	Smooth	Data; P/D = 2.0; q" on both tubes inc/dec together
D0904SC1	Smooth	Data; P/D = 2.0; 5 kW/m^2 on upper tube
D0904ASC1	Smooth	Data; P/D = 2.0; 10 kW/m^2 on upper tube
D0905SC1	Smooth	Data; P/D = 2.0; 20 kW/m^2 on upper tube
D0906SC2	Smooth	Data; P/D = 1.8; no power on lower tube
D0906ASC2	Smooth	Data; P/D = 1.8; 1 kW/m^2 on lower tube
D0907SC2	Smooth	Data; P/D = 1.8; 5 kW/m^2 on lower tube
D0907ASC2	Smooth	Data; P/D = 1.8; 10 kW/m^2 on lower tube

TABLE 4. LIST OF DATA RUNS (continued)

Data File	Tube Type	Purpose
D0908SC2	Smooth	Data; P/D = 1.8; 20 kW/m^2 on lower tube
D0908ASC2	Smooth	Data; P/D = 1.8; q" on both tubes inc/dec together
D0908ASC2	Smooth	Data; P/D = 1.8; 5 kW/m^2 on upper tube
D0909SC2	Smooth	Data; P/D = 1.8; 10 kW/m^2 on upper tube
D0909ASC2	Smooth	Data; P/D = 1.8; 20 kW/m^2 on lower tube
D0910SC3	Smooth	Data; P/D = 1.5; no power on lower tube
D0910ASC3	Smooth	Data; P/D = 1.5; 1 kW/m^2 on lower tube
D0917SC3	Smooth	Data; P/D = 1.5; 5 kW/m^2 on lower tube
D0919SC3	Smooth	Data; P/D = 1.5; 10 kW/m^2 on lower tube
D0919ASC3	Smooth	Data; P/D = 1.8; 20 kW/m^2 on lower tube
D0920SC3	Smooth	Data; P/D = 1.8; q" on both tubes inc/dec together
D0920ASC3	Smooth	Data; P/D = 1.5; 5 kW/m^2 on upper tube
D0920BSC3	Smooth	Data; P/D = 1.5; 10 kW/m^2 on upper tube
D0920CSC3	Smooth	Data; P/D = 1.5; 20 kW/m^2 on upper tube
D0921SC4	Smooth	Data; P/D = 1.2; no power on lower tube
D0921ASC4	Smooth	Data; P/D = 1.2; 1 kW/m^2 on lower tube
D0921BSC4	Smooth	Data; P/D = 1.2; 5 kW/m^2 on lower tube

45

TABLE 4. LIST OF DATA RUNS (continued)

Data File	Tube Type	Purpose
D0921CSC4	Smooth	Data; P/D = 1.2; 10 kW/m^2 on lower tube
D0922SC4	Smooth	Data; P/D = 1.2; 20 kW/m^2 on lower tube
D0922ASC4	Smooth	Data; P/D = 1.2; q" on both tubes inc/dec together
D0922BSC4	Smooth	Data; P/D = 1.2; 5 kW/m^2 on upper tube
D0922CSC4	Smooth	Data; P/D = 1.2; 10 kW/m^2 on upper tube
D0922DSC4	Smooth	Data; P/D = 1.2; 20 kW/m^2 on upper tube
D0930SC5	Smooth	Data; P/D = 1.2 rotated 30°; no power on lower tube
D0930ASC5	Smooth	Data; P/D = 1.2 rotated 30°; 1 kW/m^2 on lower tube
D0930BSC5	Smooth	Data; P/D = 1.2 rotated 30°; 5 kW/m^2 on lower tube
D0930CSC5	Smooth	Data; P/D = 1.2 rotated 30°; 10 kW/m^2 on lower tube
D0929CSC5	Smooth	Data; P/D = 1.2 rotated 30°; 20 kW/m^2 on lower tube
D0929DSC5	Smooth	Data; P/D = 1.2 rotated 30°; q" on both tubes inc/dec together
D0929BSC5	Smooth	Data; P/D = 1.2 rotated 30°; 5 kW/m^2 on upper tube
D0929ASC5	Smooth	Data; P/D = 1.2 rotated 30°; 10 kW/m^2 on upper tube
D0929SC5	Smooth	Data; P/D = 1.2 rotated 30°; 20 kW/m^2 on upper tube
D1012TBC0	TURBO-B	Repeatability; single tube
D1012ATBC0	TURBO-B	Repeatability; single tube
D1012BTBC0	TURBO-B	Repeatability; single tube

46

TABLE 4. LIST OF DATA RUNS (continued)

Data File	Tube Type	Purpose
D1019TBC1	TURBO-B	Repeatability; P/D = 2.0; no power on lower tube
D1018ATBC1	TURBO-B	Repeatability; P/D = 2.0; no power on lower tube
D1018BTBC1	TURBO-B	Data; repeatability; P/D = 2.0; no power on lower tube
D1018CTBC1	TURBO-B	Data; P/D = 2.0; 1 kW/m^2 on lower tube
D1018DTBC1	TURBO-B	Data; P/D = 2.0; 5 kW/m^2 on lower tube
D1019TBC1	TURBO-B	Data; P/D = 2.0; 10 kW/m^2 on lower tube
D1019ATBC1	TURBO-B	Data; P/D = 2.0; 20 kW/m^2 on lower tube
D1019ETBC1	TURBO-B	Data; P/D = 2.0; q" on both tubes decreased together
D1019CTBC1	TURBO-B	Data; P/D = 2.0; 5 kW/m^2 on upper tube
D1019DTBC1	TURBO-B	Data; P/D = 2.0; 10 kW/m^2 on upper tube
D1019ETBC1	TURBO-B	Data; P/D = 2.0; 20 kW/m^2 on upper tube
D1020TBC2	TURBO-B	Data; P/D = 1.8; no power on lower tube
D1020ATBC2	TURBO-B	Data; P/D = 1.8; 1 kW/m^2 on lower tube
D1020BTBC2	TURBO-B	Data; P/D = 1.8; 5 kW/m^2 on lower tube
D1020CTBC2	TURBO-B	Data; P/D = 1.8; 10 kW/m^2 on lower tube
D1020DTBC2	TURBO-B	Data; P/D = 1.8; 20 kW/m^2 on lower tube

TABLE 4. LIST OF DATA RUNS (continued)

Data File	Tube Type	Purpose
D1020ETBC2	TURBO-B	Data; P/D = 1.8; q" on both tubes decreased together
D1021TBC2	TURBO-B	Data; P/D = 1.8; 5 kW/m^2 on upper tube
D1021ATBC2	TURBO-B	Data; P/D = 1.8; 10 kW/m^2 on upper tube
D1021ATBC2	TURBO-B	Data; P/D = 1.8; 20 kW/m^2 on upper tube
D1021CTBC3	TURBO-B	Data; P/D = 1.5; no power on lower tube
D1021DTBC3	TURBO-B	Data; P/D = 1.5; 1 kW/m^2 on lower tube
D1021ETBC3	TURBO-B	Data; P/D = 1.5; 5 kW/m^2 on lower tube
D1021FTBC3	TURBO-B	Data; P/D = 1.5; 10 kW/m^2 on lower tube
D1022TBC3	TURBO-B	Data; P/D = 1.5; 20 kW/m^2 on lower tube
D1022ATBC3	TURBO-B	Data; P/D = 1.5; q" on both tubes decreased together
D1022BTBC3	TURBO-B	Data; P/D = 1.5; 5 kW/m^2 on upper tube
D1022CTBC3	TURBO-B	Data; P/D = 1.5; 10 kW/m^2 on upper tube
D1022DTBC3	TURBO-B	Data; P/D = 1.5; 20 kW/m^2 on upper tube
D1022ETBC4	TURBO-B	Data; P/D = 1.2; no power on lower tube
D1022FTBC4	TURBO-B	Data; P/D = 1.2; 1 kW/m^2 on lower tube
D1025TBC4	TURBO-B	Data; P/D = 1.2; 5 kW/m^2 on lower tube
D1025ATBC4	TURBO-B	Data; P/D = 1.2; 10 kW/m^2 on lower tube

TABLE 4. LIST OF DATA RUNS (continued)

Data File	Tube Type	Purpose
D1025BTBC4	TURBO-B	Data; P/D = 1.2; 20 kW/m^2 on lower tube
D1025CTBC4	TURBO-B	Data; P/D = 1.2; q" on both tubes decreased together
D1025DTBC4	TURBO-B	Data; P/D = 1.2; 5 kW/m^2 on upper tube
D1025ETBC4	TURBO-B	Data; P/D = 1.2; 10 kW/m^2 on upper tube
D1025FTBC4	TURBO-B	Data; P/D = 1.2; 20 kW/m^2 on upper tube
D1026TBC5	TURBO-B	Data; P/D = 1.2 rotated 30°; no power on lower tube
D1026ATBC5	TURBO-B	Data; P/D = 1.2 rotated 30°; 1 kW/m^2 on lower tube
D1026BTBC5	TURBO-B	Data; P/D = 1.2 rotated 30°; 5 kW/m^2 on lower tube
D1026CTBC5	TURBO-B	Data; P/D = 1.2 rotated 30°; 10 kW/m^2 on lower tube
D1026DTBC5	TURBO-B	Data; P/D = 1.2 rotated 30°; 20 kW/m^2 on lower tube
D1026ETBC5	TURBO-B	Data; P/D = 1.2 rotated 30°; q" on both tubes decreased together
D1027TBC5	TURBO-B	Data; P/D = 1.2 rotated 30°; 5 kW/m^2 on upper tube
D1027ATBC5	TURBO-B	Data; P/D = 1.2 rotated 30°; 10 kW/m^2 on upper tube
D1027BTBC5	TURBO-B	Data; P/D = 1.2 rotated 30°; 20 kW/m^2 on upper tube

V. DISCUSSION OF RESULTS

A. REPRODUCIBILITY/REPEATABILITY

To verify that the equipment and operating procedure being used were consistent with those used by Bertsch [Ref. 1] and Perry [Ref. 2], six reproducibility/repeatability runs were performed. Program DRPGP (from Perry's single tube work [Ref. 2]) was used for the runs conducted with a single test tube and DRPJY was used for all runs conducted with two test tubes. Figures 5.1 and 5.2 are plots of increasing and decreasing heat flux using a smooth tube in configuration C0 (which is identical to the configuration used by Perry [Ref. 2]). In Figure 5.1, the three runs completed are in very good agreement with each other. At lower heat fluxes (< 4 kW/m^2) some scatter is present which disappears at mid-range heat fluxes (4-8 kW/m^2). Perry [Ref. 2] found the same phenomenon and attributed the scatter to convection regime thermal gradients where mixing is inefficient within the liquid pool, after discovering large local variations in the tube wall and pool thermocouples of up to 5%. In this study, local variations in the tube wall and pool thermocouples were found to be up to 7% at lower heat fluxes and decreasing as heat flux increased, which supports Perry's theory. In

50
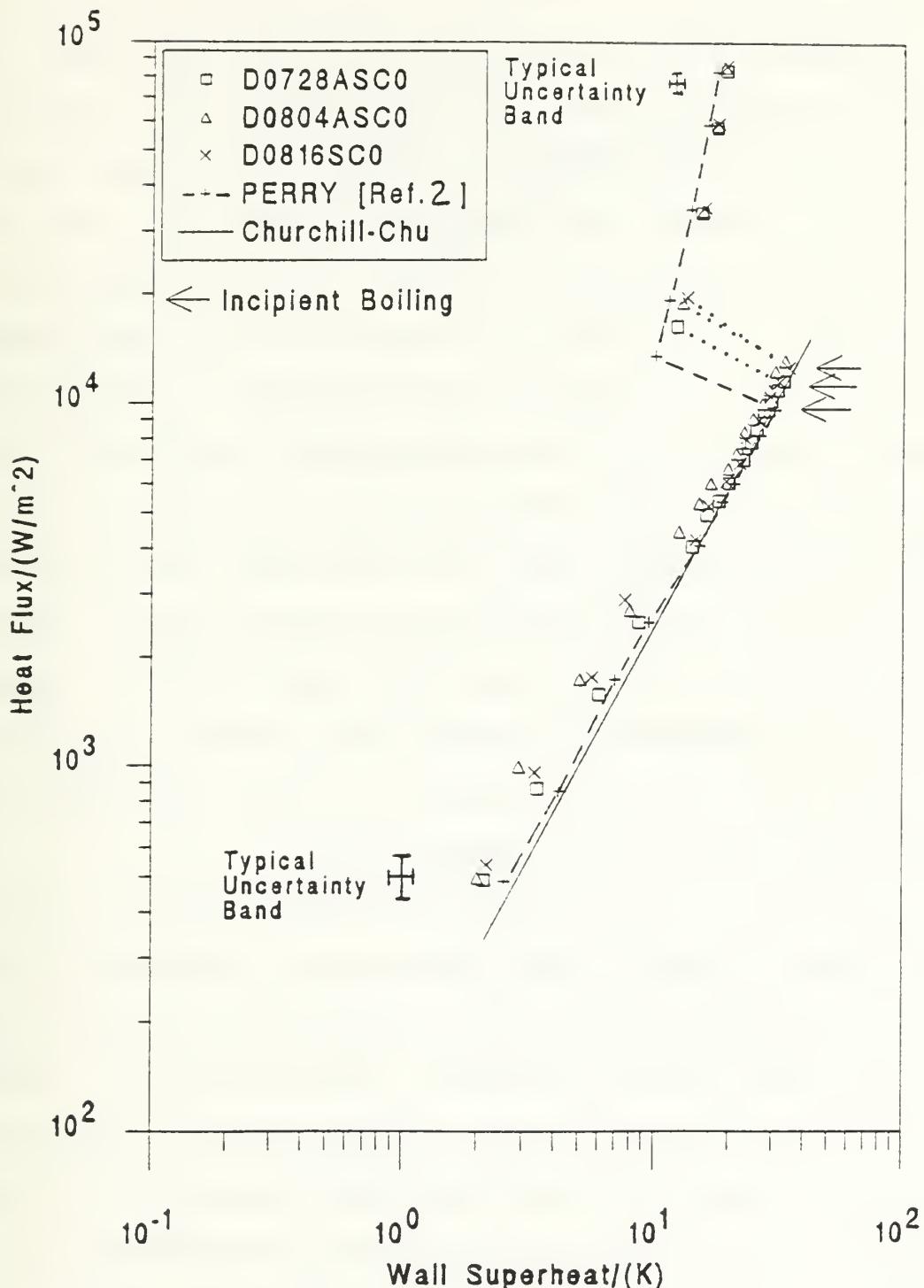
Figure 5.1   Increasing Heat Flux Repeatability Runs using
Smooth Tube Configuration C0

51

natural convection, the three data runs started to the left of the Churchill and Chu correlation [Ref. 9] (shown as a solid line) at low heat fluxes and converged toward the Churchill-Chu line as the heat flux was increased. This slight shift to the left, although consistent during the three runs, was within the uncertainty in the region. Good repeatability was also found at the onset of nucleate boiling (indicated by arrows) and in the nucleate boiling region. Comparing the repeatability runs to the representative data set of Perry [Ref. 2], at low heat fluxes the data vary slightly but are within the uncertainty band. The data merge up to the point of incipience, but why Perry's run nucleated earlier than the present data is unclear since the runs were, in essence, identical. In the boiling region, Perry's data is slightly to the left of the present data but again lie within the uncertainty band for that region.

In Figure 5.2, good repeatability is again shown for all heat fluxes. Comparing the three present repeatability runs to the representative data set of Perry [Ref. 2], again shows good reproducibility throughout. For heat fluxes < 1 kW/m^2, the slopes of the data curves change, which indicates the transition from nucleate boiling back to natural convection. Based on Figures 5.1 and 5.2, data reproducibility is considered satisfactory with the single smooth tube work carried out by Perry [Ref. 2] on the same apparatus.

52
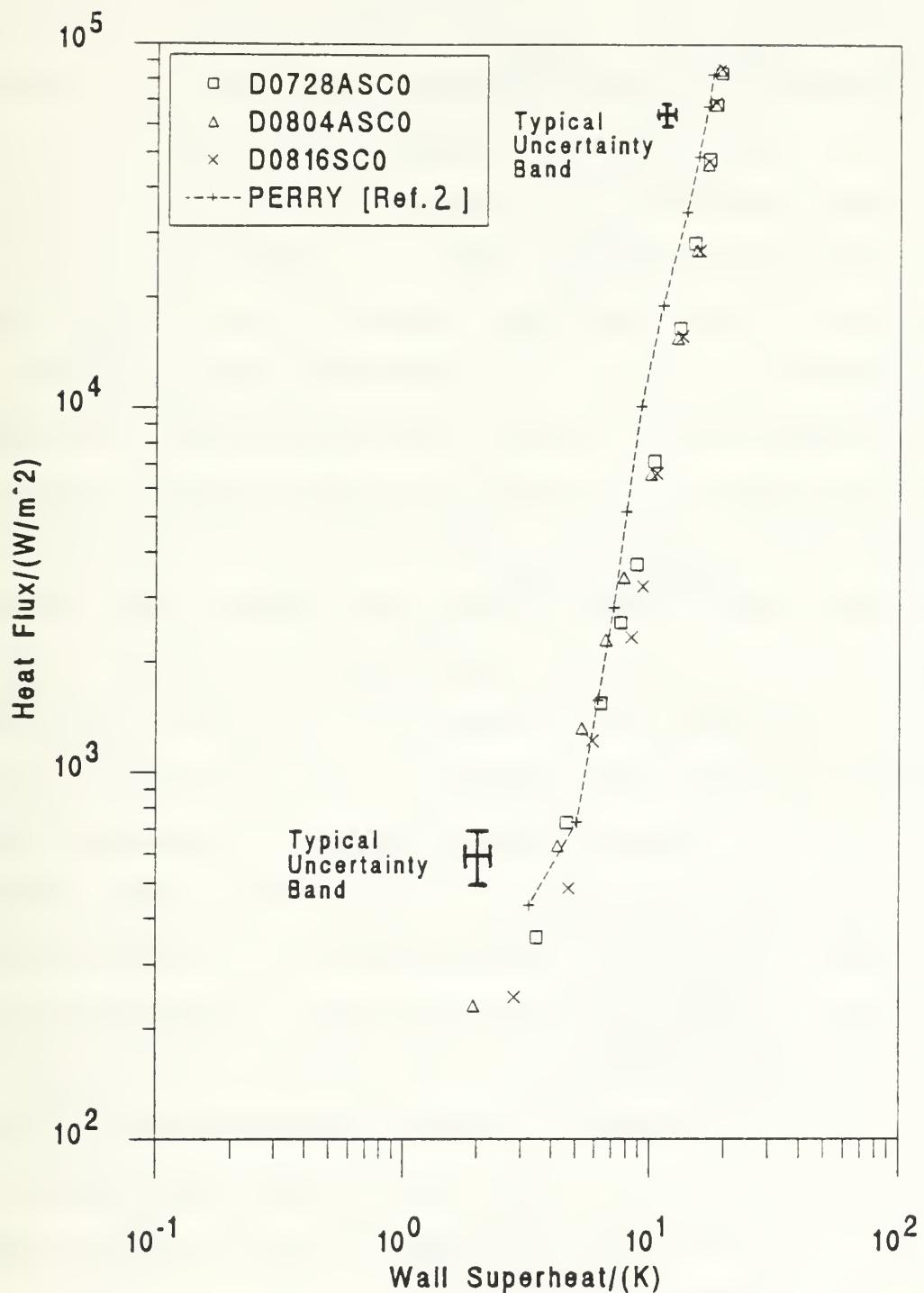
Figure 5.2 Decreasing Heat Flux Repeatability Runs using
Smooth Tube Configuration C0

53

Figure 5.3 is a comparison of decreasing heat flux repeatability runs using an enhanced tube (TURBO-B) in configuration C0 with the single tube data of Bertsch [Ref. 1]. For the present data, good repeatability is again obtained throughout. In comparing the current data with the data collected by Bertsch [Ref. 1], different boiling curves are easily seen. This was a result of two different TURBO-B test tubes being used. After examining both test tubes under a microscope (using 50x and 100x magnification), the TURBO-B test tube used in this study had wider notches between the 'mushroom-like pedestals' (see Figure 3.4), indicating that a different fabrication process was used to make the tube. Above 20 kW/m^2 on the plot, the current data curves are to the left of Bertsch's data (about 2 °C less wall superheat), indicating better heat transfer. It is believed this is due to the wider notches in the tube surface allowing more bubbles to depart the tube surface at higher heat fluxes, removing more heat than the tube used by Bertsch. At about 10 kW/m^2, the trend is reversed, the current data crosses and continues to fall below Bertsch's data (about 0.3 °C more wall superheat). At low heat fluxes, the wider notches allow the refrigerant to flood back into the boiling channels (see Figure 3.4) and reduce the number of active sites, reducing the heat transfer from the tube.

Figure 5.4 is a comparison of increasing heat flux repeatability runs using smooth tube configuration C1 with the

54
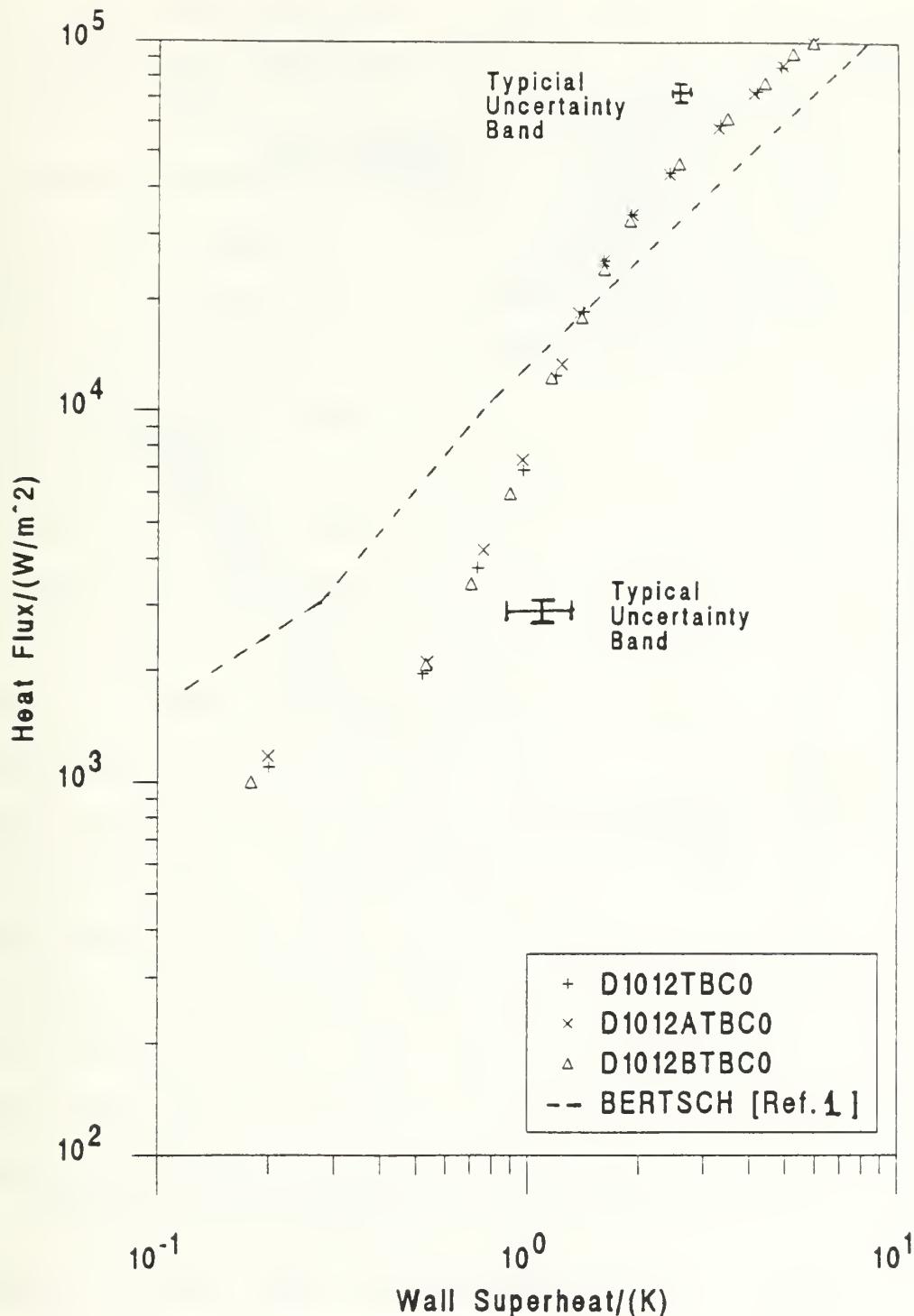
Figure 5.3   Decreasing Heat Flux Repeatability Runs using
TURBO-B Tube Configuration C0

55
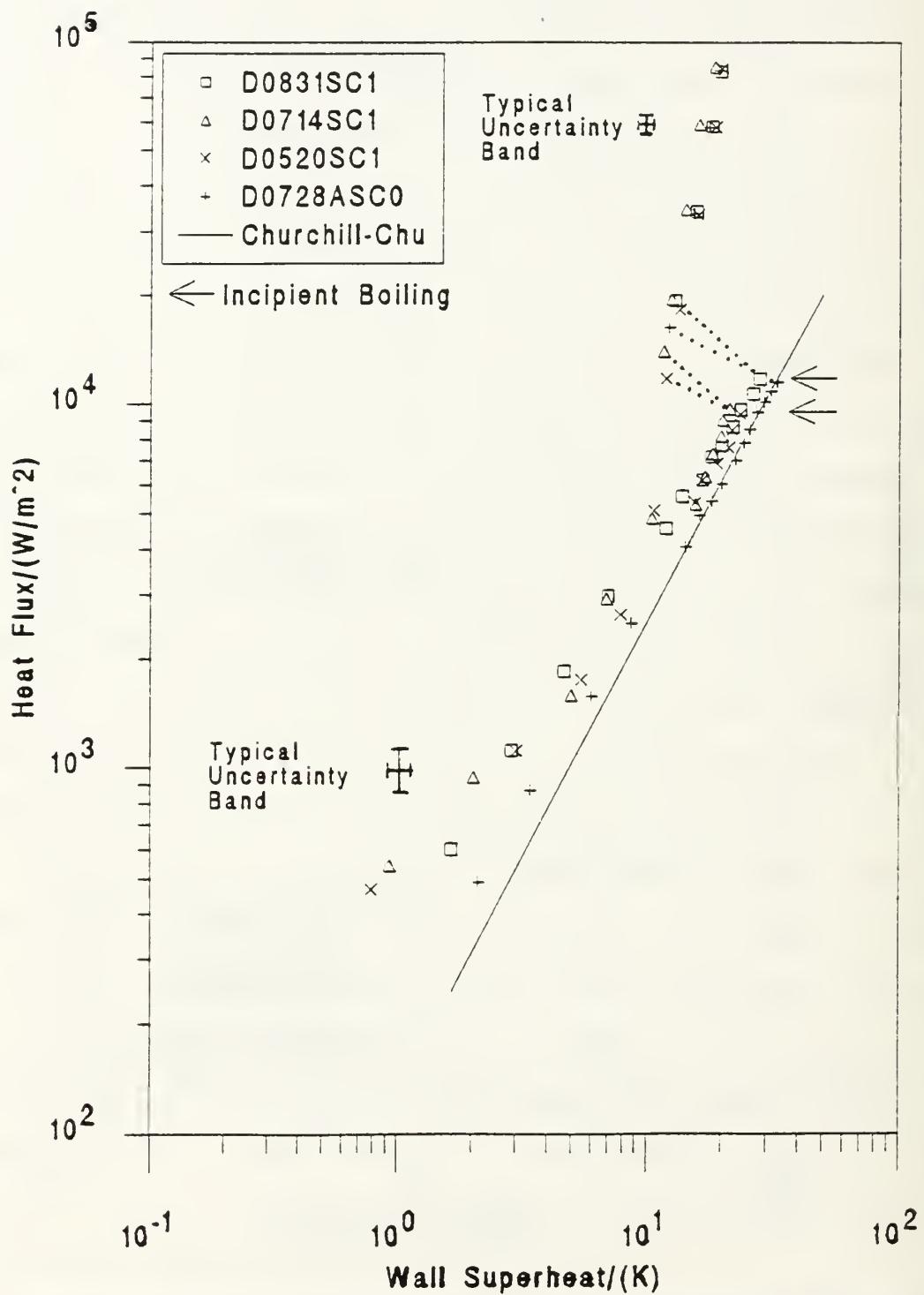
Figure 5.4   Increasing Heat Flux Repeatability Runs using
Smooth Tube Configuration C1 with the Lower Tube Unheated

56

lower tube unheated and a single smooth tube data set (D0728ASC0) from Figure 5.1. The plot shows some scatter of data at low heat fluxes that is attributed to the liquid pool temperature gradients, as discussed previously. Again, good repeatability is found in the mid-range heat flux and boiling regions. In comparison to the single tube data (configuration C0) and the Churchill and Chu correlation [Ref. 9], the upper tube heat transfer performance of the C1 configuration is clearly enhanced in natural convection. This enhancement is probably due to the liquid pool surface being much closer to the upper test tube (approximately 10 mm) when it is position C1, increasing the circulation (i.e., local fluid velocity) around the upper tube and ultimately increasing heat transfer performance of the tube. Lake [Ref. 3], in his comparison of single tube R-114 data to his C1 configuration data, found the same enhancement. He concluded that the lower tube must be modifying the flow over the upper tube. In actuality, it is probably a combination of both the decreased distance to the pool surface and the lower tube modifying the flow over the upper tube that causes the enhancement. From this plot, it was concluded that the program DRPJY was performing properly.

Figure 5.5 is the corresponding decreasing heat flux data runs for Figure 5.4. Good repeatability is again found for the C1 configuration runs. Comparing the single tube data (D0728ASC0 from Figure 5.2) to the C1 configuration data,
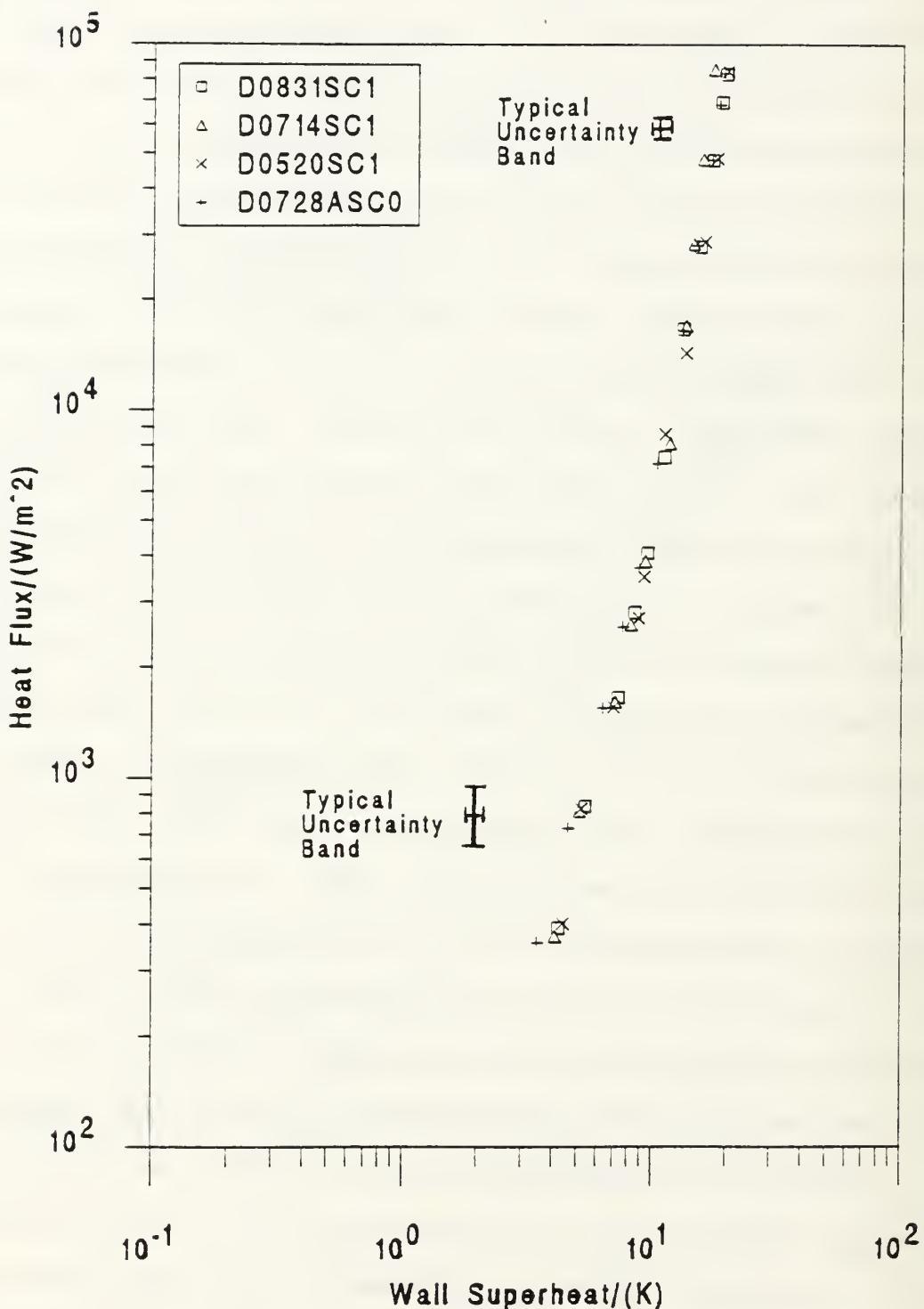
Figure 5.5 Decreasing Heat Flux Repeatability Runs using Smooth Tube Configuration C1 with the Lower Tube Unheated

indicates that in nucleate boiling with decreasing heat fluxes, both tube configurations perform equally well.

Figure 5.6 is the decreasing heat flux repeatability runs using TURBO-B tubes in configuration C1 with the lower tube unheated. Good repeatability is evident. Comparing the single TURBO-B data set (D1012TBC0) from Figure 5.3 to the C1 data, at high heat fluxes both tube configurations perform equally well, as was for the smooth tube case (Figure 5.5). At low heat fluxes (< 8 kW/m^2), the C1 configuration data is to the left of the C0 configuration data, indicating an enhancement due to the addition of the lower tube and moving the test tube closer to the surface of the liquid pool; this was not seen for the smooth tube case (Figure 5.5). As will be discussed later, the addition of a lower tube heat flux, shifts the C1 data curve even more towards the left.

Based on Figures 5.1 through 5.6, the repeatability of the current data and reproducibility of previous single tube work performed by Perry [Ref. 2], is considered satisfactory.

B. INFLUENCE OF THE LOWER TUBE

To investigate the effects of a lower heated tube on an upper tube, five different tube configurations and fixed lower tube heat flux settings were used. The five tube configurations selected were P/D ratios of 2.0, 1.8, 1.5, 1.2

59
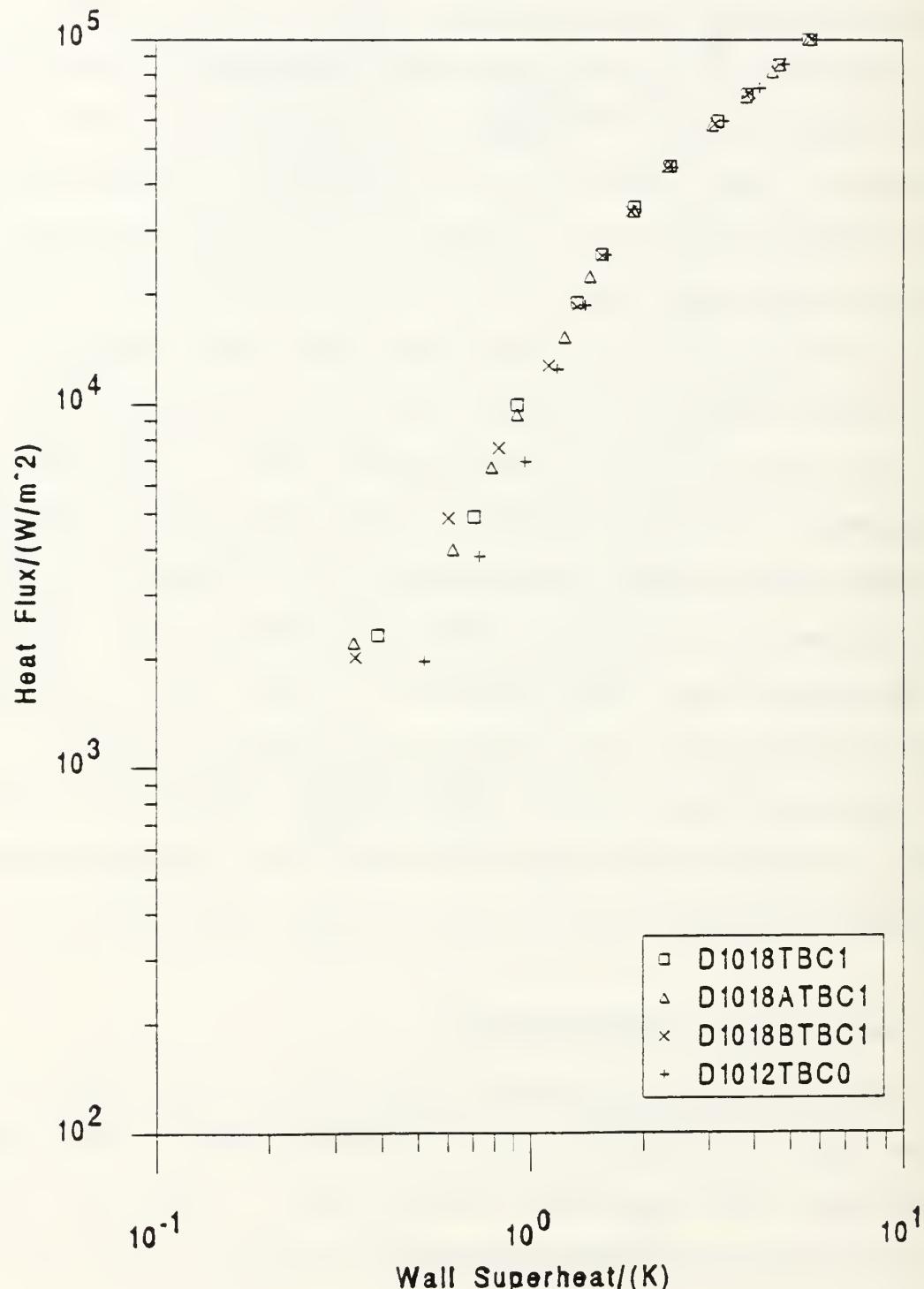
Figure 5.6 Decreasing Heat Flux Repeatability Runs using
TURBO-B Tube Configuration C1 with the Lower Tube Unheated

60

and 1.2 (rotated 30°). P/D of 2.0 was selected because it matches not only the vertical pitch used in naval shipboard flooded evaporators, but also the pitch used in the flooded evaporator bundle apparatus at the Naval Postgraduate School Heat Transfer Laboratory. The fixed lower tube heat flux settings (LTHFS) used were 0, 1, 5, 10 and 20 kW/m^2. In addition to these runs, data runs for each tube configuration were also done using a lower tube heat flux setting that was equal to the upper tube heat flux setting (UTHFS). Finally, at a fixed UTHFS of 5, 10 and 20 kW/m^2, the LTHFS was varied to investigate the influence of the strength of the convection effects from below. For each data run, the same tube surface was used for the upper and lower tube; mixing of the tube types was not allowed. For the smooth tube runs, the upper tube was started in the natural convection region at low heat fluxes, was run up and down through various heat flux settings, and was returned to the natural convection region. For the TURBO-B tubes, only decreasing upper tube heat flux runs were recorded to prevent overlapping/repeating data (the TURBO-B tubes did not enter the natural convection region at low heat fluxes).

To evaluate the effect of a lower heated tube on an upper tube, the data is presented by the effect of changing the P/D ratio for a common LTHFS, the effect of varying the LTHFS for a common P/D ratio and the effect of varying the lower tube heat flux for a fixed upper tube heat flux setting.

61

1. The Effect of Tube Spacing

a. *Smooth Tubes with Lower Tube Unheated*

Figure 5.7 shows the increasing heat flux data taken for the five tube configurations (C1-C5) with the lower tube unheated and the corresponding Churchill and Chu correlation [Ref. 9]. As seen in the repeatability runs, at low heat fluxes the data is shifted to the left of the Churchill-Chu line and as the heat flux is increased, the data tends to approach the Churchill-Chu line up to the incipient boiling point (indicated by arrows). This implies that the circulation occurring within the evaporator enhances the natural convection that occurs from a single tube immersed in an *infinite* expanse of fluid. Following nucleation of the upper tube, the boiling curve for P/D of 1.8 is to the left of the others and appears to be yielding the best heat transfer performance. It is unclear why this is so, because it is so repeatable and the same smooth test tubes were used. Lake [Ref. 3] also found that P/D of 1.8 gave the best heat transfer performance.

Figure 5.8 shows the corresponding decreasing heat flux data for Figure 5.7. With decreasing heat flux, a P/D of 1.8 again provides the best heat transfer performance until the lowest heat flux region, as did Lake's data [Ref. 3].

62
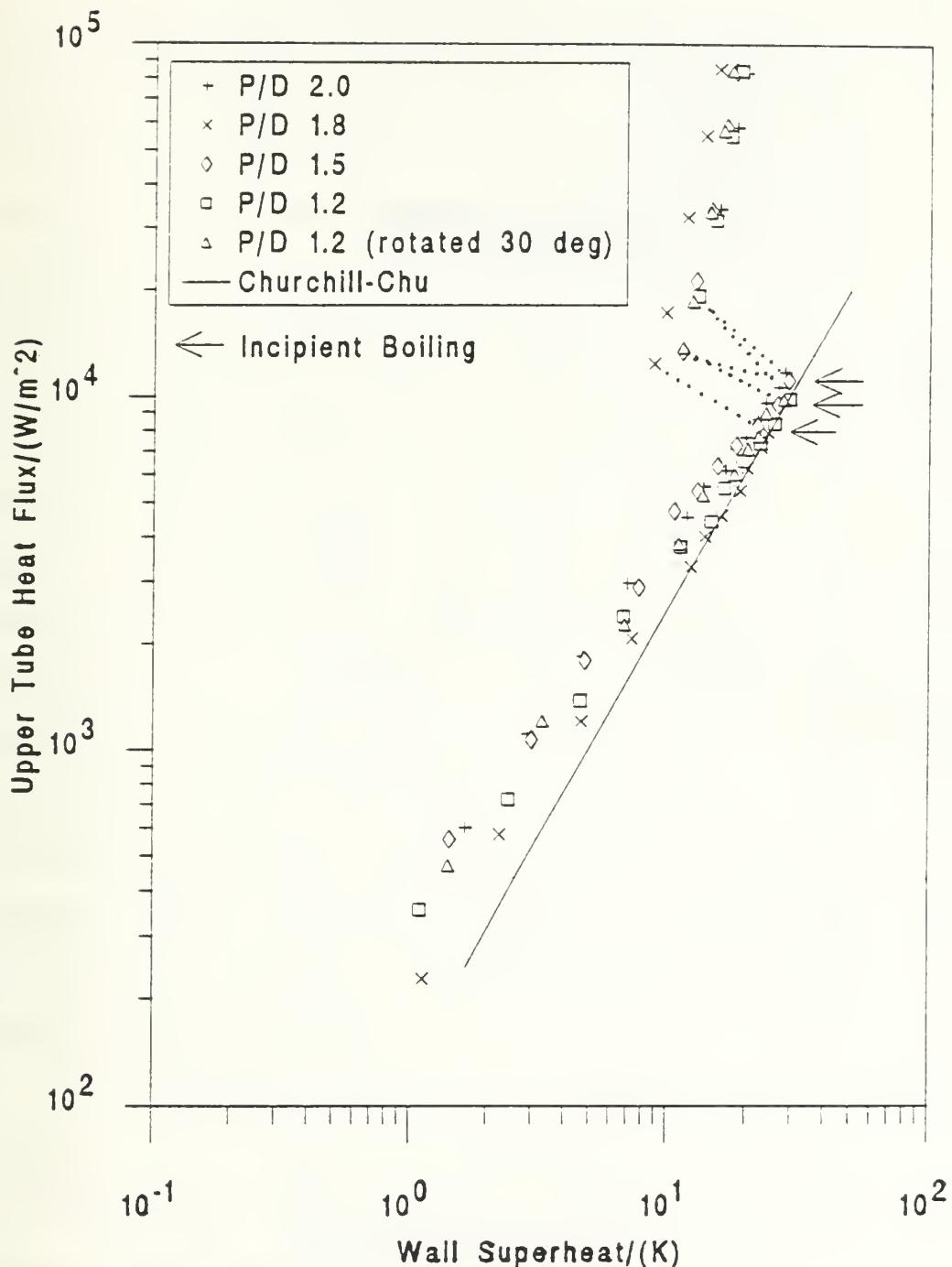
Figure 5.7 Comparison of Smooth Tube P/D Ratios for
Increasing Heat Flux with the Lower Tube Unheated

63
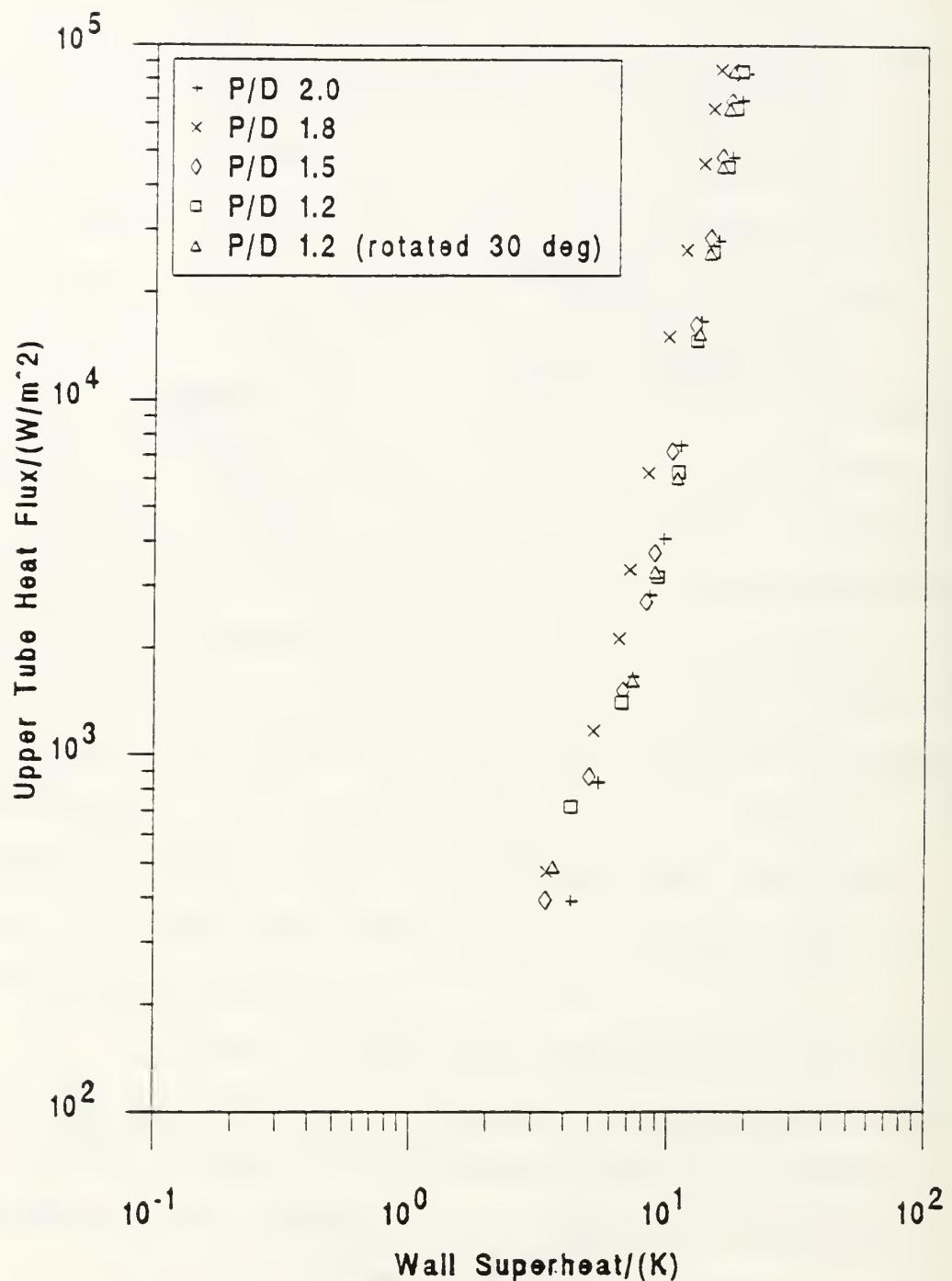
Figure 5.8 Comparison of Smooth Tube P/D Ratios for
Decreasing Heat Flux with the Lower Tube Unheated

64

b. *Smooth Tubes with LTHFS of 1 kW/m^2*

Figure 5.9 shows the increasing heat flux data taken for the five tube configurations (C1-C5) with a heat flux of 1 kW/m^2 on the lower tube. Both the upper and lower tubes for all configurations started in the natural convection region. At low heat fluxes, some scatter is present which becomes smaller as the data approaches the incipient boiling points and tends towards the Churchill and Chu correlation [Ref. 9], as seen previously. Note that the data for a P/D of 1.2 crosses the Churchill-Chu line and appears to nucleate earlier than the others. For this small spacing, the heated plume from the lower tube can actually reduce natural convection from the top tube since the local ambient pool temperature is increased. This creates a larger wall temperature and a larger wall superheat (Twall - Tsat). After nucleation, a P/D of 1.8 again provides better heat transfer in the boiling region than the other P/D ratios. This trend suggests that in the boiling region the enhancement provided by a P/D of 1.8 is due to the tube spacing itself and not from heating the lower tube.

Figure 5.10 is the decreasing heat flux data for to Figure 5.9. A P/D of 1.8 provides the best heat transfer performance until approximately 4 kW/m^2, which is where the boiling curves seem to merge. With a LTHFS of 1 kW/m^2, it appears to force the decreasing boiling curves to merge at a
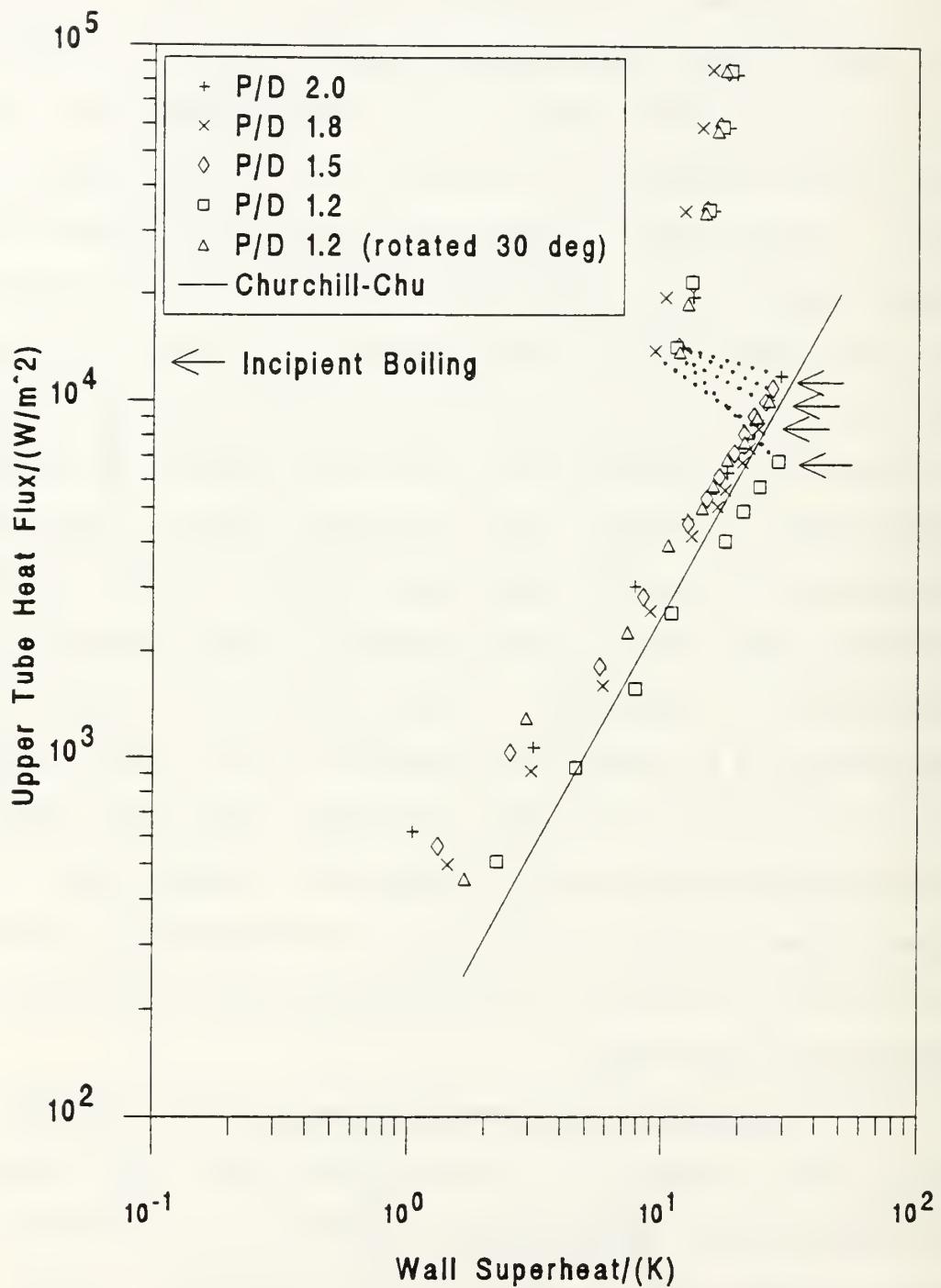
Figure 5.9 Comparison of Smooth Tube P/D Ratios for
Increasing Heat Flux with 1 kW/m² on the Lower Tube

66
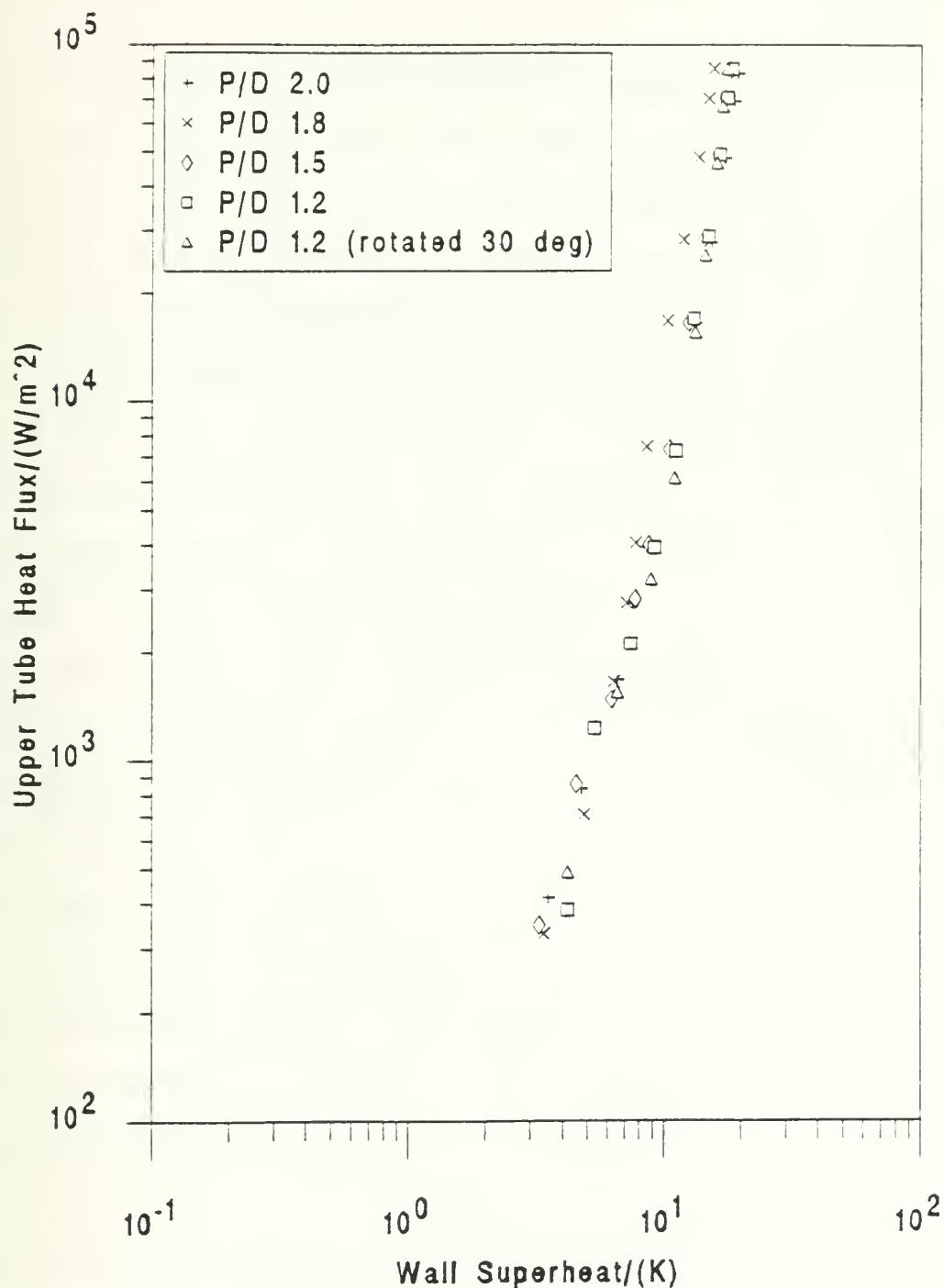
Figure 5.10 Comparison of Smooth Tube P/D Ratios for Decreasing Heat Flux with 1 kW/m^2 on the Lower Tube

67

higher heat flux (4 kW/m²) than with the lower tube unheated (< 1 kW/m²).

c. Smooth Tubes with LTHFS of 5 kW/m²

Figure 5.11 shows the increasing heat flux data taken for the five tube configurations (C1-C5) with 5 kW/m² on the lower tube. Both upper and lower tubes for all the configurations started in the natural convection region. At low heat fluxes, the data is to the left of the Churchill and Chu correlation [Ref. 9], as seen in Figures 5.7 and 5.9. As the heat flux is increased, some interesting things happen. The data for a P/D of 1.2 (rotated 30°) quickly crosses the Churchill-Chu line and begins to parallel it, then nucleates at a low heat flux of about 3 kW/m² . This is believed to be an anomaly and not an effect. Of the remaining P/D ratios, 1.8 is the only one to tend toward the Churchill-Chu line with increasing heat flux. The P/D ratios of 2.0, 1.5 and 1.2 seem to parallel the Churchill-Chu line, probably due to the LTHFS intensifying the forced convection around the upper tube. In all cases, the lower tube remained in natural convection until the upper tube nucleated. Once the upper tube nucleated, the lower tube also nucleated. In the boiling region, a P/D of 1.8 again gave the best enhancement.

Figure 5.12 is the decreasing heat flux data for Figure 5.11. Above 10 kW/m², P/D of 1.8 is clearly providing
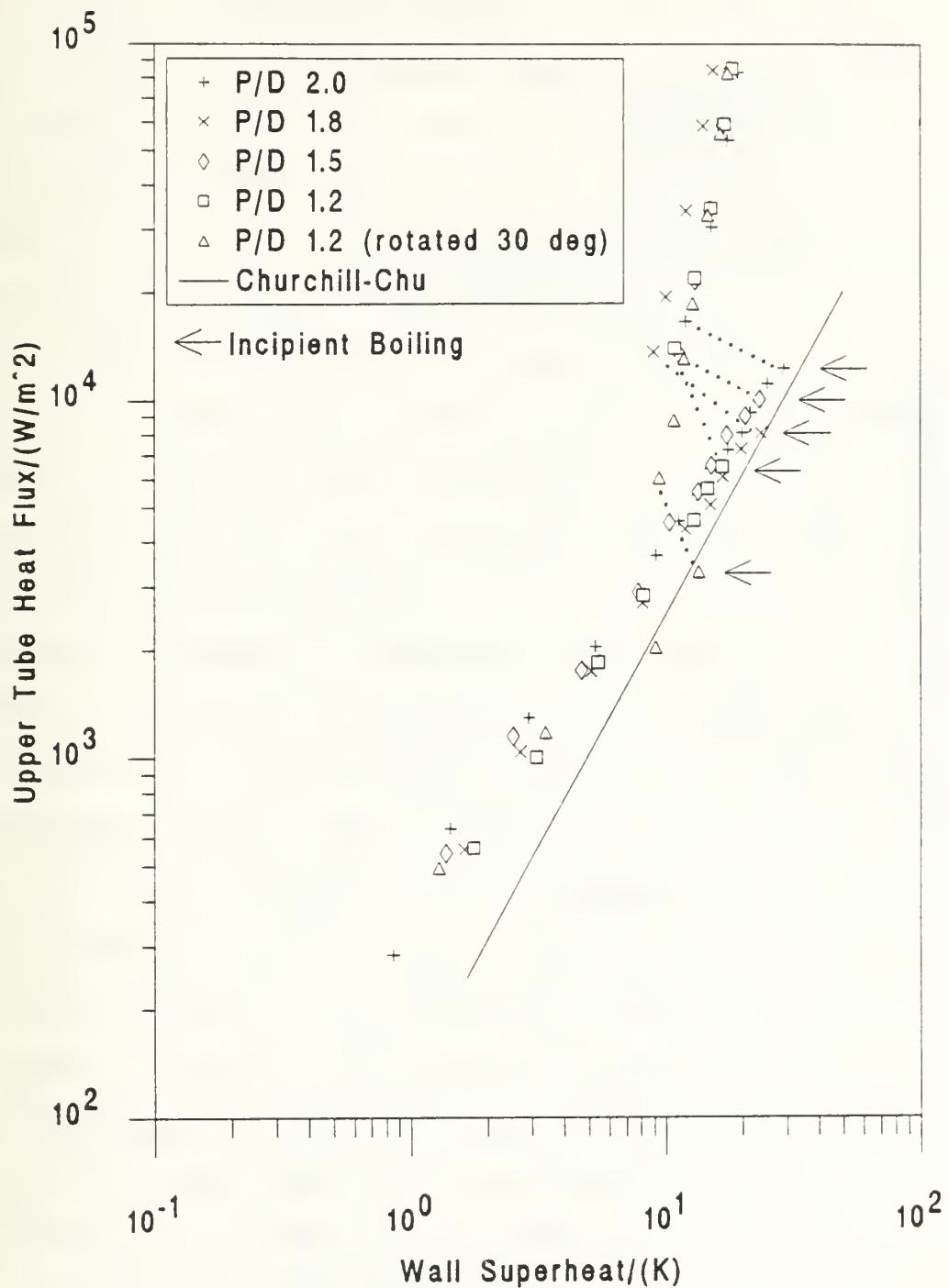
Figure 5.11 Comparison of Smooth Tube P/D Ratios for
Increasing Heat Flux with 5 kW/m² on the Lower Tube
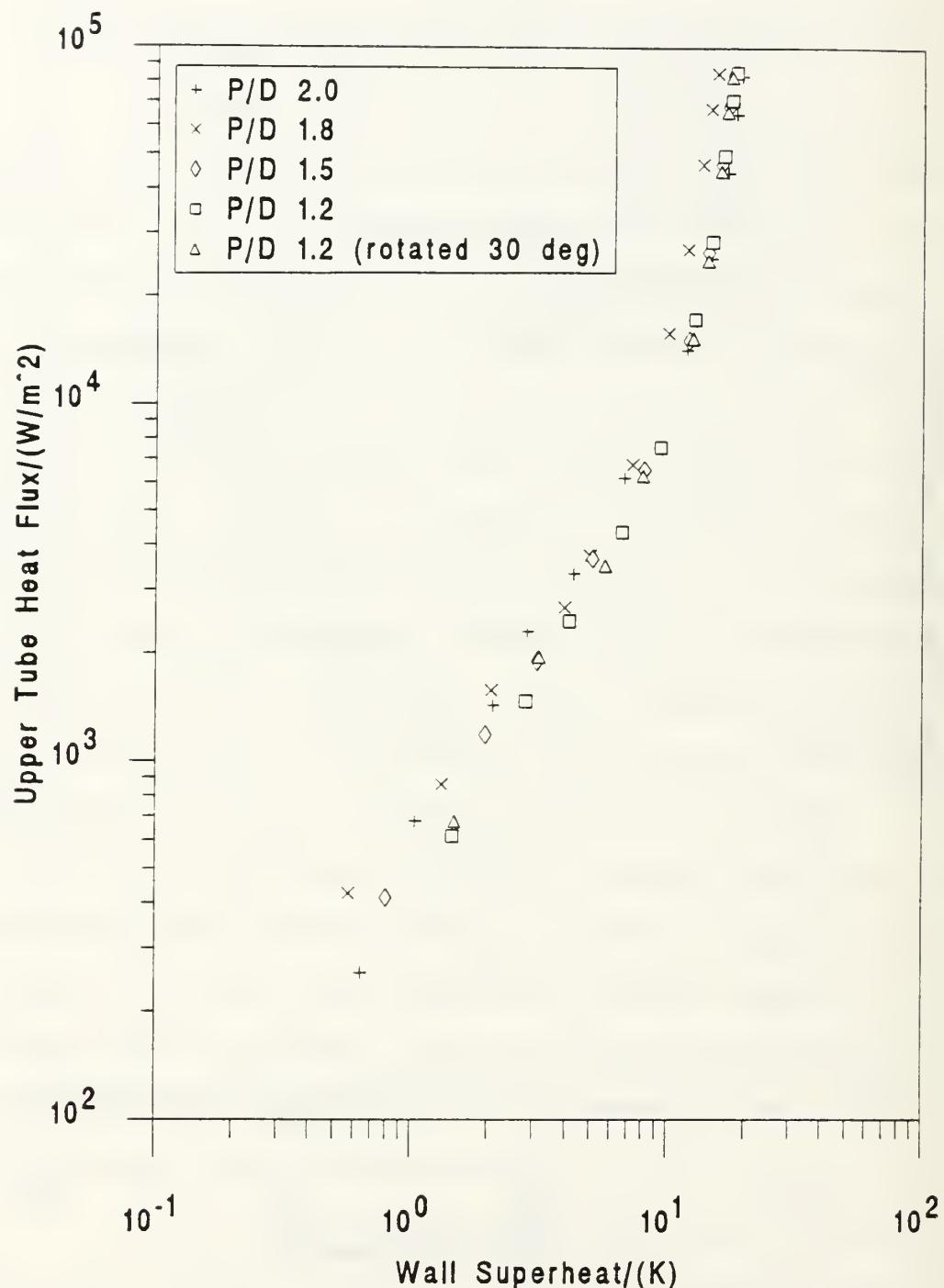
Figure 5.12   Comparison of Smooth Tube P/D Ratios for
Decreasing Heat Flux with 5 kW/m^2 on the Lower Tube

70

the best heat transfer. Below 10 kW/m², the upper tube is returning to natural convection, but the lower tube is still nucleating. The bubbles departing the lower tube impinge upon the upper tube causing a significant increase in heat transfer performance, from bubble sweeping, compared to the data for a LTHFS of 0 and 1 kW/m². Also, a LTHFS of 5 kW/m² eliminates any upper tube hysteresis effect.

d. *Smooth Tubes with LTHFS of 10 kW/m²*

Figure 5.13 shows the increasing heat flux data taken for the five tube configurations (C1-C5) with 10 kW/m² on the lower tube. For this LTHFS, the lower tube nucleated at the start of the run for a P/D of 1.5, but the upper tube remained in natural convection. The effect of the bubbles from the lower tube impacting and sweeping over the upper tube is seen to significantly enhance the heat transfer performance of the upper tube in the low heat flux regions. For the other P/D ratios, the incipient boiling points were very random; at the largest spacing, nucleation occurred quickly, whereas at the smallest spacing, nucleation was delayed. Possibly, the largest spacing (P/D of 2.0) allowed the heated plume from the lower tube to thin the boundary layer around the upper tube, but the closest spacing (P/D of 1.2) enabled the heated plume to 'skirt' around the upper tube and not disturb the upper tube boundary layer as much, delaying the point of incipience. Again, once the upper tube

71
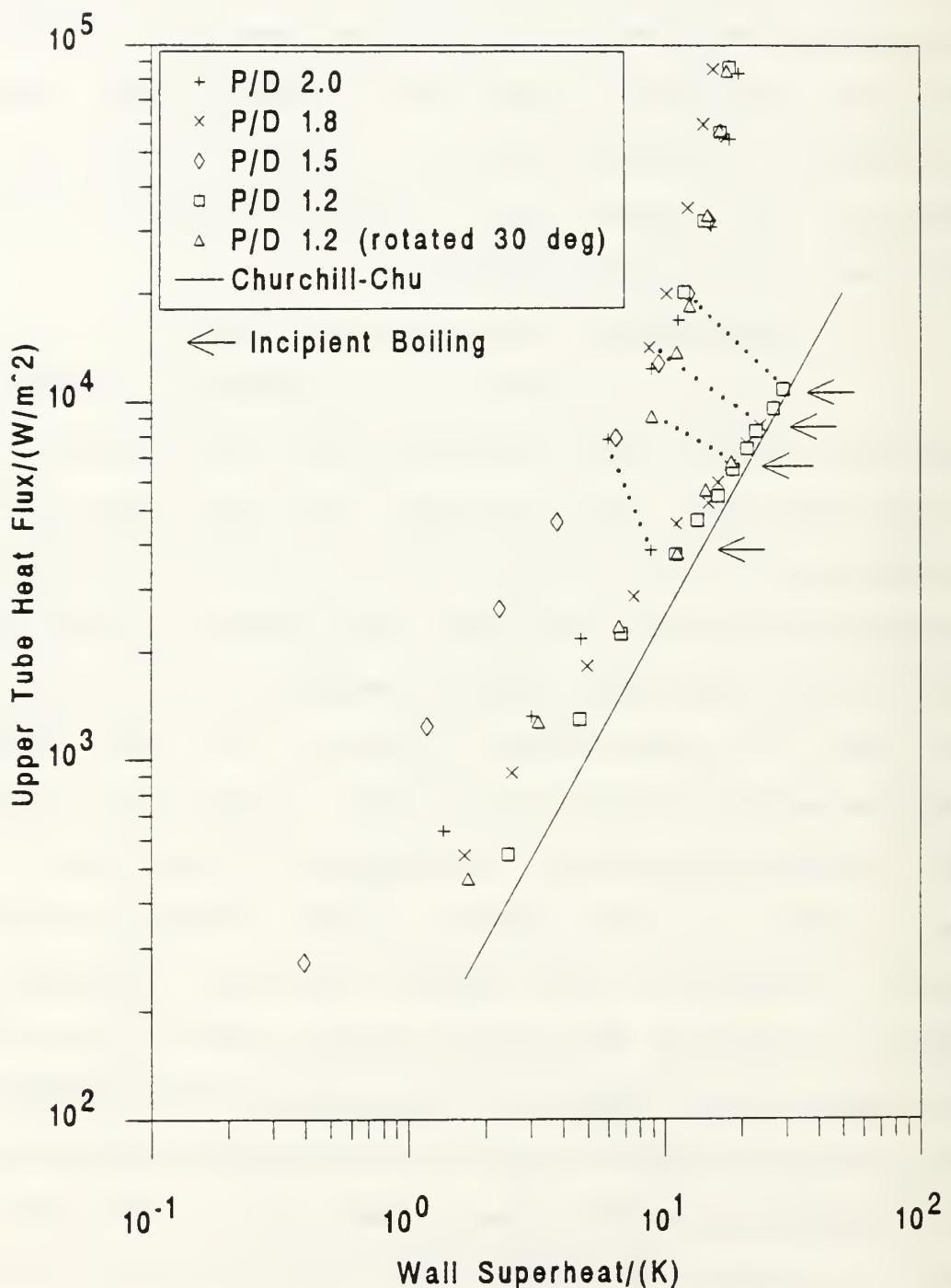
Figure 5.13 Comparison of Smooth Tube P/D Ratios for
Increasing Heat Flux with 10 kW/m^2 on the Lower Tube

72

nucleated, the lower tube also nucleated shortly thereafter. In the fully developed nucleate boiling region, a P/D of 1.8 still gives the best performance.

Figure 5.14 is the decreasing heat flux data for Figure 5.13. A P/D of 1.8 provided the best heat transfer until the heat flux was lowered to about 15 kW/m^2, where no gain over the other P/D ratios is noticed. This concurs with the findings of Lake [Ref. 3]. Below 10 kW/m^2, the nucleating lower tube is definitely enhancing the upper tube performance for all P/D ratios, although, the P/D of 1.2 (rotated 30°) is slightly to the right of the other curves. This is probably caused by the angular offset of the upper tube, not allowing the bubbles from the lower tube to directly impinge upon the upper tube. Therefore, a 30° rotation slightly decreases the performance of the upper tube compared to an in-line tube configuration.

e. *Smooth Tubes with LTHFS of 20 kW/m²*

Figure 5.15 shows the increasing heat flux data taken for the five tube configurations (C1-C5) with 20 kW/m^2 on the lower tube. In each run, the lower tube was nucleating at the beginning of the run and remained nucleating throughout. The only effect from P/D spacing is noticed above 20 kW/m^2 where a P/D of 1.8 again provides the best performance.
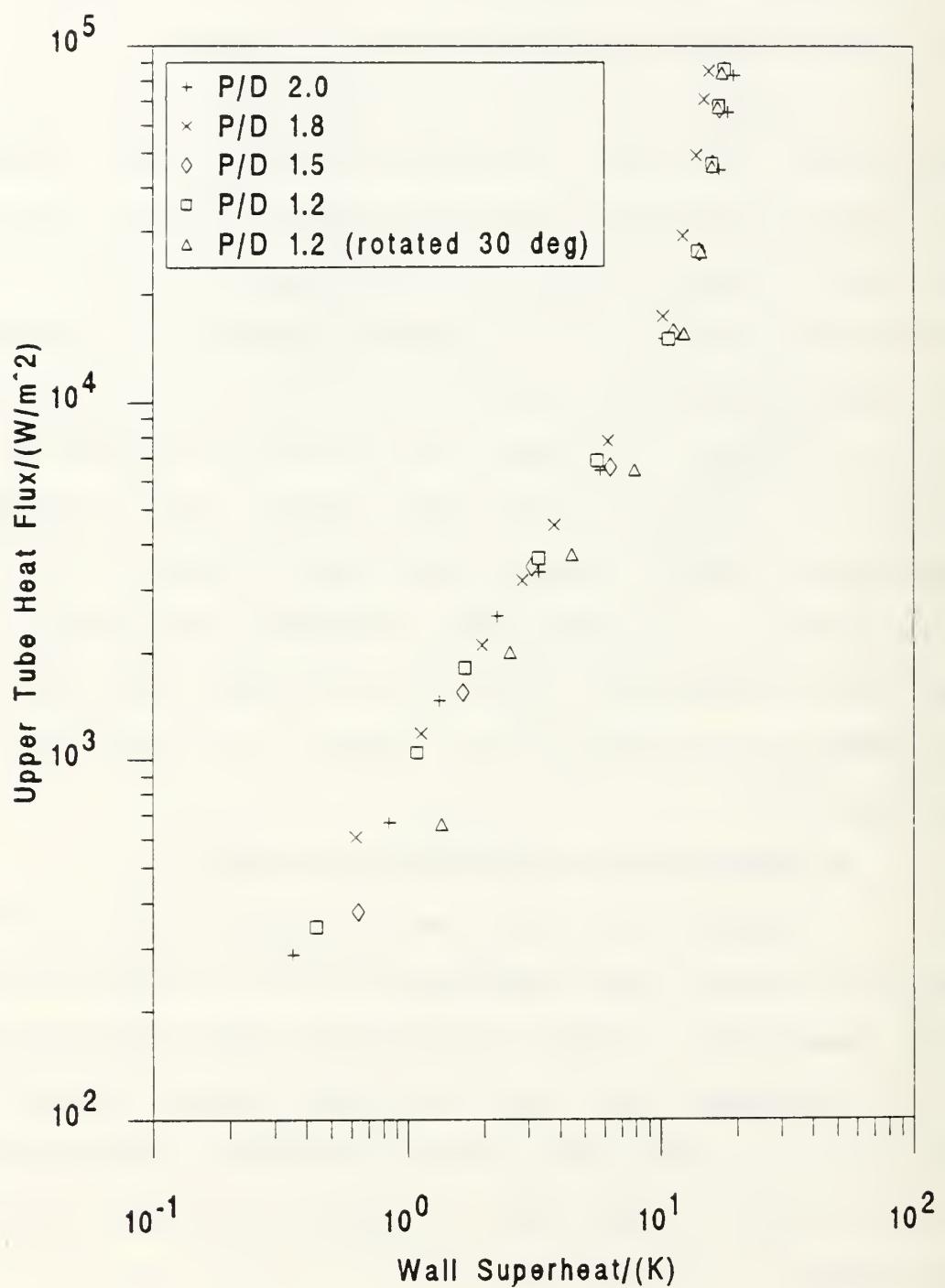
Figure 5.14 Comparison of Smooth Tube P/D Ratios for
Decreasing Heat Flux with 10 kW/m² on the Lower Tube

74
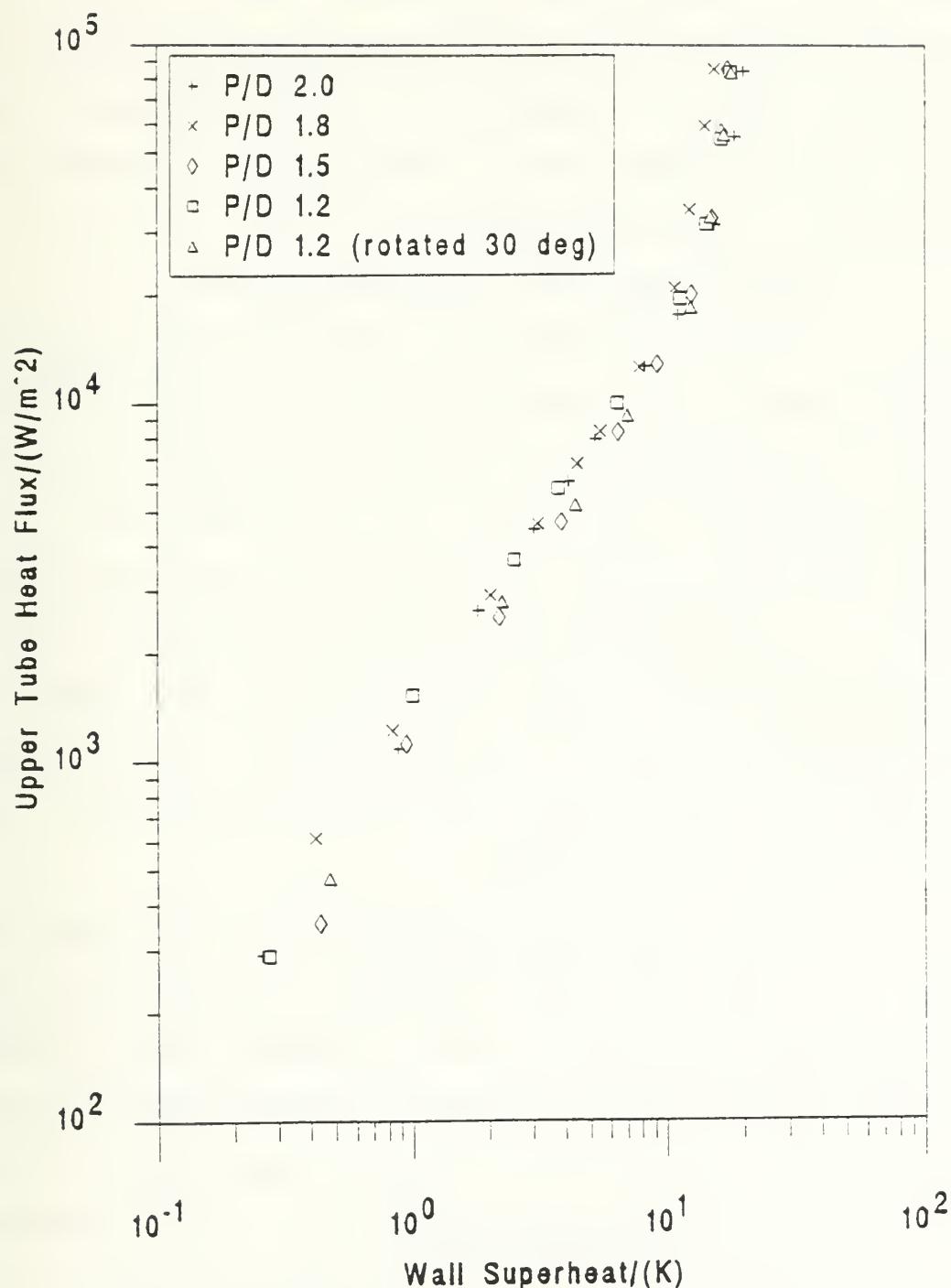
Figure 5.15 Comparison of Smooth Tube P/D Ratios for
Increasing Heat Flux with 20 kW/m^2 on the Lower Tube

75

Figure 5.16 is the decreasing heat flux data for Figure 5.15. Again, below 20 kW/m^2, only a P/D of 1.2 (rotated 30°) drops slightly below the other curves at mid-range heat fluxes. It appears that this LTHFS enables more bubbles from the lower tube to impinge upon the upper tube, compared to a LTHFS of 10 kW/m^2.

f. Smooth Tubes with UTHFS equal LTHFS

Figure 5.17 shows the increasing heat flux data taken for the five tube configurations (C1-C5) with the UTHFS equal to the LTHFS throughout the entire length of the run. At the beginning of all the runs, both tubes were in the natural convection region. In the natural convection region, a P/D of 1.2 (rotated 30°) is the only configuration that is very close to the Churchill and Chu correlation [Ref. 9]. This was not expected nor can be explained. Again, a random incipient point was obtained and in the boiling region, a P/D of 1.8 was the best performer.

Figure 5.18 is the decreasing heat flux data for Figure 5.17. Above 20 kW/m^2, a P/D of 1.8 still provides the best performance and below 20 kW/m^2 it appears that as the P/D decreases, so does the enhancement of the upper tube. Between 9 and 5 kW/m^2, it's believed that the tubes shift from the boiling region back to natural convection. This may cause the decrease of enhancement because, as speculated earlier, as the
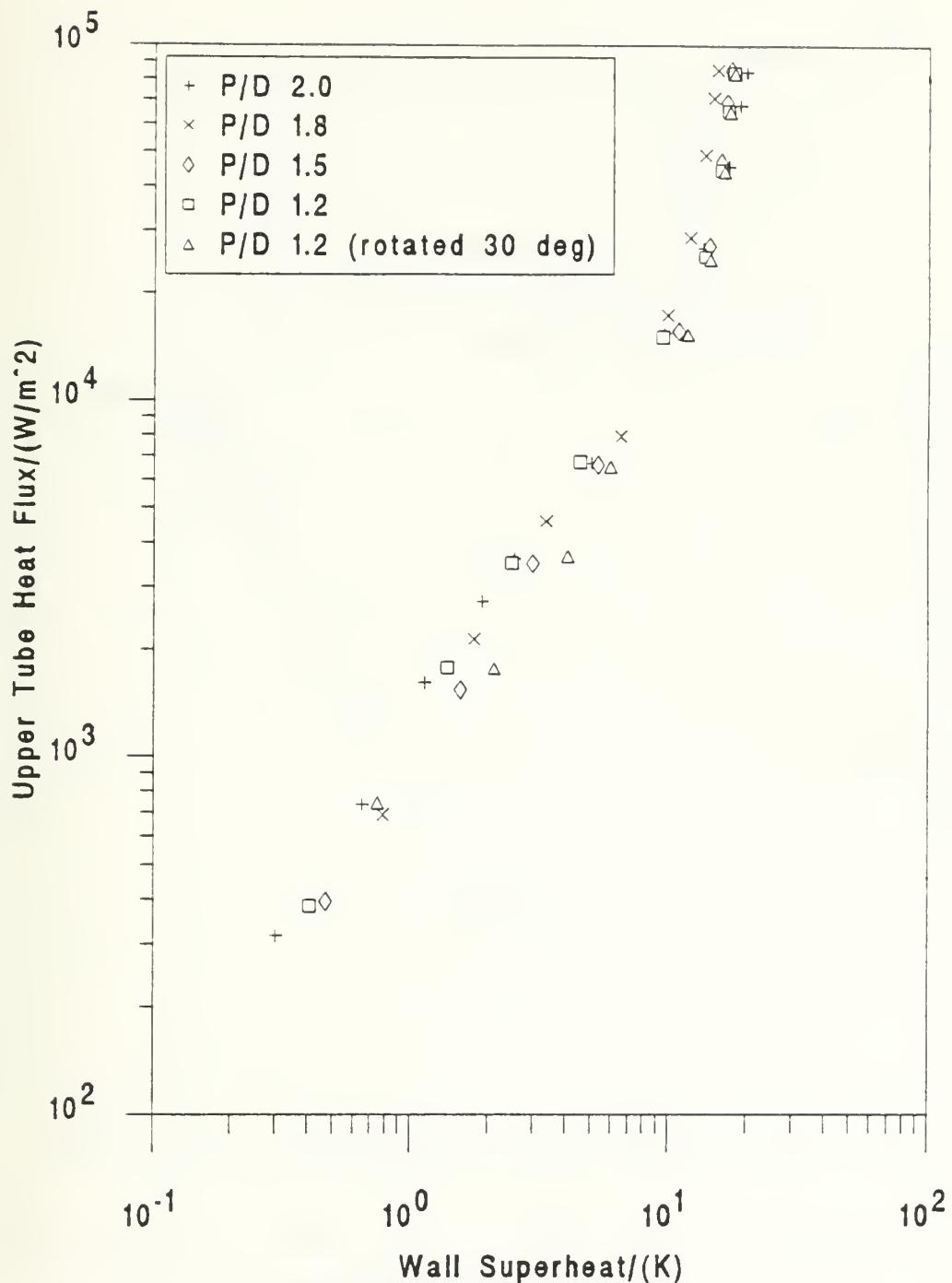
Figure 5.16 Comparison of Smooth Tube P/D Ratios for Decreasing Heat Flux with 20 kW/m² on the Lower Tube
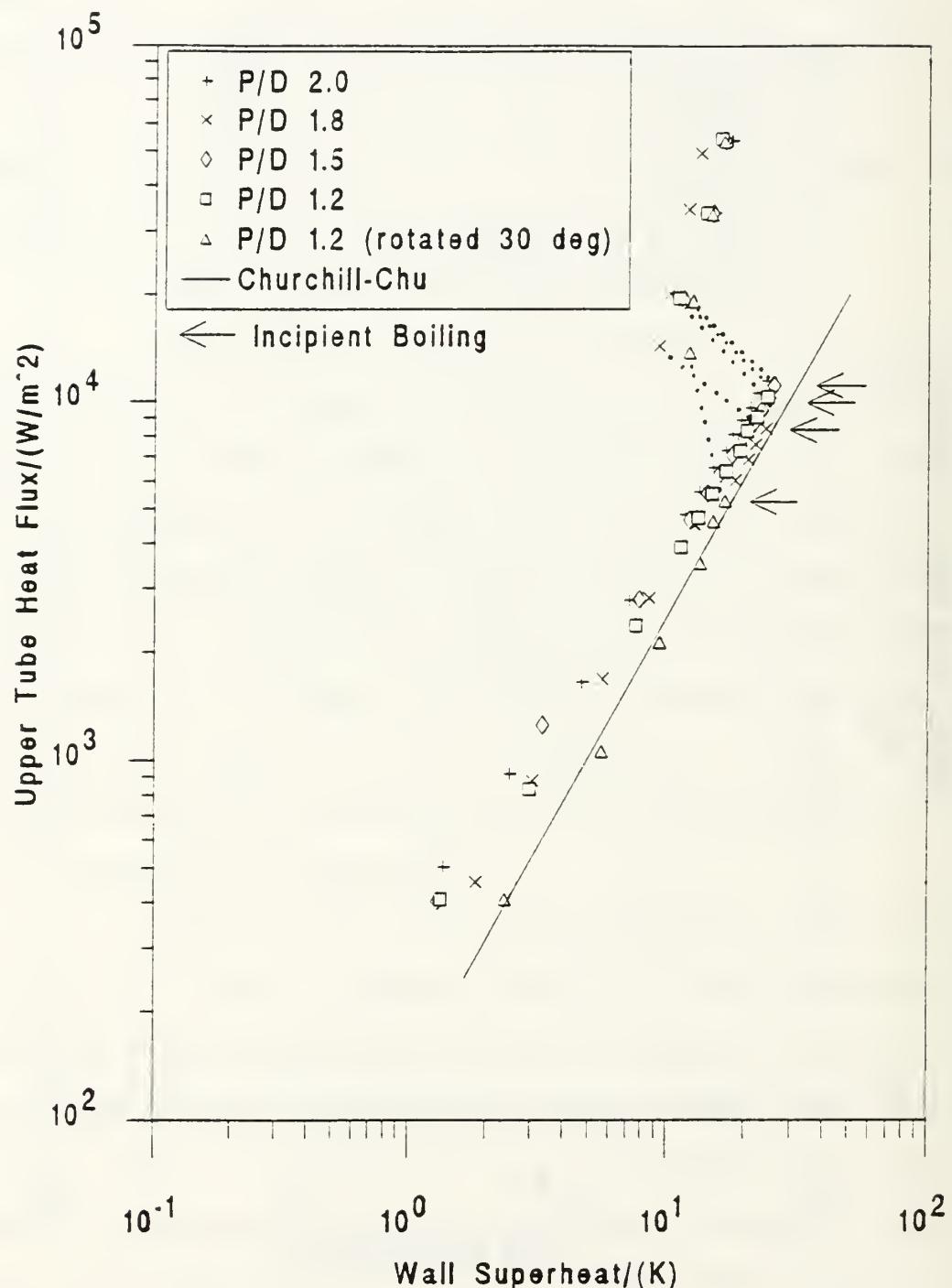
Figure 5.17   Comparison of Smooth Tube P/D Ratios for
Increasing Heat Flux with UTHFS equal to LTHFS

78
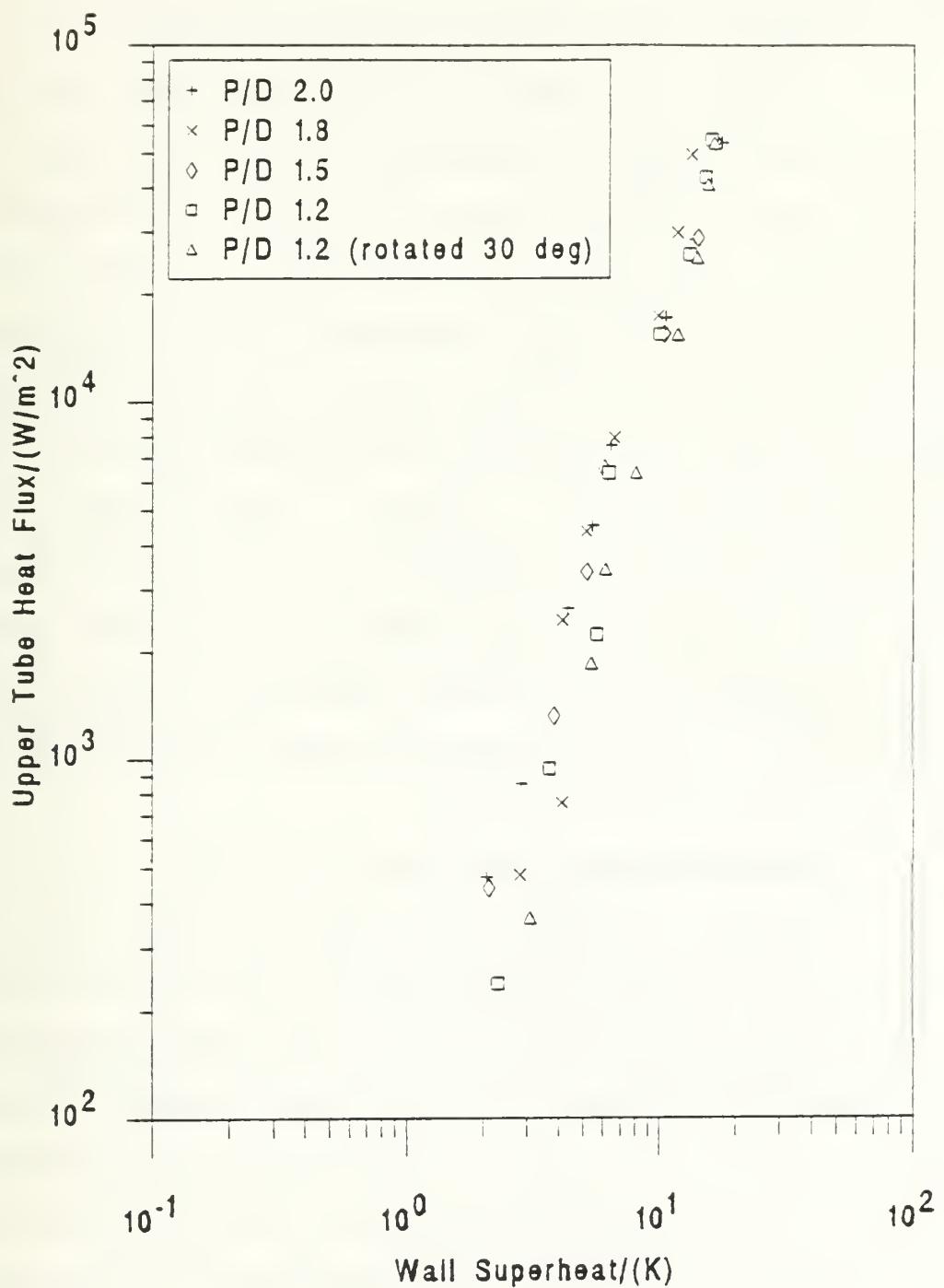
Figure 5.18 Comparison of Smooth Tube P/D Ratios for
Decreasing Heat Flux with UTHFS equal to LTHFS

79

P/D is decreased so too are the convection effects from the lower tube.

g. TURBO-B Tubes with Lower Tube Unheated

Figure 5.19 shows the decreasing heat flux data taken for the five tube configurations (C1-C5) with lower tube unheated. At the start of each run, an undetermined amount of nucleation was occurring from the lower tube due to the vigorous boiling action off the upper tube at the run start heat flux (100 kW/m^2). A very consistent boiling curve above 10 kW/m^2 indicates that there is no enhancement from the lower tube at any P/D ratio. Below 5 kW/m^2, the rotated configuration data agrees well with the single tube data in Figure 5.3. This indicates that the lower tube is not modifying the flow around the upper tube and the upper tube is performing as a single tube which provides less heat transfer than the in-line configurations.

h. TURBO-B Tubes with LTHFS of 1 kW/m^2

Figure 5.20 shows the decreasing heat flux data taken for the five tube configurations (C1-C5) with 1 kW/m^2 on the lower tube. At the start of each run, both the upper and lower tubes were nucleating. Very little change is noticed between Figures 5.19 and 5.20. Above 20 kW/m^2, the plots are identical. Below 10 kW/m^2, the LTHFS of 1 kW/m^2 moved the data curves slightly to the left. This indicates that the greater
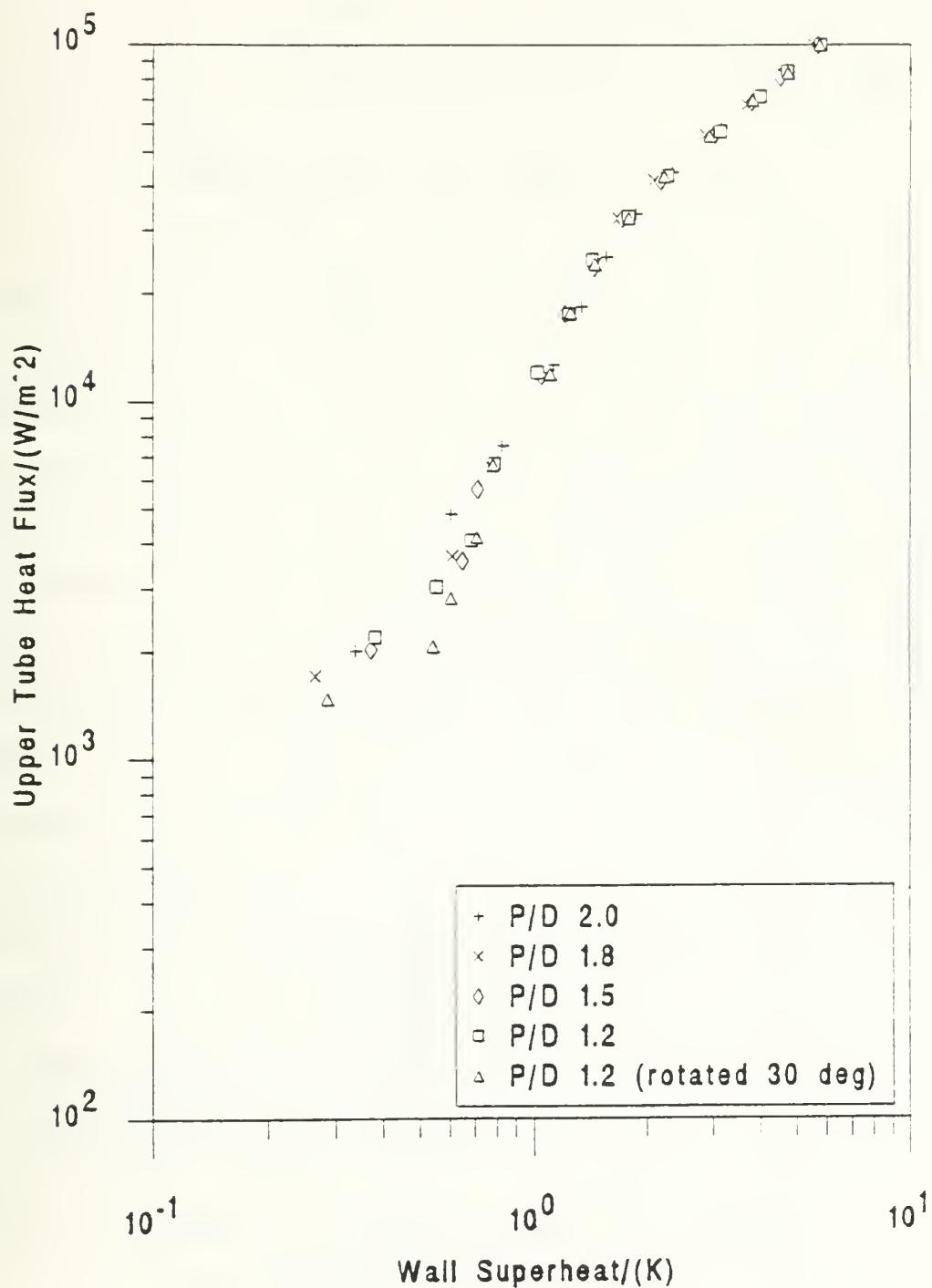
Figure 5.19 Comparison of TURBO-B Tube P/D Ratios for
Decreasing Heat Flux with the Lower Tube Unheated

81
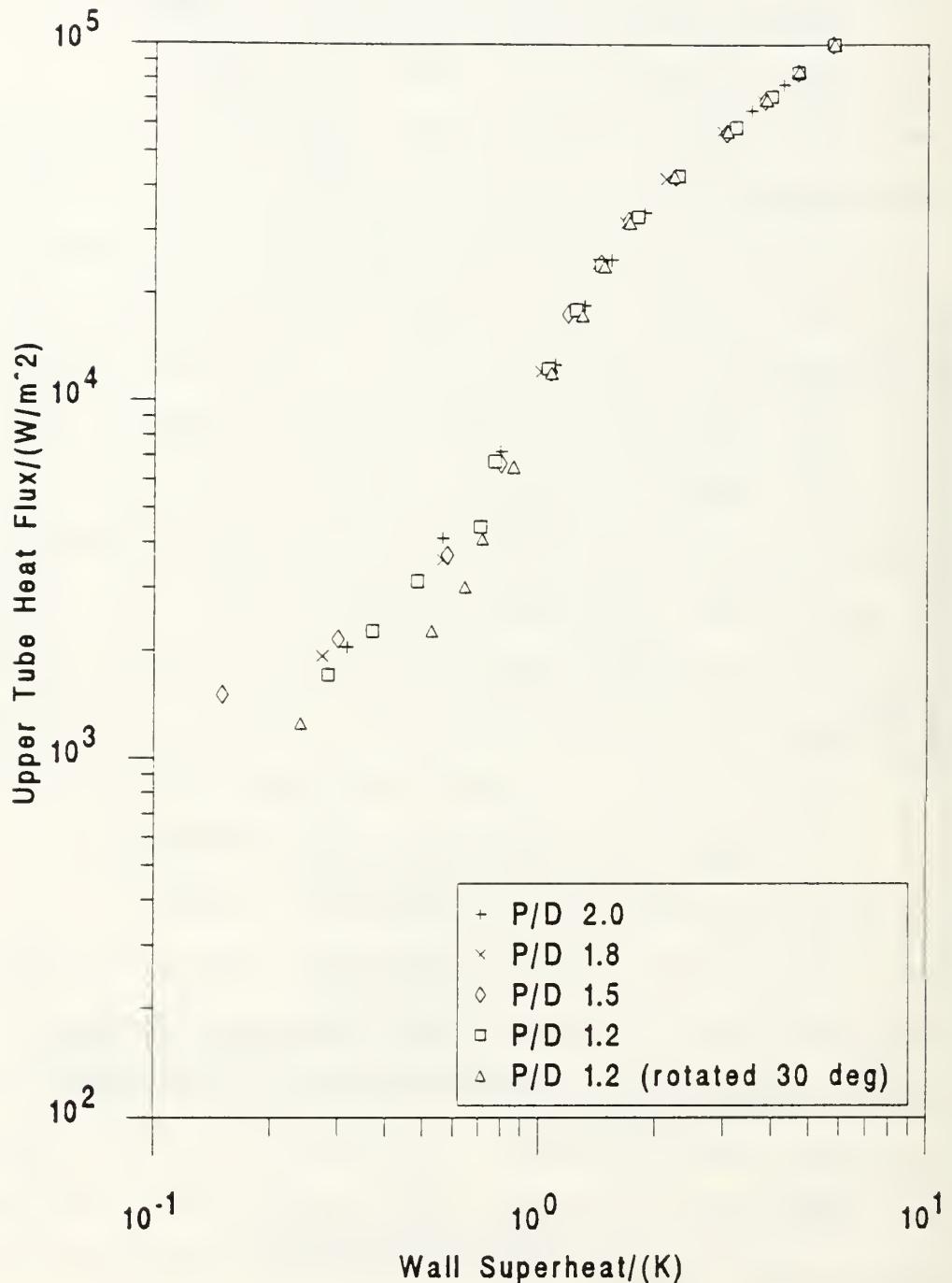
Figure 5.20   Comparison of TURBO-B Tube P/D Ratios for
Decreasing Heat Flux with 1 kW/m^2 on the Lower Tube

82

the LTHFS, the more enhanced the mid-range and lower heat flux region becomes. As seen in the previous figure, a P/D of 1.2 (rotated 30°) is again less enhanced than the other P/D ratios.

i. *TURBO-B Tubes with LTHFS of 5 kW/m²*

Figure 5.21 shows the decreasing heat flux data taken for the five tube configurations (C1-C5) with 5 kW/m² on the lower tube. At the start of each run, both tubes were vigorously boiling. Above 20 kW/m², the data is consistent with the two previous plots, but below 10 kW/m², a definite separation between a P/D of 1.2 (rotated 30°) and the other P/D ratios is seen. Also for heat fluxes < 10 kW/m², the in-line configurations provide better heat transfer than the same configurations seen in Figure 5.20. This indicates that as LTHFS increases, more bubbles depart the lower tube and increase the upper tube heat transfer performance for the in-line configurations. For the rotated configuration, the bubbles must be departing the lower TURBO-B tube differently (compare to a lower smooth tube) and are not impinging upon the upper TURBO-B tube. This explains the approximately 40 - 45% decrease in heat transfer performance for the rotated configuration compared to the in-line configurations.

j. *TURBO-B Tubes with LTHFS of 10 kW/m²*

Figure 5.22 shows the decreasing heat flux data taken for the five tube configurations (C1-C5) with 10 kW/m²
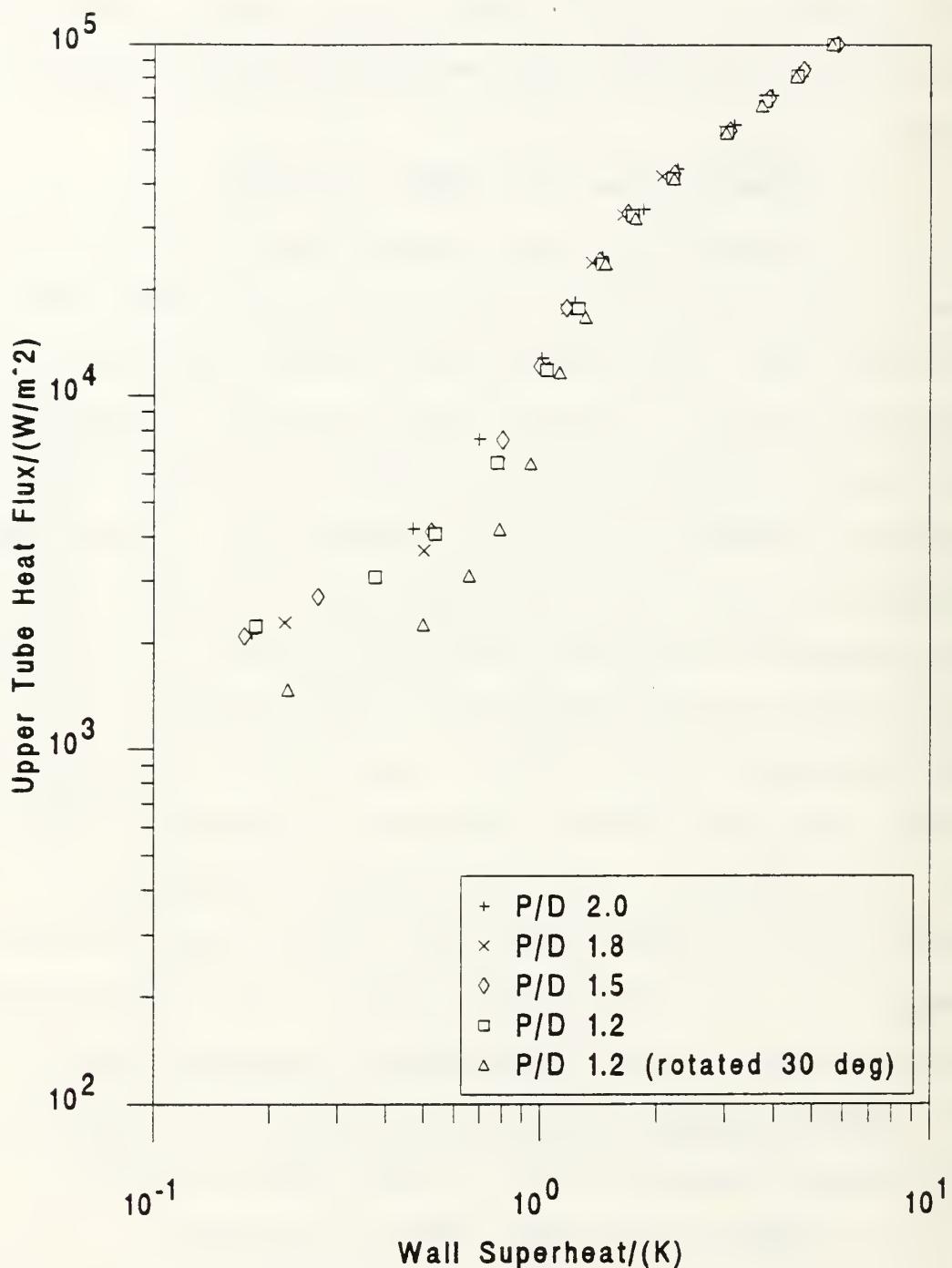
Figure 5.21 Comparison of TURBO-B Tube P/D Ratios for
Decreasing Heat Flux with 5 kW/m^2 on the Lower Tube

84
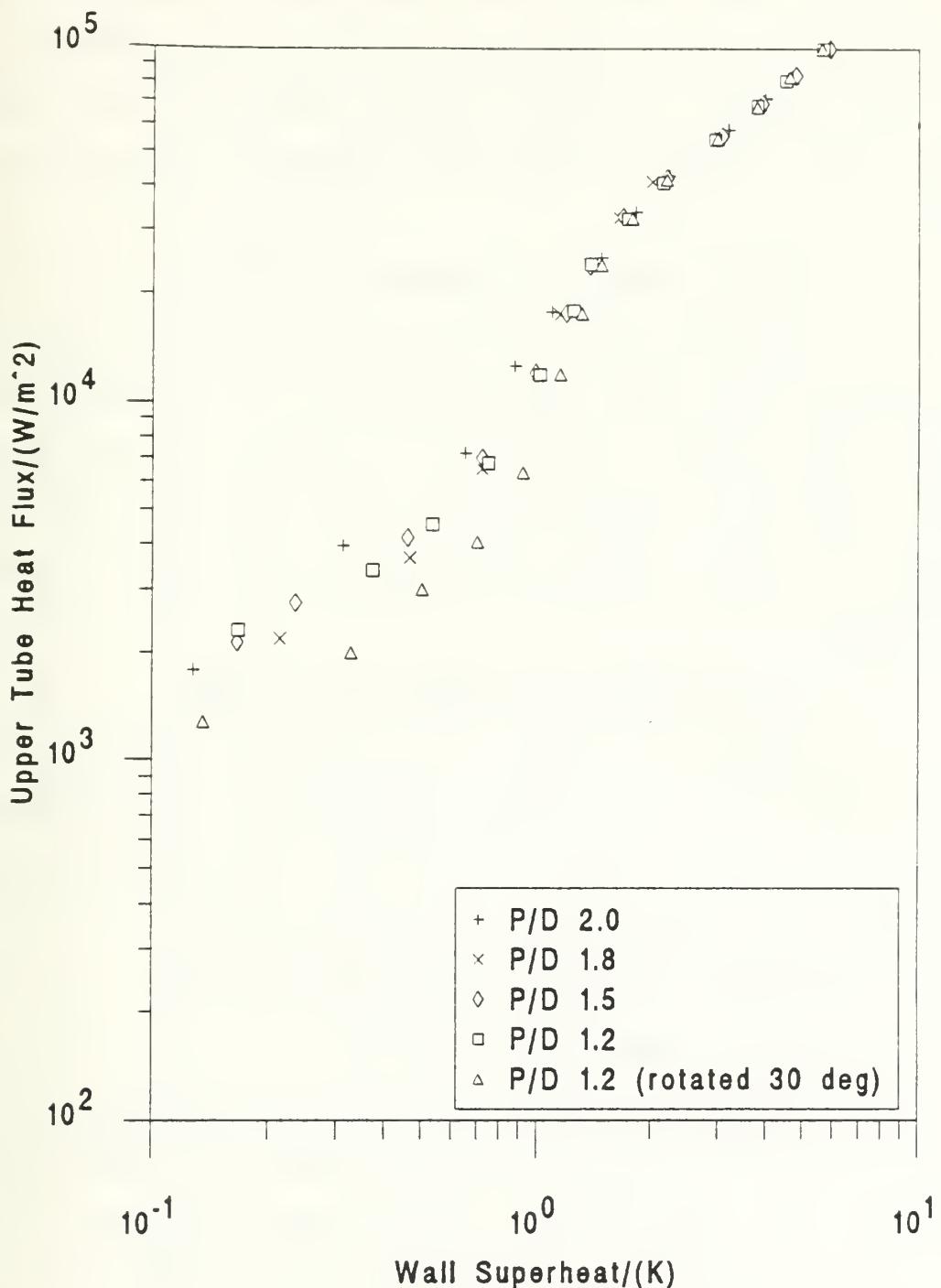
Figure 5.22 Comparison of TURBO-B Tube P/D Ratios for
Decreasing Heat Flux with 10 kW/m^2 on the Lower Tube

on the lower tube. Again, both tubes were nucleating at the beginning of each run. There are no obvious changes above 20 kW/m^2 from the previous plots. Below 10 kW/m^2, all the curves seem to have shifted to the left compared to the previous case.

k. TURBO-B Tubes with LTHFS of 20 kW/m^2

Figure 5.23 shows the decreasing heat flux data taken for the five tube configurations (C1-C5) with 20 kW/m^2 on the lower tube. Figures 5.22 and 5.23 show similar results, therefore, increasing the LTHFS from 10 to 20 kW/m^2 provides a small change in upper tube heat transfer performance.

l. TURBO-B Tubes with UTHFS equal LTHFS

Figure 5.24 shows the decreasing heat flux data taken for the five tube configurations (C1-C5) with the UTHFS equal to the LTHFS. There is not much change in this plot relative to the trend set by the previous plots.

2. The Effect of a Fixed Lower Tube Heat Flux

a. Smooth Tubes with P/D of 2.0

Figure 5.25 shows the increasing heat flux data taken for a P/D of 2.0 at five different heat flux settings on the lower tube. The Churchill and Chu correlation [Ref. 9] is also shown for comparison. For a LTHFS of 20 kW/m^2, the lower tube had nucleated immediately at the beginning of the run and remained nucleating for the length of the run. All other

86
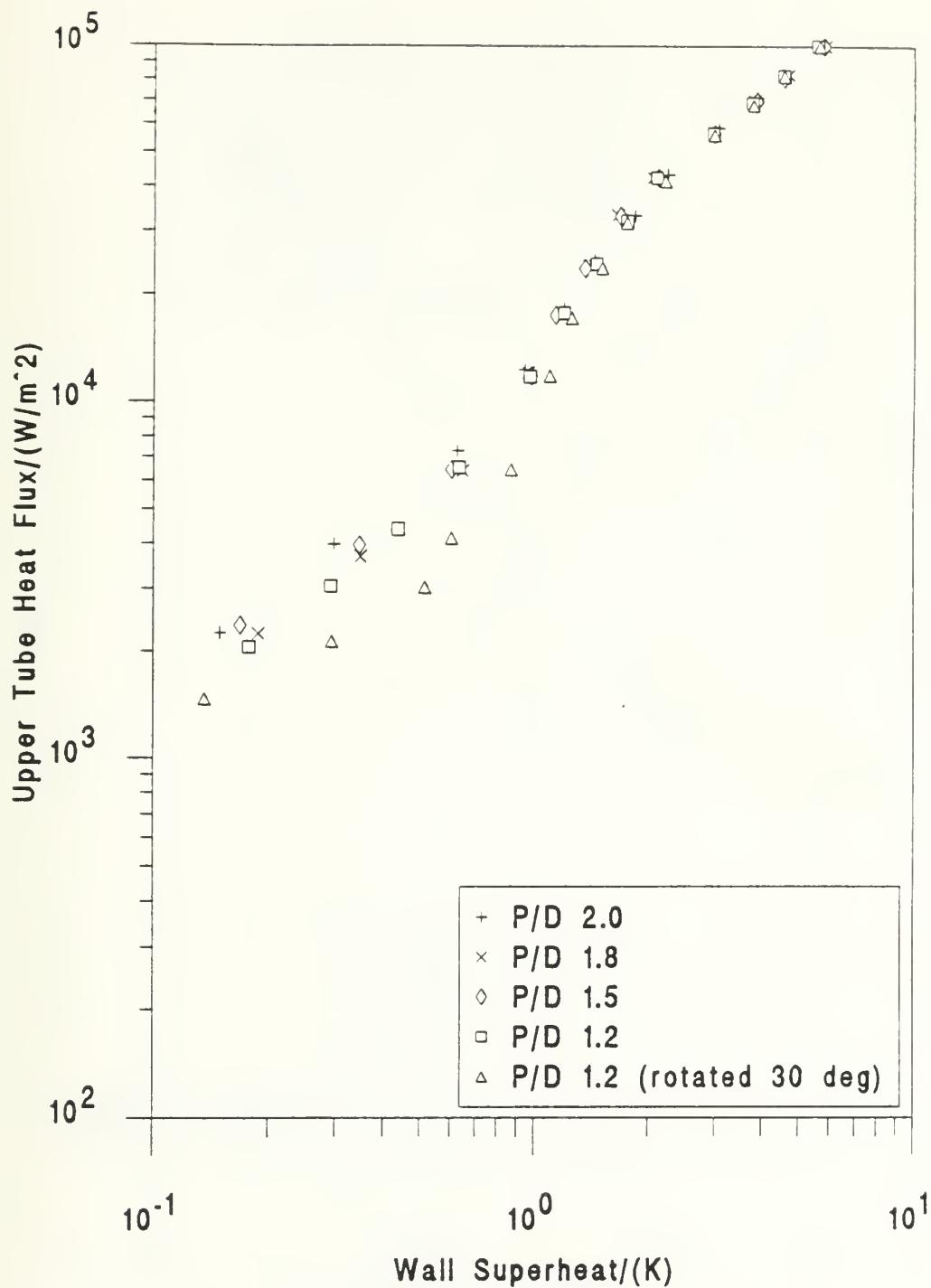
Figure 5.23 Comparison of TURBO-B Tube P/D Ratios for
Decreasing Heat Flux with 20 kW/m² on the Lower Tube

87
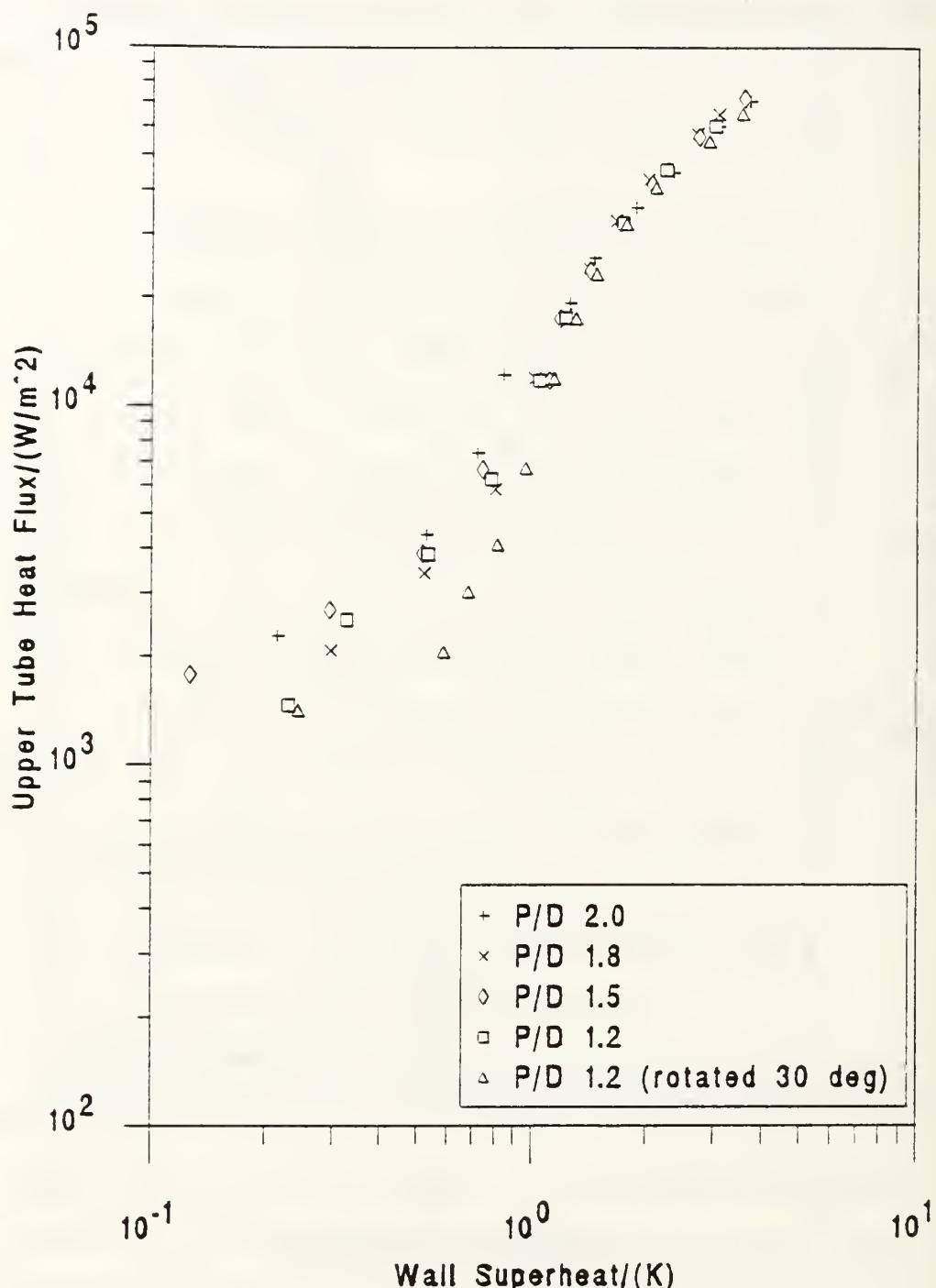
Figure 5.24   Comparison of TURBO-B Tube P/D Ratios for
Decreasing Heat Flux with the UTHFS equal to the LTHFS
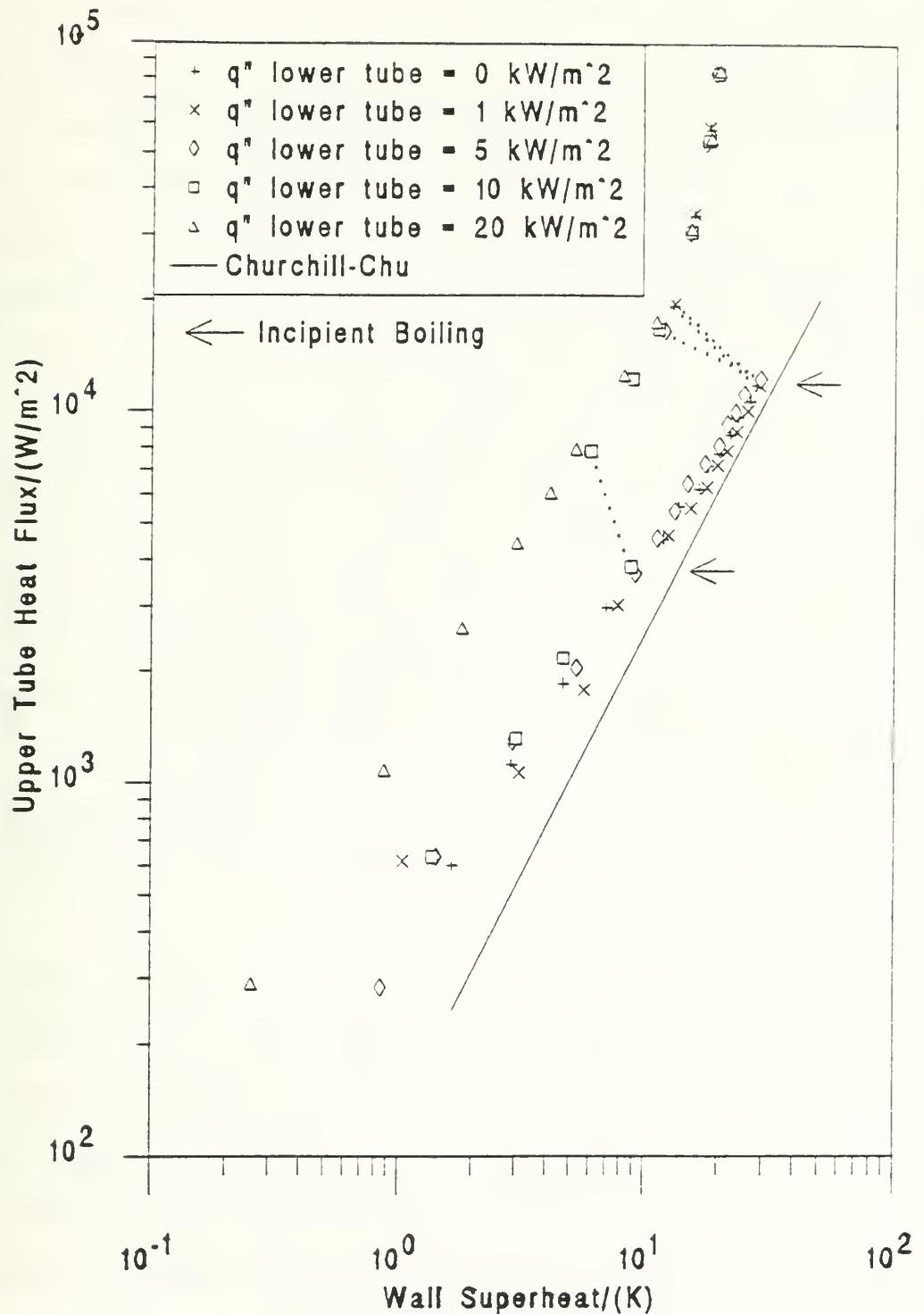
Figure 5.25 Comparison of Lower Tube Heat Flux Settings on
Increasing Heat Flux of Smooth Tubes with P/D of 2.0

89

LTHFS data runs, started in natural convection. In the natural convection region, the data are shifted to the left of the Churchill and Chu correlation [Ref. 9], but approach it as heat flux is increased. This is probably caused by strong circulation patterns within the small evaporator enhancing the heat transfer mentioned previously. In natural convection, the effect of a LTHFS had little influence on the upper tube heat transfer behavior; in fact, this is repeated for all the P/D ratios. The point of incipience was very repeatable, with the exception of a LTHFS of 10 kW/m^2. A heat flux of 10 kW/m^2 is approximately the heat flux that 'trips' the nucleation sites causing boiling to occur from a smooth tube, so shortly after the run started, the lower tube nucleated and caused the upper tube to nucleate quickly. At high heat fluxes, all the data falls on one nucleate boiling curve indicating that the LTHFS has little effect on the heat transfer from the upper tube in this region.

Figure 5.26 shows the decreasing heat flux data for the data run for Figure 5.25. Important to note that the upper tube starts and finishes each run in natural convection, but the lower tube might not. For a LTHFS of 0 and 1 kW/m^2, the lower tube starts and finishes in natural convection; for a LTHFS of 20 kW/m^2, it starts and finishes in nucleate boiling; and for a LTHFS of 5 and 10 kW/m^2, it starts in natural convection and finishes in nucleate boiling. At high heat fluxes, all the data lay on one nucleate boiling curve as
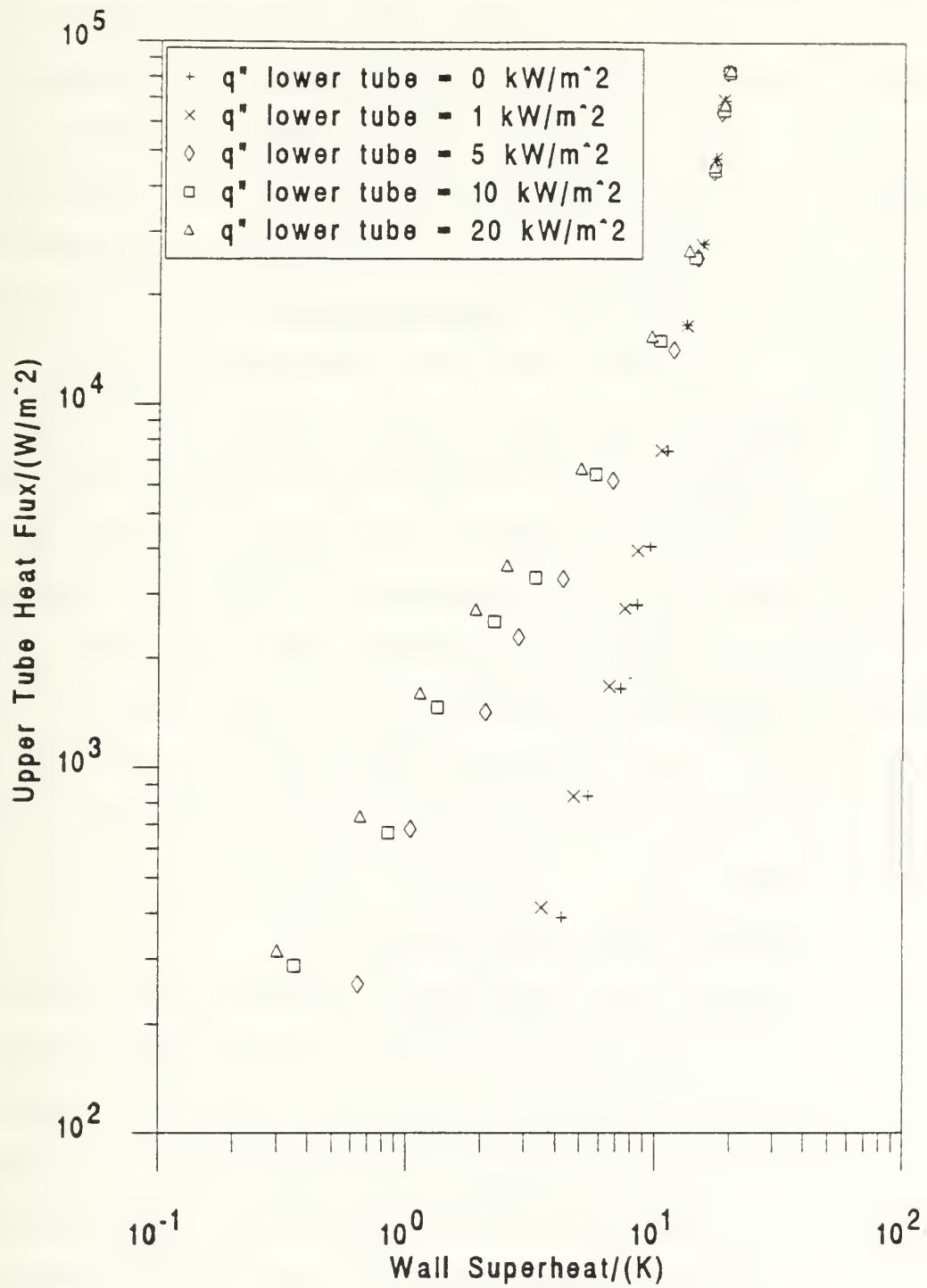
Figure 5.26   Comparison of Lower Tube Heat Flux Settings on
Decreasing Heat Flux of Smooth Tubes with P/D of 2.0

91

expected. Below 20 kW/m^2, five separate curves are seen. The curves with a LTHFS of 0 and 1 kW/m^2 return to the natural convection region, indicating a deactivation of the nucleation sites as the upper tube heat flux is decreased, showing the hysteresis effect of the upper tube. At a heat flux below 5 kW/m^2, the curves with a LTHFS of 5, 10 and 20 kW/m^2 begin to parallel the natural convection curve found on the increasing heat flux plot and have significant enhancement over the 0 and 1 kW/m^2 curves at low heat fluxes. Also, the hysteresis effect is eliminated by the vigorously nucleating lower tube. This same phenomena was found by Lake [Ref. 3]. He attributed this enhancement to strong convection effects on the upper tube from the bubbles nucleating off the lower tube. Therefore, significant enhancement of heat transfer of an upper tube is possible when the lower tube is nucleating and very little enhancement is noticed when both tubes are in natural convection.

b. Smooth Tubes with P/D of 1.8

Figure 5.27 shows the increasing heat flux data taken for a P/D of 1.8 at five lower tube heat flux settings. For a LTHFS of 20 kW/m^2, the lower tube had nucleated immediately at the beginning of the run and remained nucleating for the entire length of the run. All other LTHFS started in natural convection. In the natural convection region, the data are shifted to the left of the Churchill and
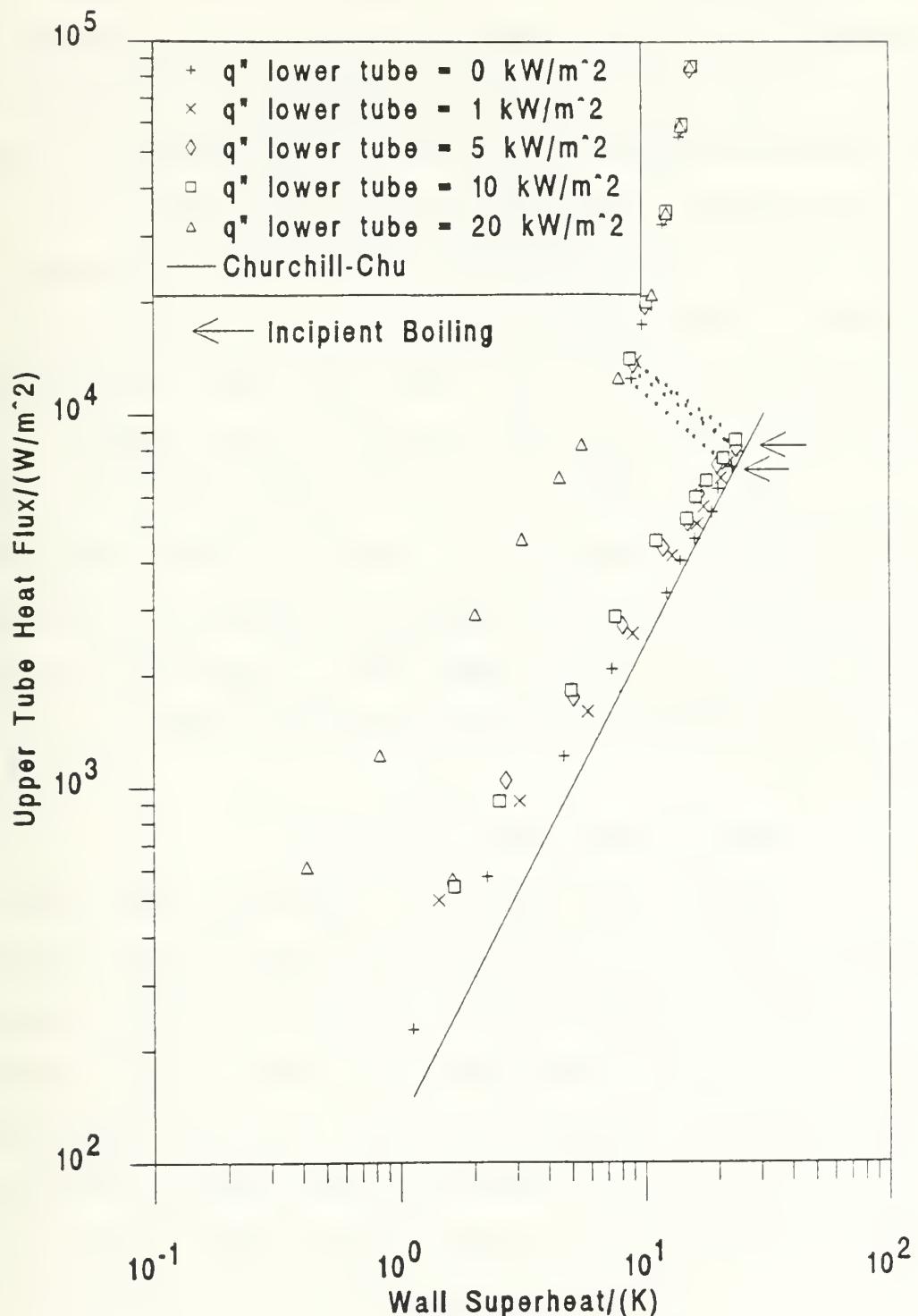
Figure 5.27 Comparison of Lower Tube Heat Flux Settings on Increasing Heat Flux of Smooth Tubes with P/D of 1.8

93

Chu correlation [Ref. 9], but approach it as heat flux is increased, as was the case with a P/D of 2.0. Again, the effect of the LTHFS had little influence of the upper tube heat transfer behavior. The point of incipience was again, very repeatable. This time, unlike for a P/D of 2.0, the lower tube remained in natural convection until the upper tube nucleated. Again, at high heat fluxes, all the data falls on one nucleate boiling curve indicating that the LTHFS has little effect upon the heat transfer in this region.

Figure 5.28 shows the decreasing heat flux data for the data runs for Figure 5.27. The data trend is similar to that found in Figure 5.26. Therefore, significant enhancement of heat transfer from an upper tube is again seen when the lower tube is nucleating with larger than 5 kW/m^2 on the lower tube.

c. Smooth Tubes with P/D of 1.5

Figure 5.29 shows the increasing heat flux data taken for a P/D of 1.5 at five lower tube heat flux settings. For a LTHFS of 10 and 20 kW/m^2, the lower tube had nucleated immediately at the beginning of the run and remained nucleating for the length of the run. All other LTHFS started in natural convection. This plot shows similar results seen on Figure 5.27 and most of the comments still apply.
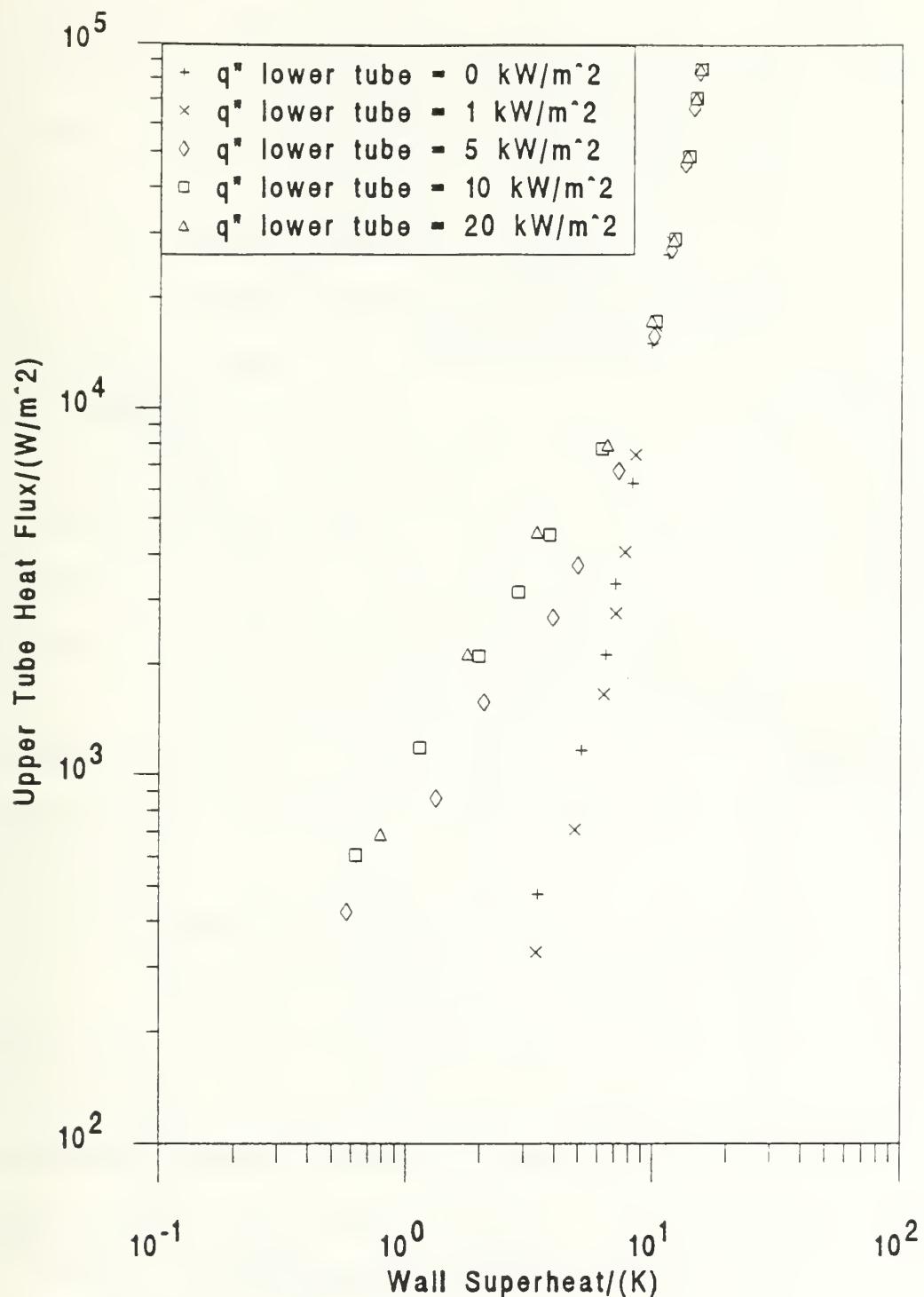
Figure 5.28 Comparison of Lower Tube Heat Flux Settings on
Decreasing Heat Flux of Smooth Tubes with P/D of 1.8
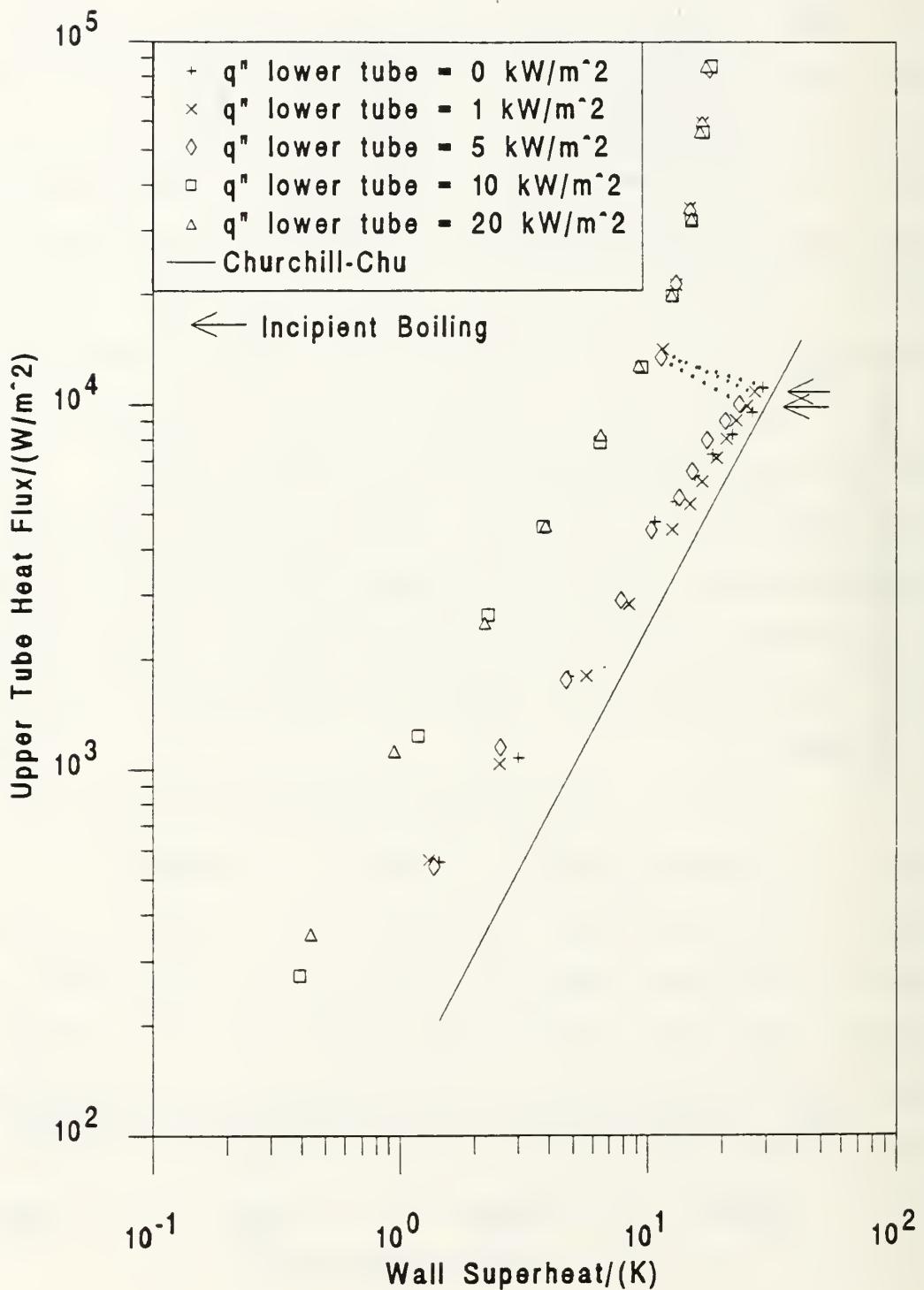
Figure 5.29 Comparison of Lower Tube Heat Flux Settings on
Increasing Heat Flux of Smooth Tubes with P/D of 1.5

96

Figure 5.30 shows the decreasing heat flux data for the data runs shown in Figure 5.29. Again, similar results are obtained as before. Significant enhancement in the heat transfer from an upper tube is obtained when the lower tube is nucleating with a heat flux larger than 5 kW/m^2.

d. Smooth Tubes with P/D of 1.2

Figure 5.31 shows the increasing heat flux data taken for a P/D of 1.2 at five lower tube heat flux settings. For a LTHFS of 20 kW/m^2, the lower tube had nucleated immediately at the beginning of the run and remained nucleating for the length of the run. All other LTHFS started in natural convection. This plot shows similar results seen on Figure 5.29 and most of the comments still apply.

Figure 5.32 shows the decreasing heat flux data for the data runs shown in Figure 5.31. This plot shows similar results seen on Figure 5.30 and again, most of the comments still apply.

e. Smooth Tubes with P/D of 1.2 (Rotated 30°)

Figure 5.33 shows the increasing heat flux data taken for a P/D of 1.2 (rotated 30°), at five lower tube heat flux settings. For a LTHFS of 20 kW/m^2, the lower tube had nucleated immediately at the beginning of the run and remained nucleating for the length of the run. All other LTHFS started in natural convection. The increasing data for this configuration is more concentrated than the others seen

97
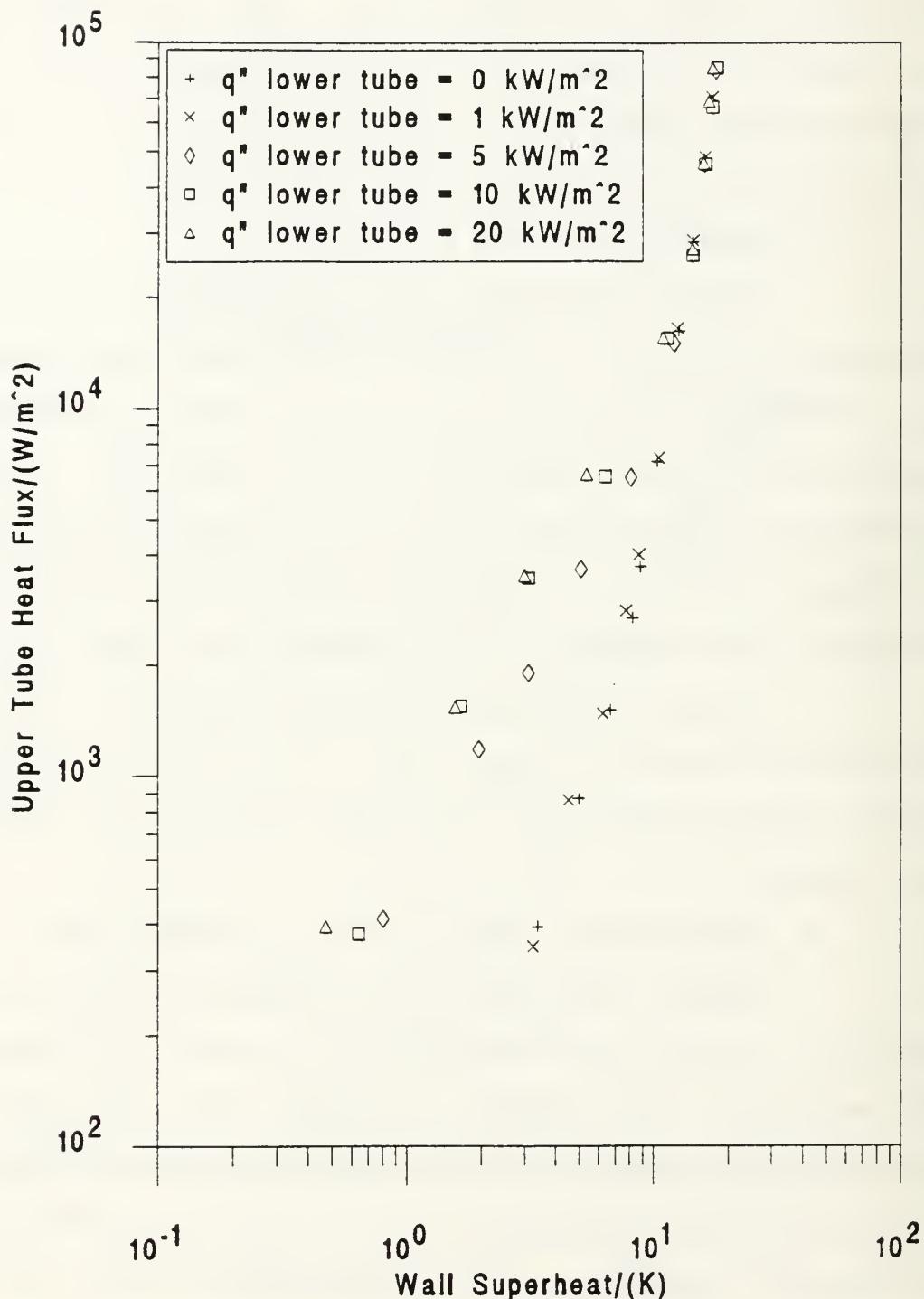
Figure 5.30 Comparison of Lower Tube Heat Flux Settings on
Decreasing Heat Flux of Smooth Tubes with P/D of 1.5
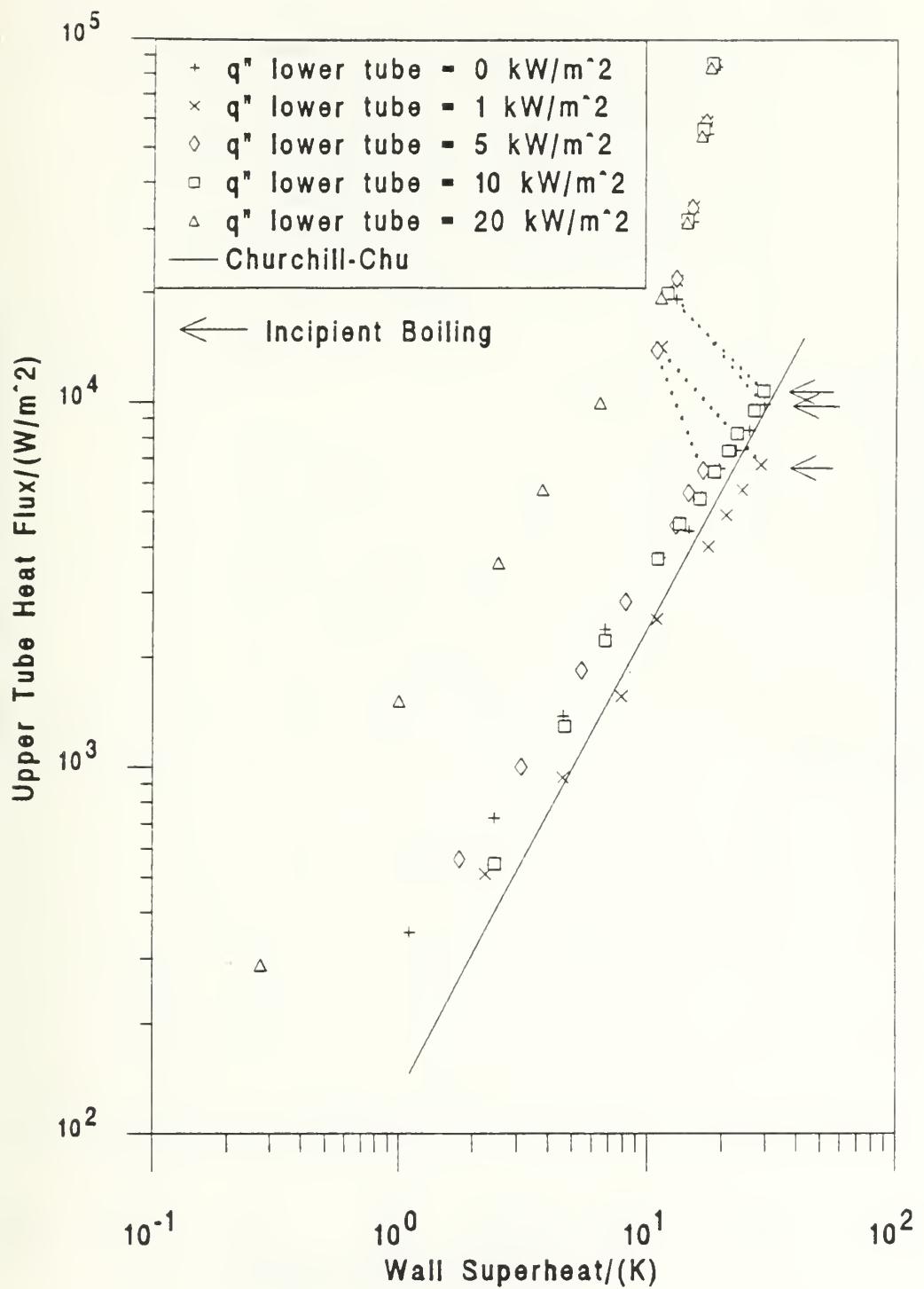
Figure 5.31 Comparison of Lower Tube Heat Flux Settings on
Increasing Heat Flux of Smooth Tubes with P/D of 1.2
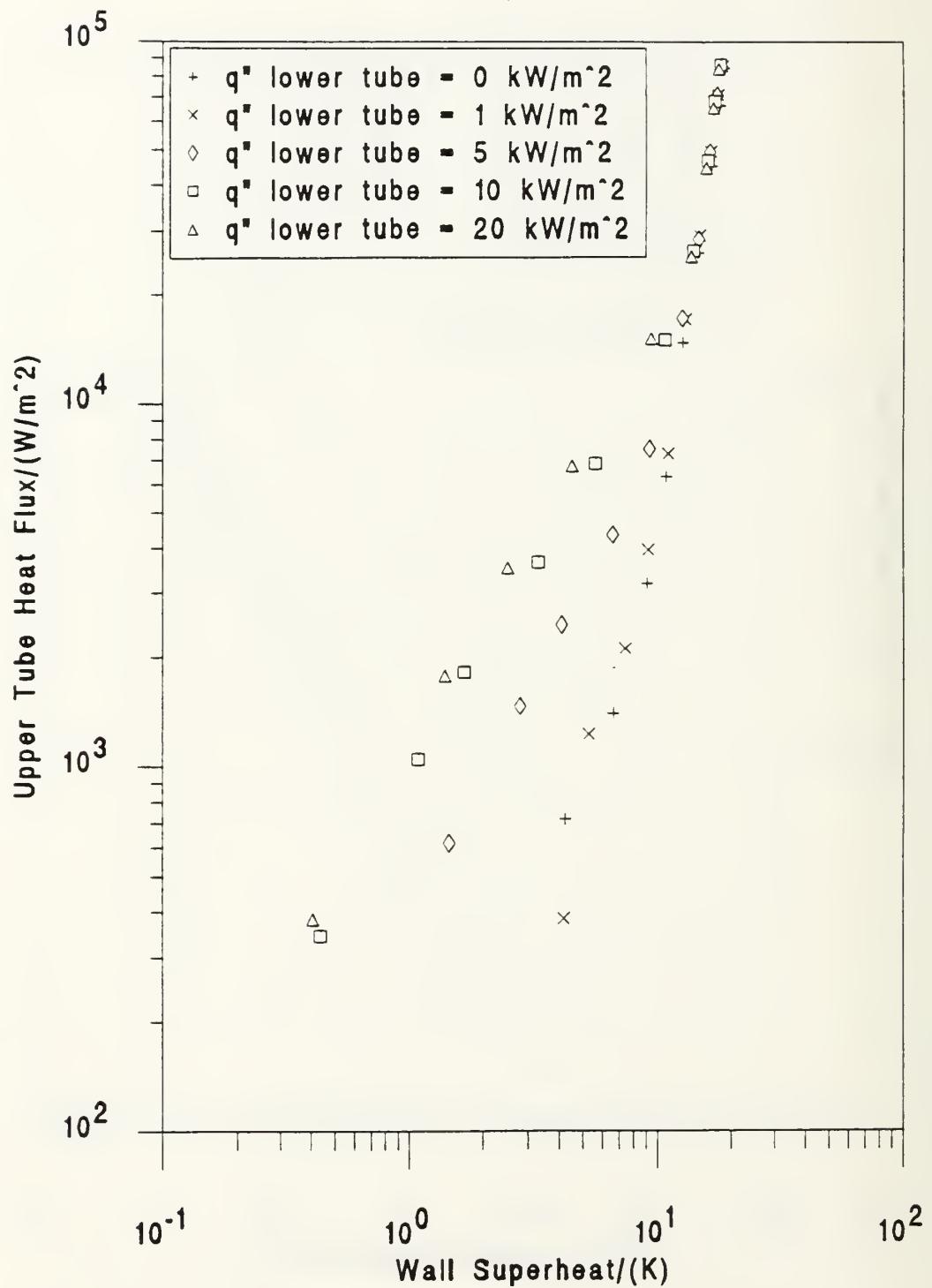
Figure 5.32 Comparison of Lower Tube Heat Flux Settings on
Decreasing Heat Flux of Smooth Tubes with P/D of 1.2
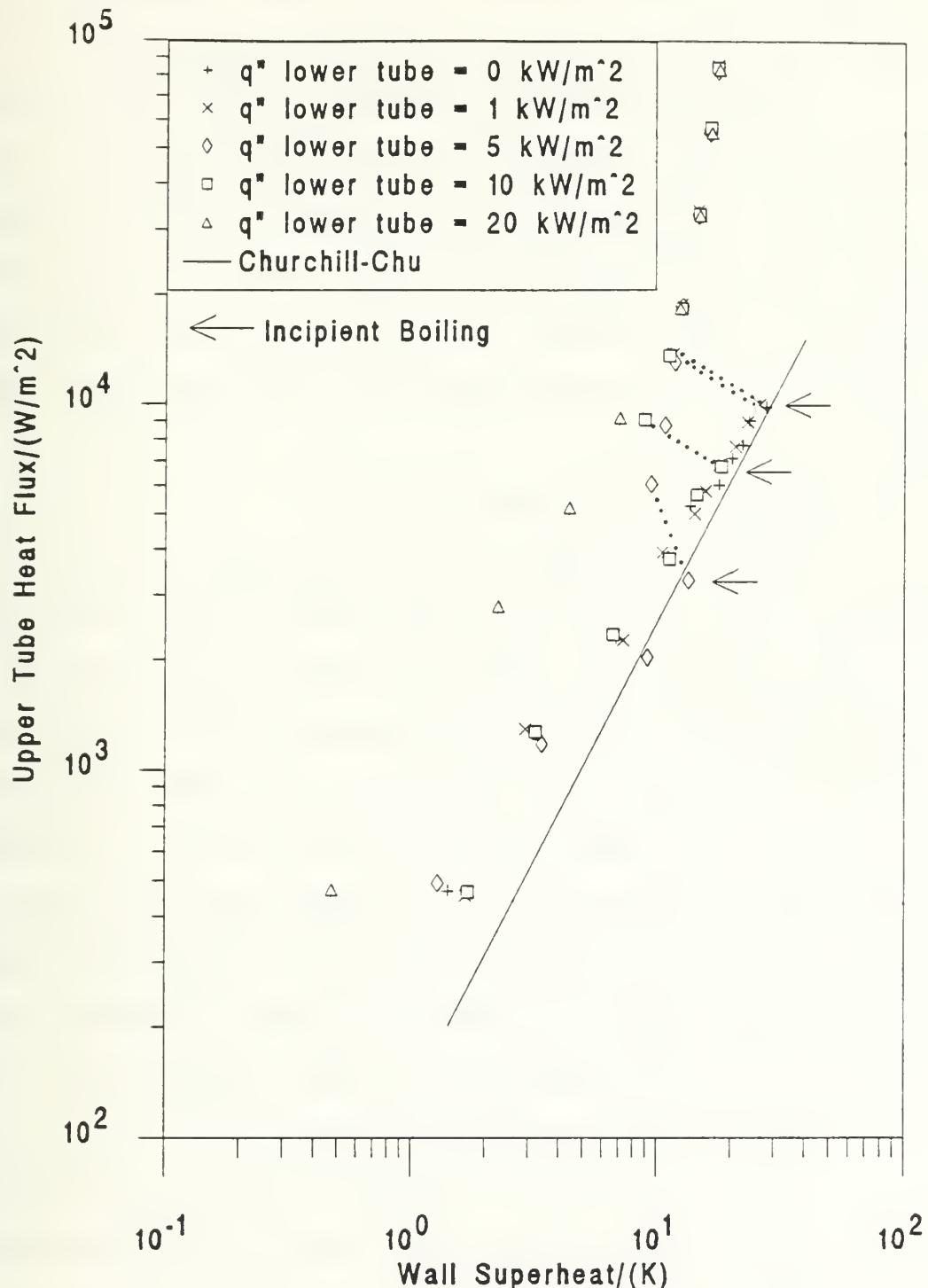
Figure 5.33 Comparison of Lower Tube Heat Flux Settings on
Increasing Heat Flux of Smooth Tubes with P/D of 1.2
(Rotated 30°)

101

previously. This might be due to the offset orientation of the upper tube causing the data to be less scattered.

Figure 5.34 shows the decreasing heat flux data for the data runs shown in Figure 5.33. At high heat fluxes, all the data lay on one nucleate boiling curve. Below 10 kW/m^2, separate curves are formed and as seen before. Significant enhancement of heat transfer from an upper tube is obtained when the lower tube is nucleating with a heat flux larger than 5 kW/m^2.

f. TURBO-B Tubes with P/D of 2.0

Figure 5.35 shows the decreasing heat flux data for the TURBO-B tubes taken at five lower tube heat flux settings. At the start of each run, a very consistent boiling curve is seen above 20 kW/m^2, indicating that above a UTHFS of 20 kW/m^2, there is no enhancement from increasing the LTHFS. Below 10 kW/m^2, raising the LTHFS does increase the heat transfer performance of the upper tube. At an upper tube heat flux of 2 kW/m^2, an increase in performance of 2.4 is found going from an unheated lower tube to a LTHFS of 20 kW/m^2, compared to an increase of 3.6 for the smooth tube array (Figure 5.26).

g. TURBO-B Tubes with P/D of 1.8

Figure 5.36 shows the decreasing heat flux data for the TURBO-B tubes taken at five lower tube heat flux settings. Similar results are found compared to the P/D of 2.0 case. At
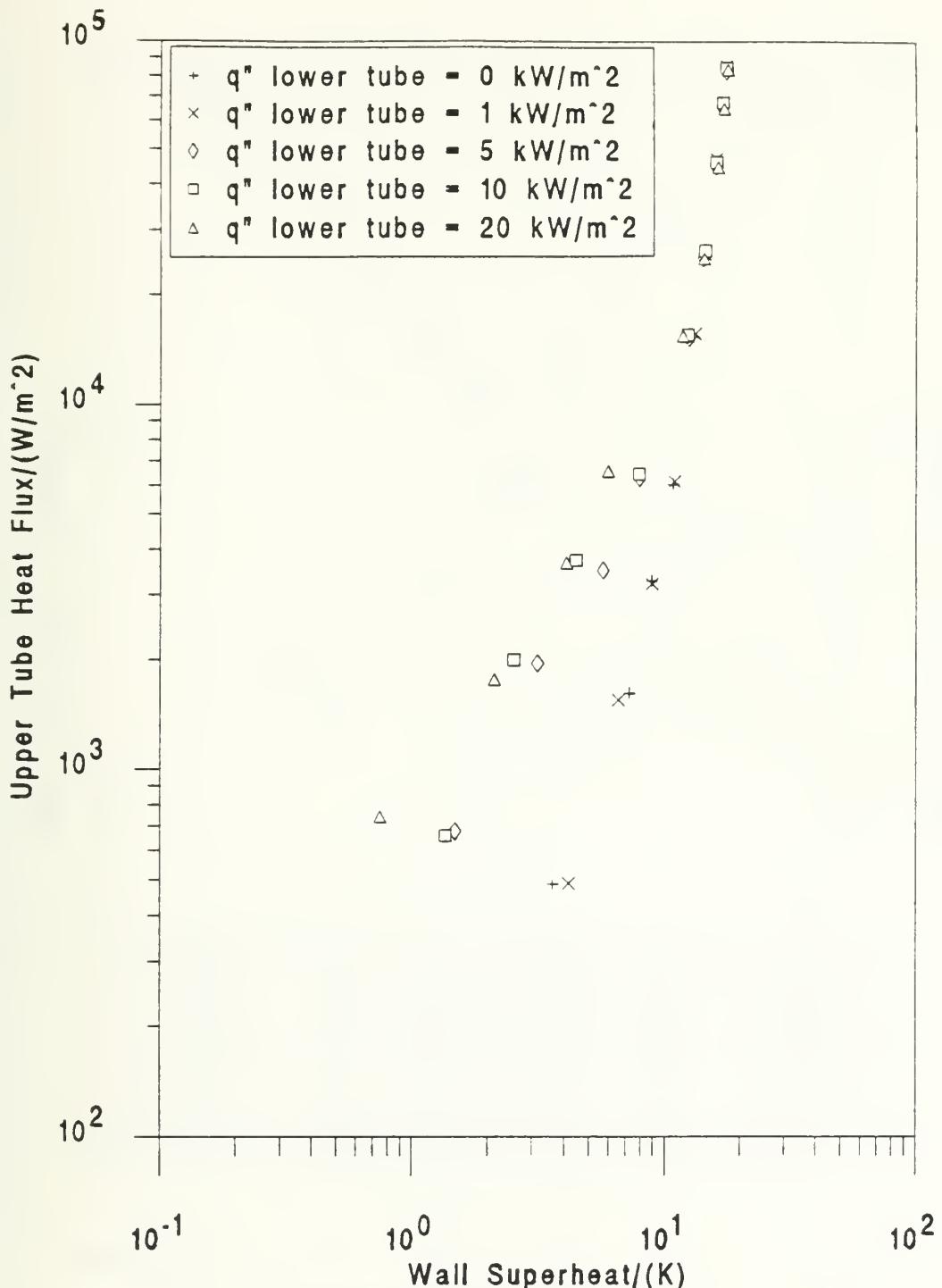
Figure 5.34   Comparison of Lower Tube Heat Flux Settings on
Decreasing Heat Flux of Smooth Tubes with P/D of 1.2
(Rotated 30°)

103
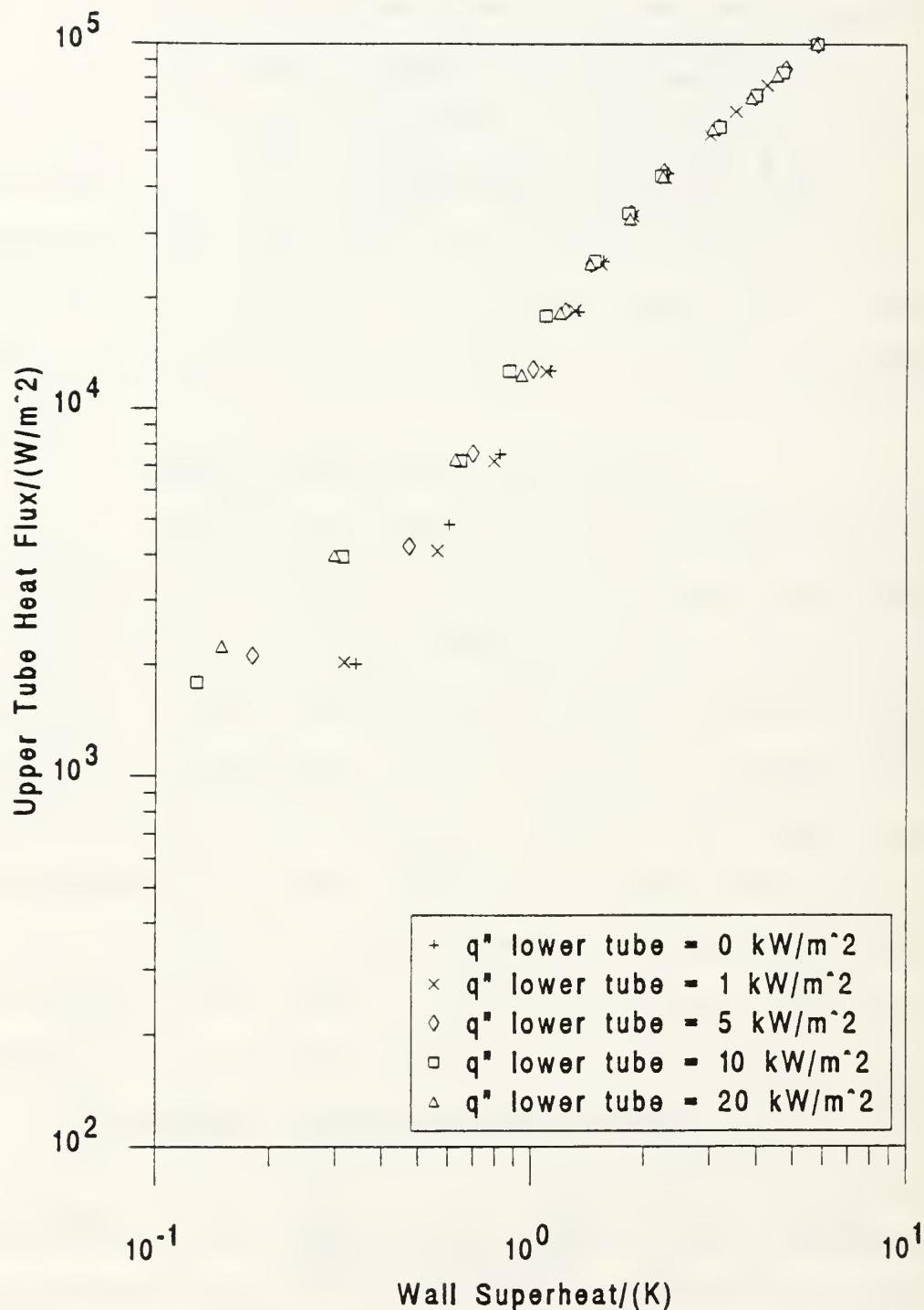
Figure 5.35 Comparison of Lower Tube Heat Flux Settings on
Decreasing Heat Flux of TURBO-B Tubes with P/D of 2.0
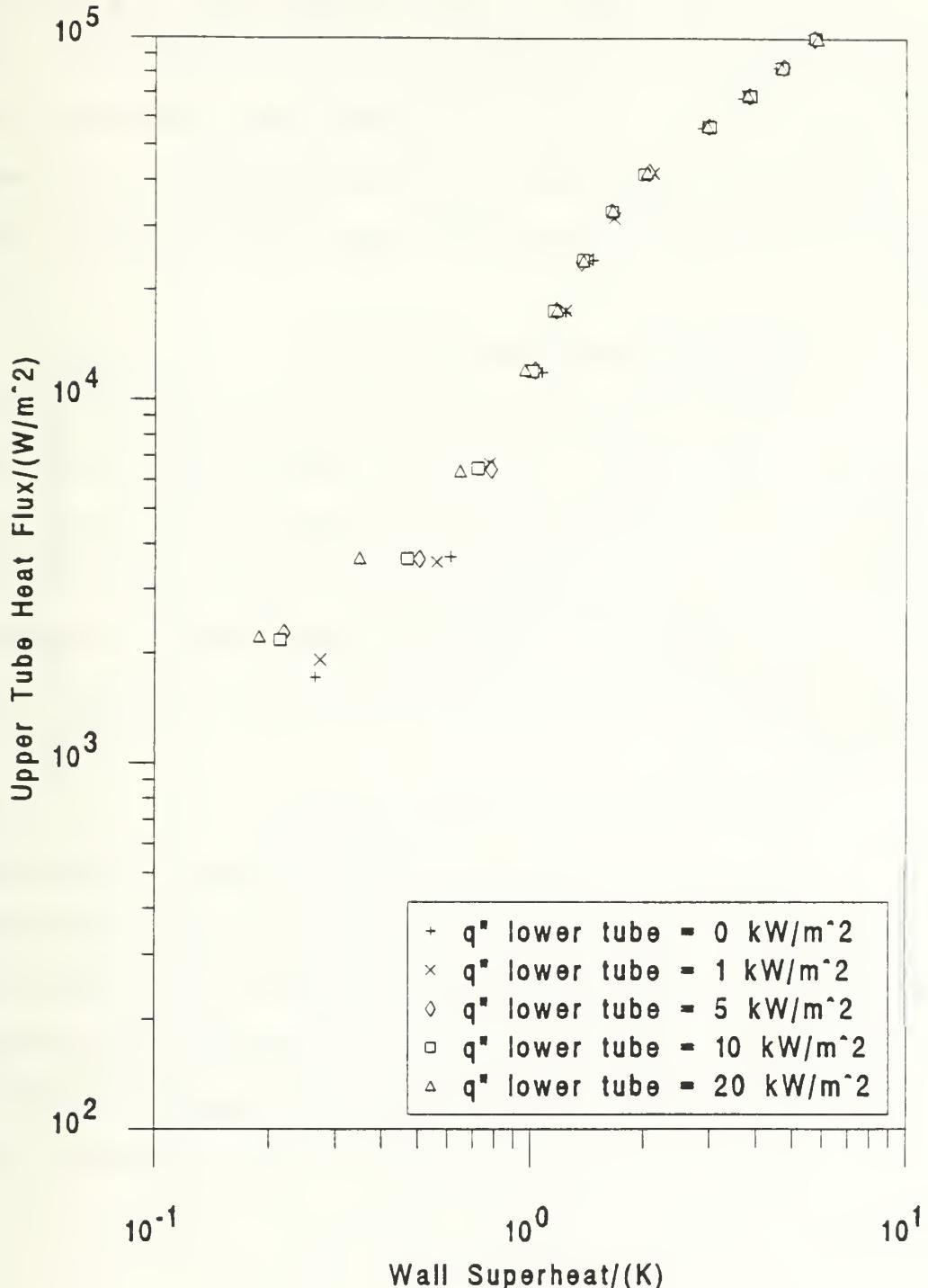
Figure 5.36 Comparison of Lower Tube Heat Flux Settings on
Decreasing Heat Flux of TURBO-B Tubes with P/D of 1.8

105

an upper tube heat flux of 2 kW/m², an increase in performance of 1.6 is found going from a unheated lower tube to a LTHFS of 20 kW/m², compared to an increase of 3.7 for the smooth tube array (Figure 5.28). Unlike the smooth tube case where a P/D of 1.8 produced the best heat transfer performance in nucleate boiling, no optimal P/D ratio was found for the TURBO-B tube array.

h. *TURBO-B Tubes with P/D of 1.5*

Figure 5.37 shows the decreasing heat flux data for the TURBO-B tubes taken at five lower tube heat flux settings. Similar results are found compared to the P/D of 1.8 case. At an upper tube heat flux of 2 kW/m², an increase in performance of 2.2 is found going from a unheated lower tube to a LTHFS of 20 kW/m², compared to an increase of 3.5 for the smooth tube array (Figure 5.30).

i. *TURBO-B Tubes with P/D of 1.2*

Figure 5.38 shows the decreasing heat flux data for the TURBO-B tubes taken at five lower tube heat flux settings. Similar results are found compared to the P/D of 1.5 case. At an upper tube heat flux of 2 kW/m², an increase in performance of 2.2 is found going from a unheated lower tube to a LTHFS of 20 kW/m², compared to an increase of 5.4 for the smooth tube array (Figure 5.32).
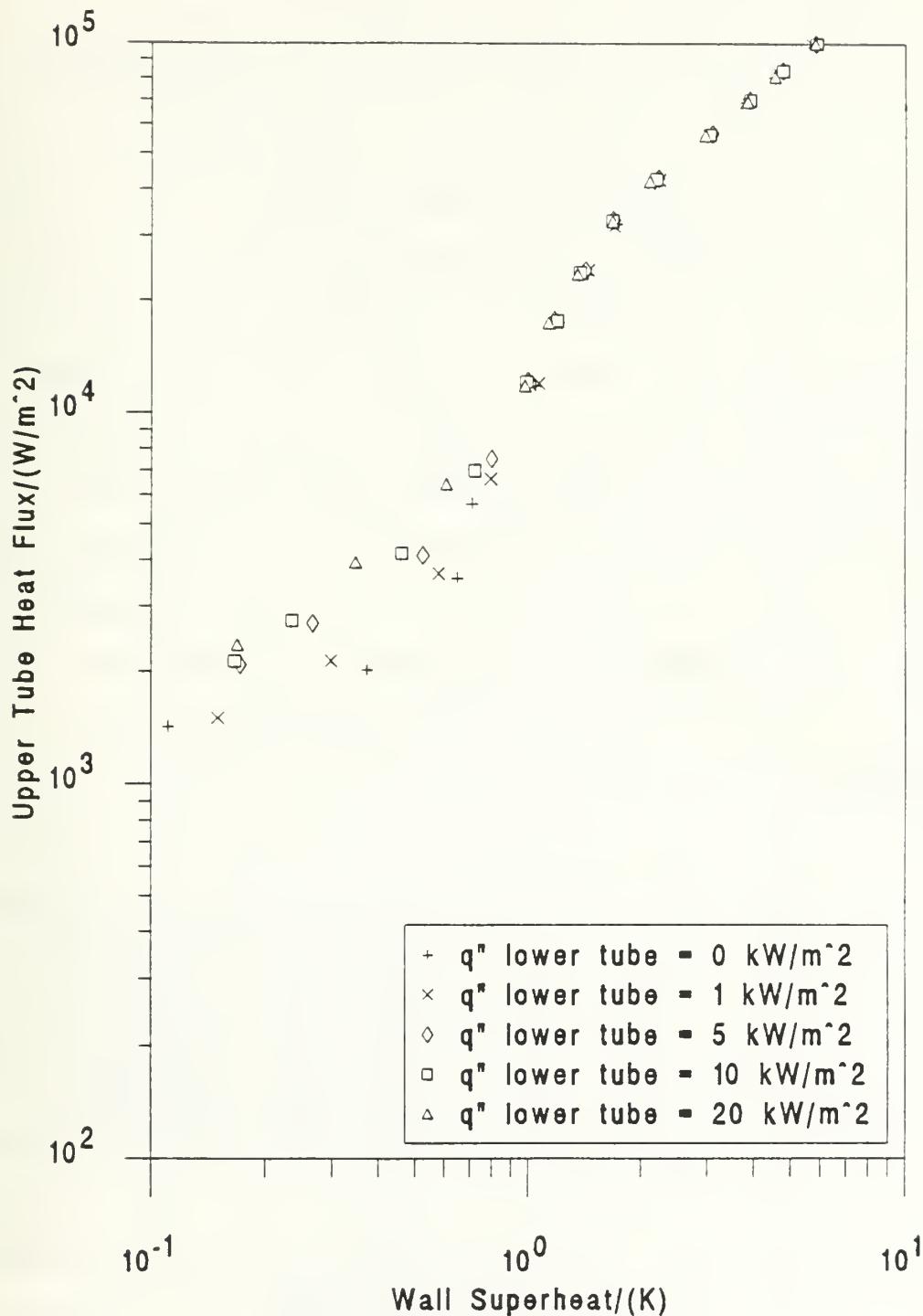
Figure 5.37 Comparison of Lower Tube Heat Flux Settings on Decreasing Heat Flux of TURBO-B Tubes with P/D of 1.5

107
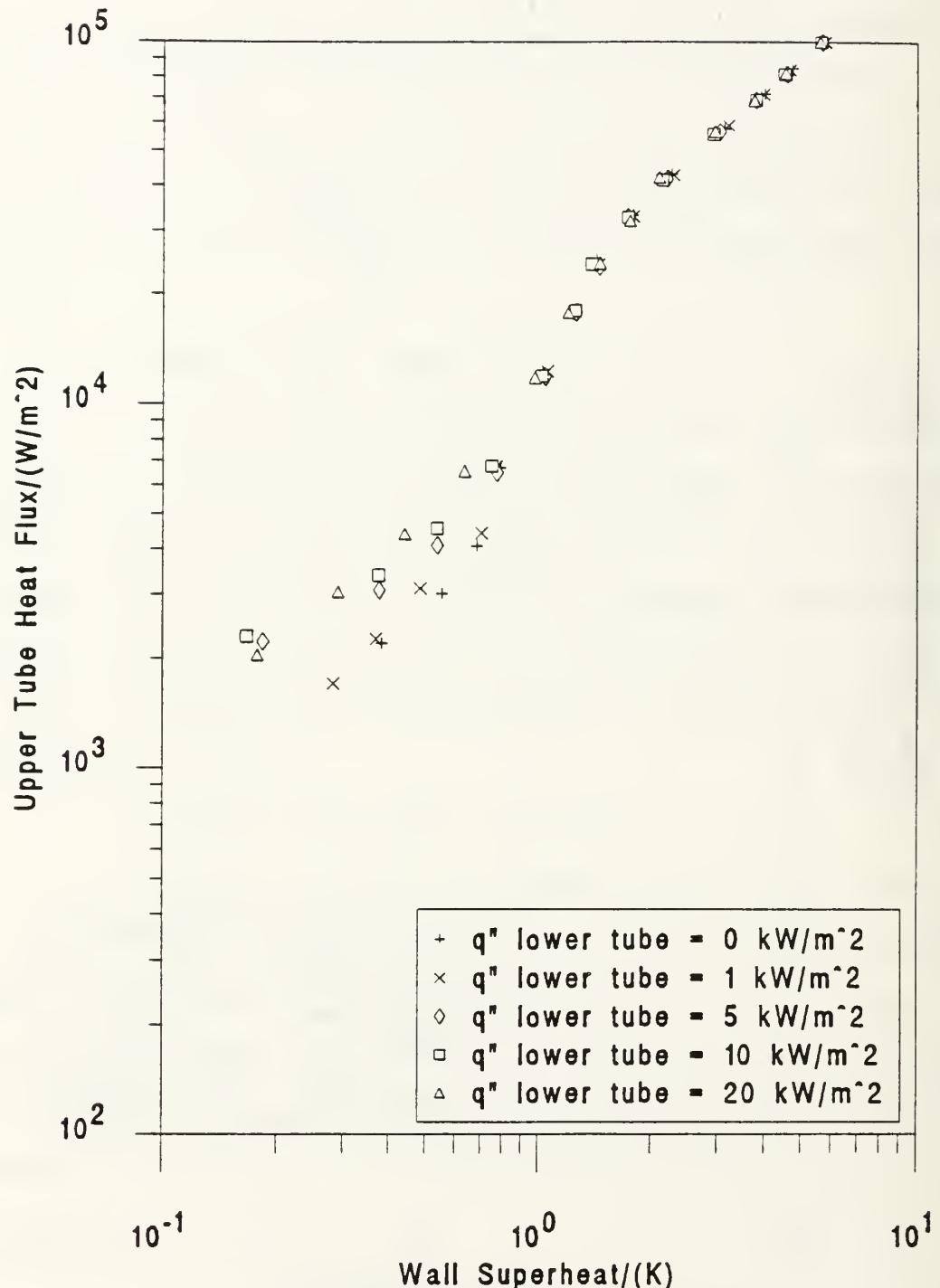
Figure 5.38   Comparison of Lower Tube Heat Flux Settings on
Decreasing Heat Flux of TURBO-B Tubes with P/D of 1.2

j. TURBO-B Tubes with P/D of 1.2 (Rotated 30°)

Figure 5.39 shows the decreasing heat flux data for the TURBO-B tubes taken at five lower tube heat flux settings. A very consistent boiling curve is again seen above 10 kW/m². Below 10 kW/m², the data seems less scattered and slightly to the left of any other configuration, indicating that rotating the upper tube reduces the enhancement produced from increasing the LTHFS in the low heat flux regions. At an upper tube heat flux of 2 kW/m², an increase in performance of 1.7 is found going from a unheated lower tube to a LTHFS of 20 kW/m², compared to an increase of 3.5 for the smooth tube array (Figure 5.34).

3. The Effect of a Variable Lower Tube Heat Flux

a. Smooth Tubes with P/D of 2.0

Figure 5.40 shows the heat transfer performance of an upper tube, held at a constant heat flux, as the lower tube heat flux is varied. The three fixed UTHFS used were 5, 10 and 20 kW/m². The labeling in the plot legend describes which data were taken using increasing or decreasing lower tube heat flux. The sharp transitions in the increasing curves are the points where the lower tube nucleated and caused the upper tube to shift from natural convection to nucleate boiling (visually verified during the data run), significantly increasing the upper tube heat transfer coefficient, as expected. The maximum upper tube heat transfer coefficient
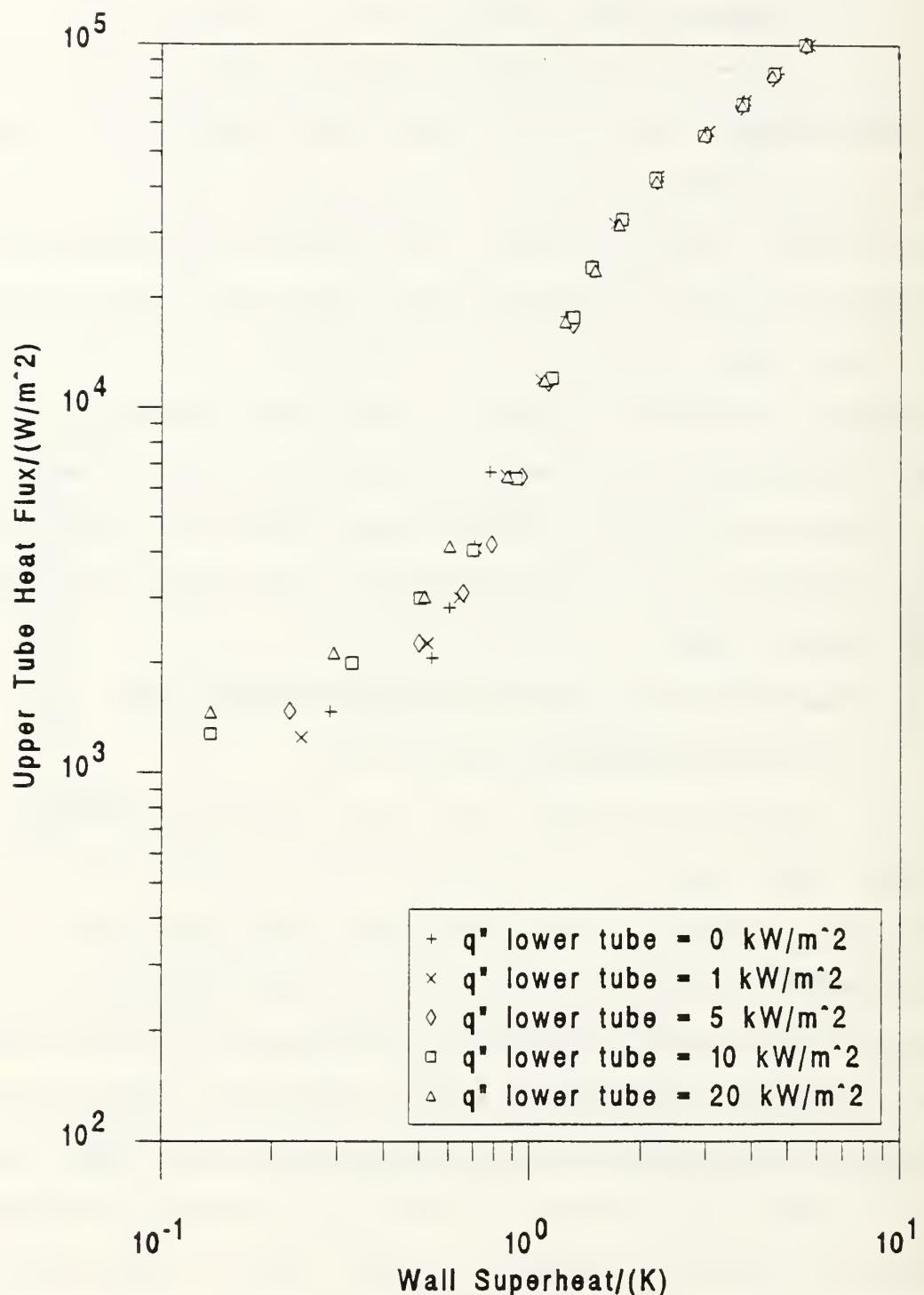
Figure 5.39   Comparison of Lower Tube Heat Flux Setting on
Decreasing Heat Flux of TURBO-B Tubes with P/D of 1.2
(Rotated 30°)
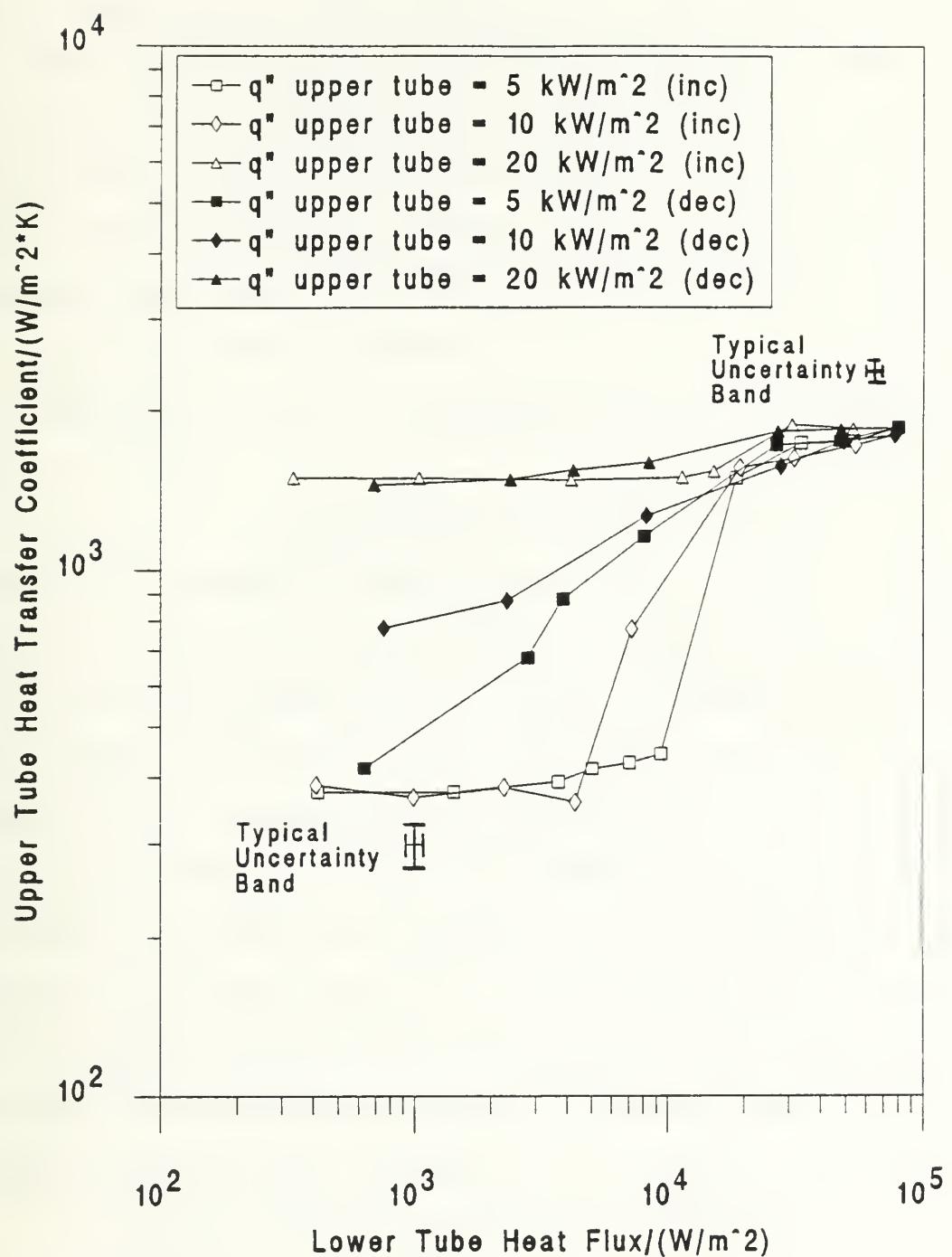
Figure 5.40   Heat Transfer Performance of a Smooth Upper
Tube at a Constant Heat Flux for a P/D of 2.0

for all three UTHFS was 1850 W/m$^2 \cdot$K, which indicates that at a lower tube heat flux of 80 kW/m^2, the heat transfer performance of the upper tube is independent of the lower tube heat flux. The decreasing curves show that for an UTHFS of 20 kW/m^2, the lower tube heat flux has little influence on the upper tube heat transfer. For the UTHFS of 10 kW/m^2, as the lower tube heat flux is decreased, the upper tube remains in nucleate boiling, but for the UTHFS of 5 kW/m^2, the upper tube returns to the natural convection region as the lower tube heat flux is decreased.

b. *Smooth Tubes with P/D of 1.8*

Figure 5.41 shows the heat transfer performance of an upper tube, held at a constant heat flux, as the lower tube heat flux is varied. Similar results were obtained as in the P/D of 2.0 case, except that the curves did not merge at the highest heat flux setting. The maximum heat transfer coefficient for the UTHFS of 5 and 10 kW/m^2 converged at approximately 1700 W/m$^2 \cdot$K and for the UTHFS of 20 kW/m^2 the value was about 1900 W/m$^2 \cdot$K. It is not known why the curves did not merge at high lower tube heat fluxed. Comparing these results to the P/D of 2.0 results, at the smallest lower tube heat fluxes, the P/D of 1.8 provides better heat transfer.
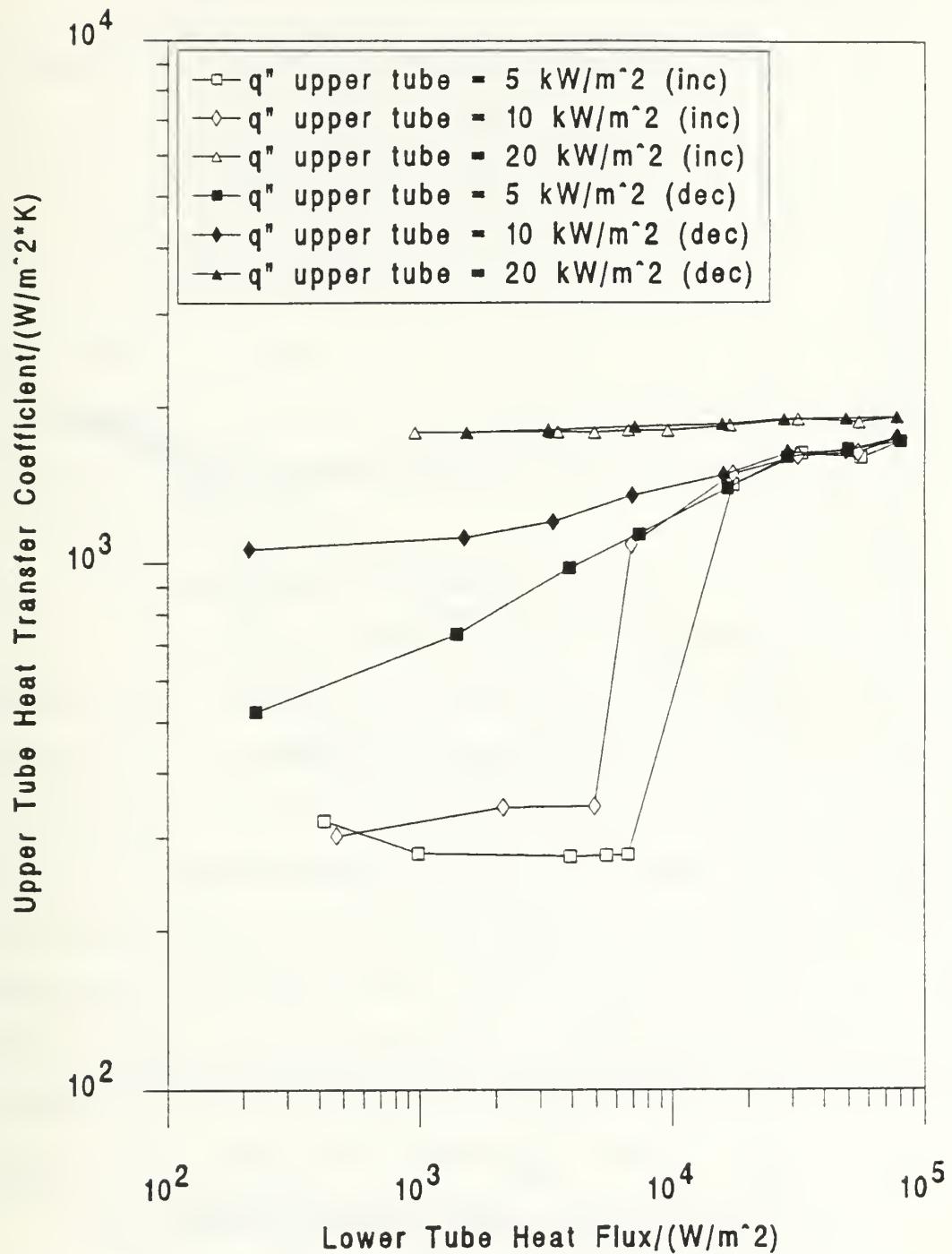
Figure 5.41   Heat Transfer Performance of a Smooth Upper
Tube at a Constant Heat Flux for a P/D of 1.8

113
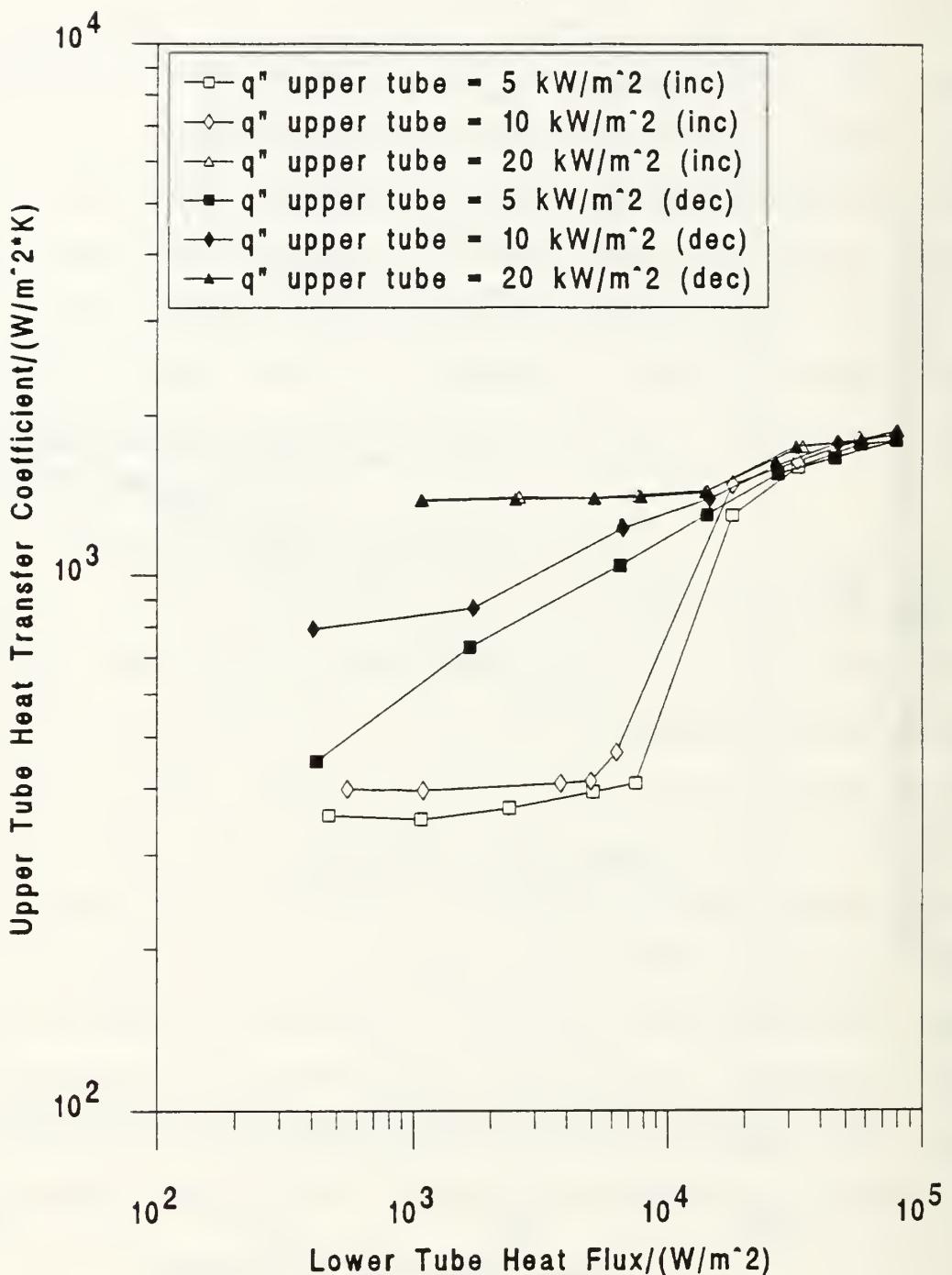
Figure 5.42   Heat Transfer Performance of a Smooth Upper
Tube at a Constant Heat Flux for a P/D of 1.5

114

c. Smooth Tubes with P/D of 1.5

Figure 5.42 shows the heat transfer performance of an upper tube, held at a constant heat flux, as the lower tube heat flux is varied. The maximum heat transfer coefficient for all three of the UTHFS converged at approximately 1800 $W/m^2 \cdot K$, similar to the P/D of 2.0 case. The decreasing curves show very similar behavior found at a P/D of 2.0. Comparing these results to data of a P/D of 2.0 and 1.8, a P/D of 2.0 and 1.5 are similar in the amount of enhancement achieved, whereas a P/D of 1.8 outperforms them both, in the mid to low heat flux regions.

d. Smooth Tubes with P/D of 1.2

Figure 5.43 shows the heat transfer performance of an upper tube, held at a constant heat flux, as the lower tube heat flux is increased. The maximum heat transfer coefficient for all three of the UTHFS converged, as did the P/D of 2.0 and 1.5, at approximately 1990 $W/m^2 \cdot K$, highest value of all the configurations tested. Therefore, the best heat transfer performance was given by a P/D ratio of 1.8 when the lower tube heat flux was held constant, but a P/D ratio of 1.2 when the upper tube heat flux was held constant. No decreasing curves were recorded for these data runs.

e. Smooth Tubes with P/D of 1.2 (Rotated 30°)

Figure 5.44 shows the heat transfer performance of an upper tube, held at a constant heat flux, as the lower tube
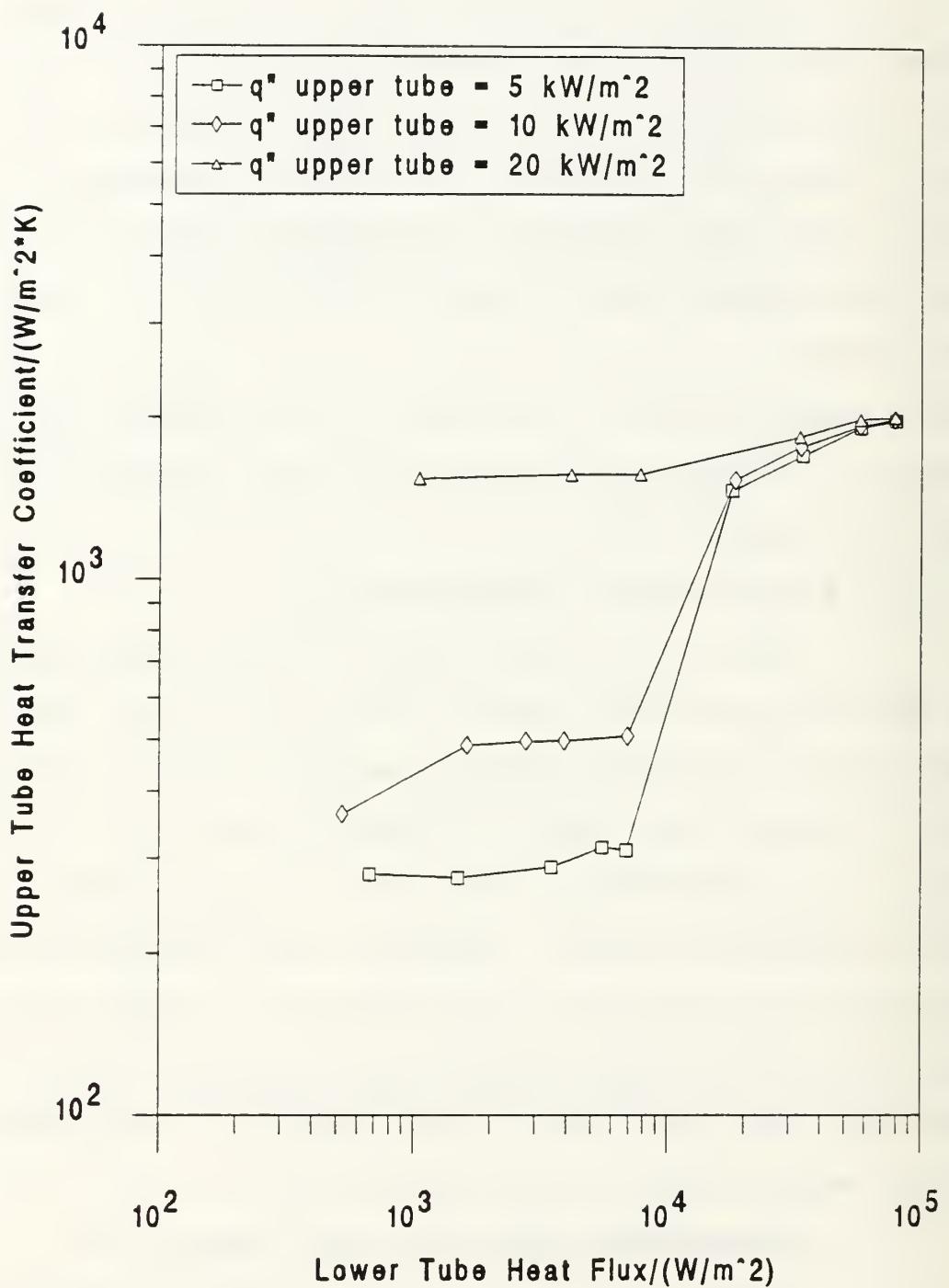
Figure 5.43 Heat Transfer Performance of a Smooth Upper
Tube at a Constant Heat Flux for a P/D of 1.2

116
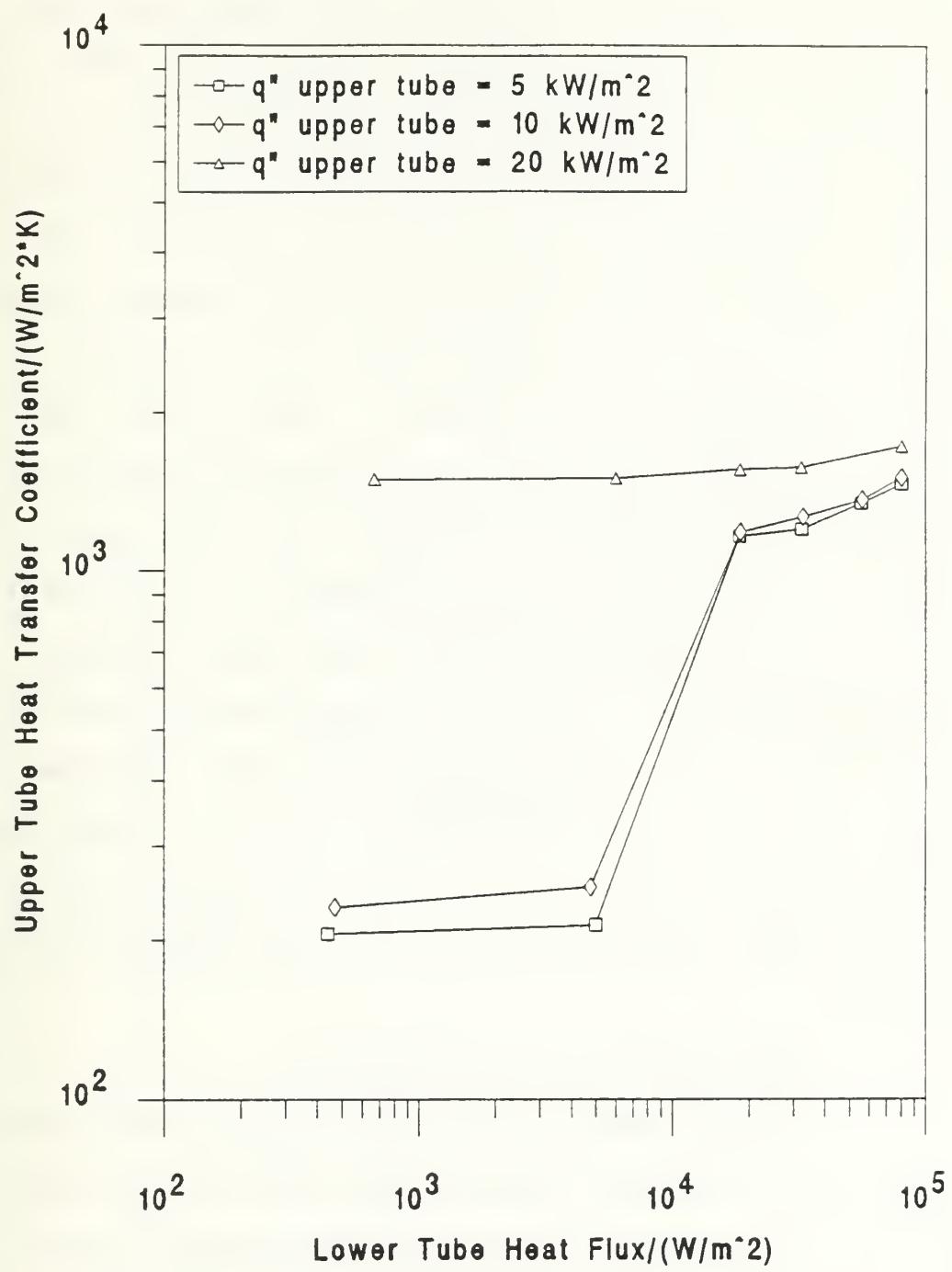
Figure 5.44   Heat Transfer Performance of a Smooth Upper
Tube at a Constant Heat Flux for a P/D of 1.2 (Rotated 30°)

heat flux is increased. As seen for the P/D of 1.8 case, the curves do not merge at the highest lower tube heat flux. The maximum heat transfer coefficient for the two lower curves converged at about 1500 $W/m^2 \cdot K$ and the upper curve was 1725 $W/m^2 \cdot K$. Comparing Figures 5.43 and 5.44, for an UTHFS of 20 kW/m^2, the data curves are identical for lower tube heat fluxes up to 8 kW/m^2, indicating that the forced convection effects from the lower tube have very little influence on the upper tube heat transfer behavior. Above lower tube heat fluxes of 10 kW/m^2, the in-line configuration provides better heat transfer performance because the lower tube is in nucleate boiling and all of the bubbles are impacting the upper tube providing enhancement by *bubble pumping;* as opposed to the offset configuration, where most of the bubbles coming off the lower tube miss the upper tube. The same idea holds true for the other data curves. The in-line configurations are more enhanced due to *bubble pumping* from the lower tube. No decreasing curves were recorded for these data runs.

f. TURBO-B Tubes with P/D of 2.0

Figure 5.45 shows the heat transfer performance of an upper tube, held at a constant heat flux, as the lower tube heat flux is decreased. At high lower tube heat fluxes, all three of the UTHFS appear to perform almost equally. For an UTHFS of 20 kW/m^2, the lower tube heat flux has little
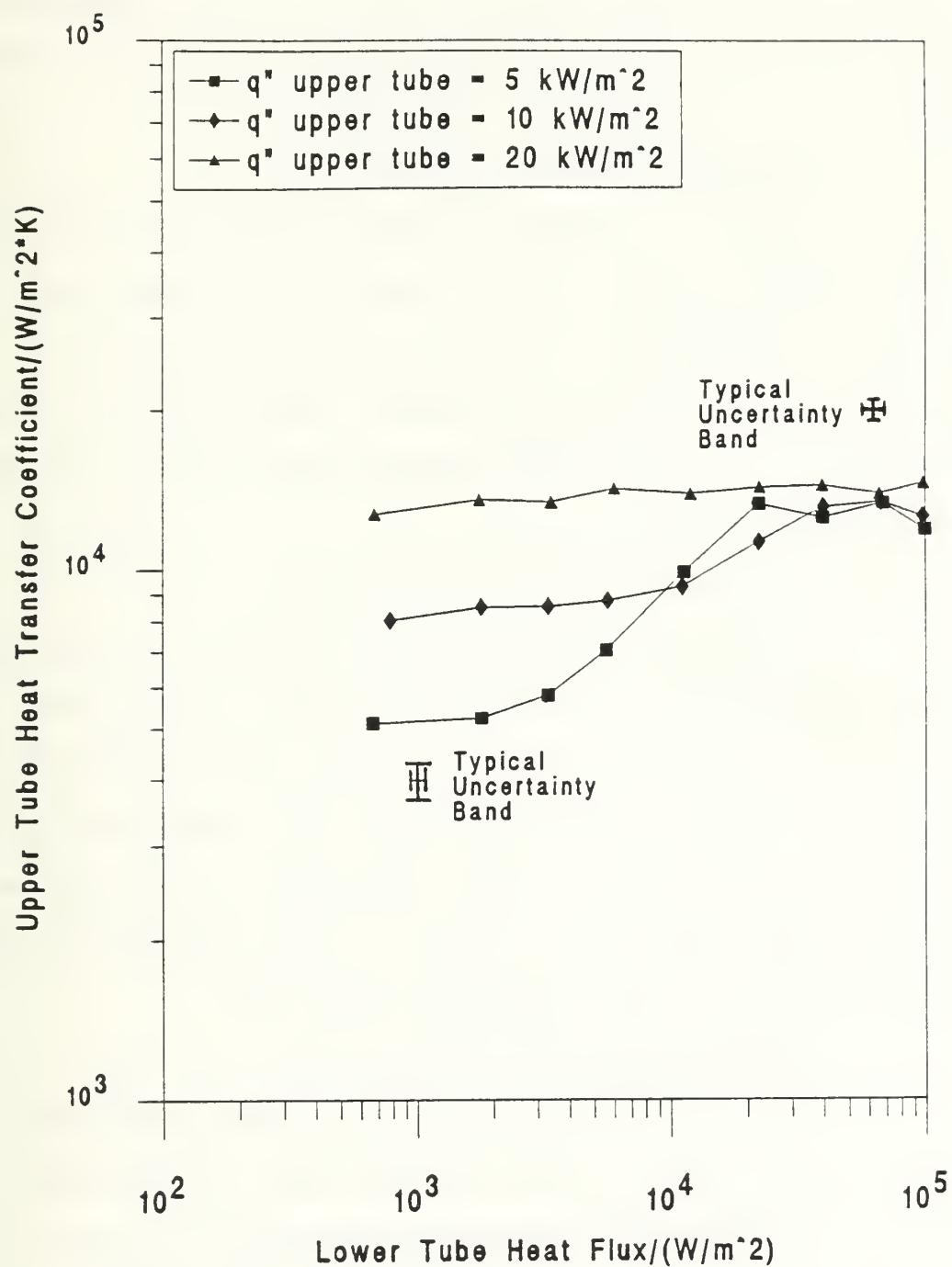
Figure 5.45 Heat Transfer Performance of a TURBO-B Upper
Tube at a Constant Heat Flux for a P/D of 2.0

119

influence on the upper tube heat transfer and for an UTHFS of 5 and 10 kW/m^2, as the lower tube heat flux is decreased so follows the performance of the upper tube (more for 5 than 10 kW/m^2).

g. TURBO-B Tubes with P/D of 1.8

Figure 5.46 shows the heat transfer performance of an upper tube, held at a constant heat flux, as the lower tube heat flux is decreased. Comparing these curves to the ones for a P/D of 2.0, a small enhancement in performance is gained in the mid and low heat flux regions using a P/D of 1.8, which is an expected result.

h. TURBO-B Tubes with P/D of 1.5

Figure 5.47 shows the heat transfer performance of an upper tube, held at a constant heat flux, as the lower tube heat flux is decreased. There is very little difference in performance between a P/D of 1.5 and 1.8. Comparing the P/D of 1.5 to the 2.0 data, a small decrease in performance is noted for lower tube heat fluxes > 20 kW/m^2 using the P/D of 1.5 configuration, which cannot be explained.

i. TURBO-B Tubes with P/D of 1.2

Figure 5.48 shows the heat transfer performance of an upper tube, held at a constant heat flux, as the lower tube heat flux is decreased. Similar performance is noted for a P/D ratio of 1.2 and 1.5, therefore, the comments made previously still apply.
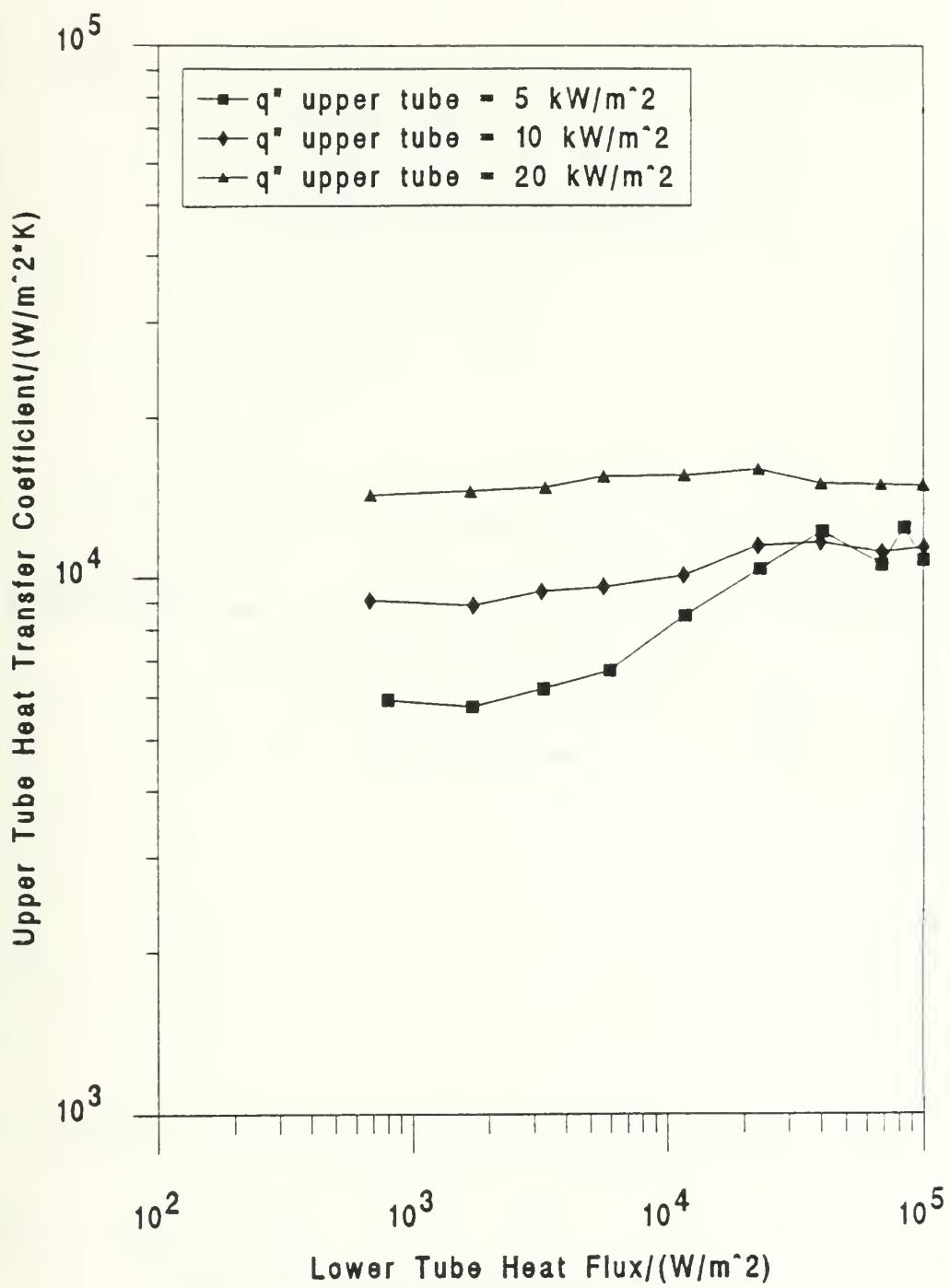
Figure 5.46   Heat Transfer Performance of a TURBO-B Upper
Tube at a Constant Heat Flux for a P/D of 1.8

121
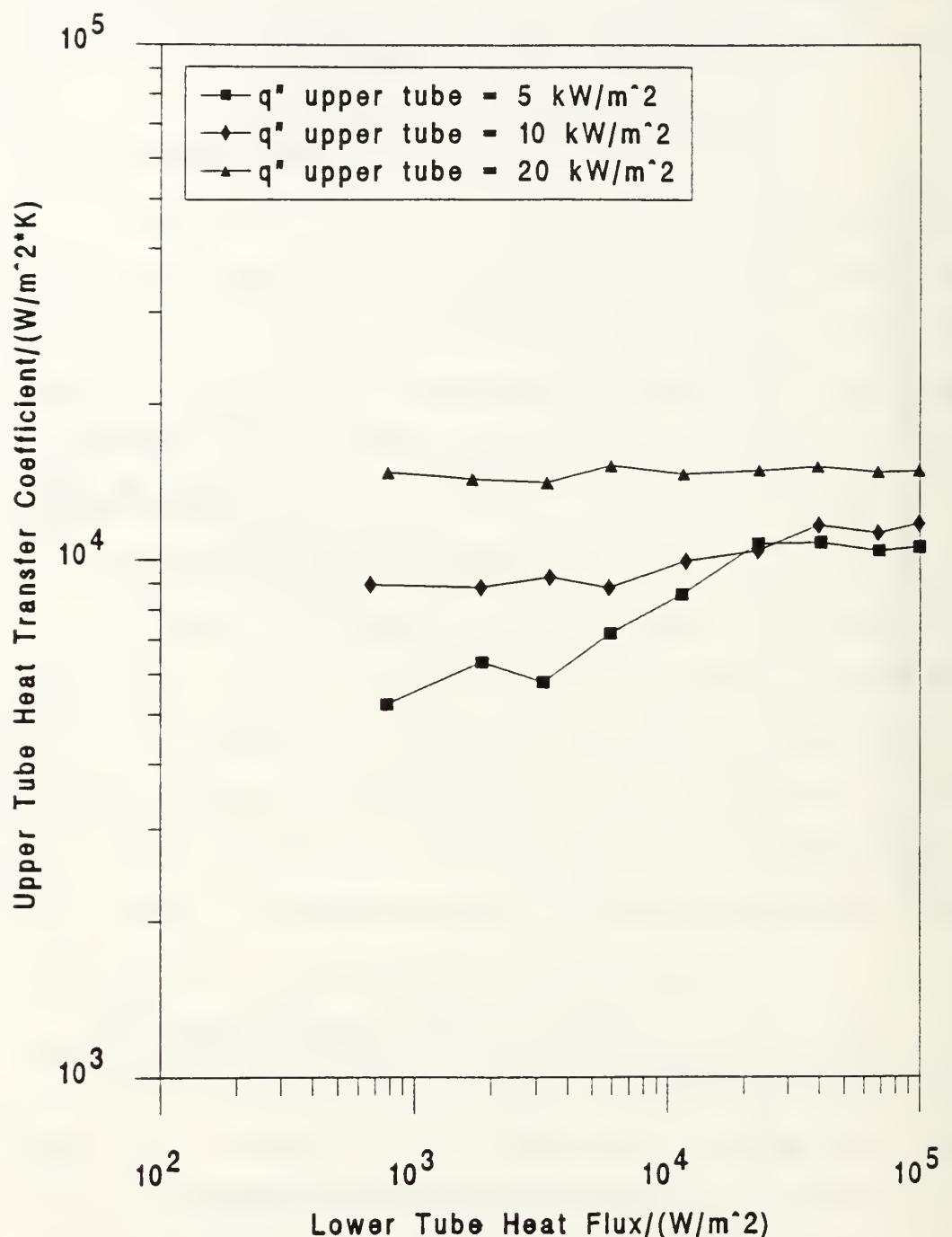
Figure 5.47   Heat Transfer Performance of a TURBO-B Upper
Tube at a Constant Heat Flux for a P/D of 1.5
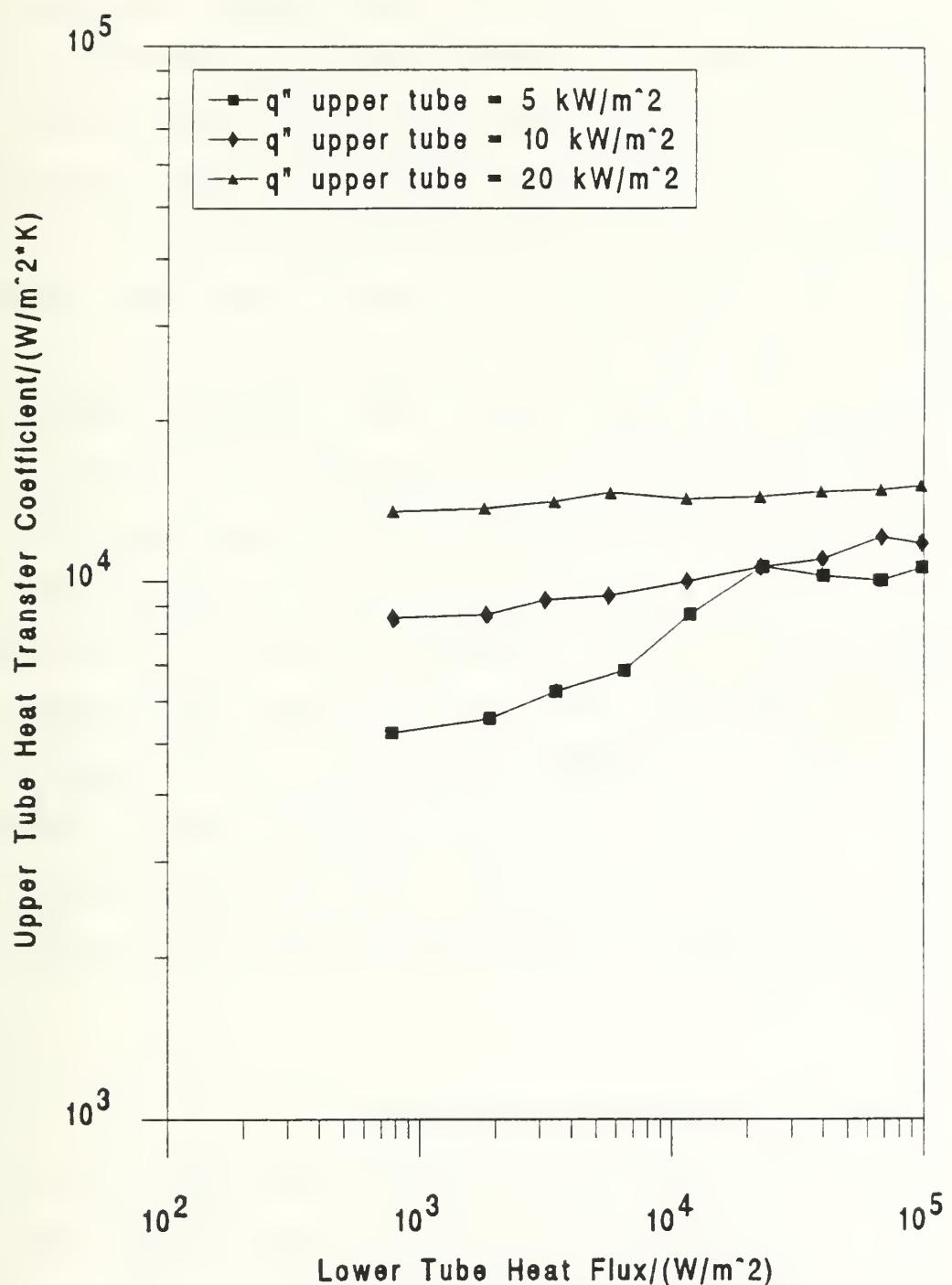
Figure 5.48   Heat Transfer Performance of a TURBO-B Upper
Tube at a Constant Heat Flux for a P/D of 1.2

123

j. TURBO-B Tubes with P/D of 1.2 (Rotated 30°)

Figure 5.49 shows the heat transfer performance of an upper tube, held at a constant heat flux, as the lower tube heat flux is decreased. Comparing Figures 5.48 and 5.49, for an UTHFS of 20 kW/m^2, the data curves are almost identical, indicating that the lower tube orientation and heat flux have very little influence on the upper tube heat transfer behavior. For the other two data curves, the in-line configuration provides better heat transfer performance because of *bubble pumping,* discussed earlier. For the offset configuration, all of the data curves do not merge and are almost horizontal lines, indicating there is no enhancement by *bubble pumping.* It is believed that most of the bubbles coming off the lower tube miss the upper tube because the bubbles depart the TURBO-B tube surface at the upper most section of the tube, which is different than how bubbles depart the smooth tube surface. This phenomena needs to be further investigated. No decreasing curves were recorded for these data runs.

C. R-124/R-114 PERFORMANCE COMPARISON

Figure 5.50 compares the decreasing heat flux data for R-124 found in this study with the R-114 data of Lake [Ref. 3] for smooth tube configurations listed in the plot legend, with the lower tube unheated. In the mid to high heat flux

124
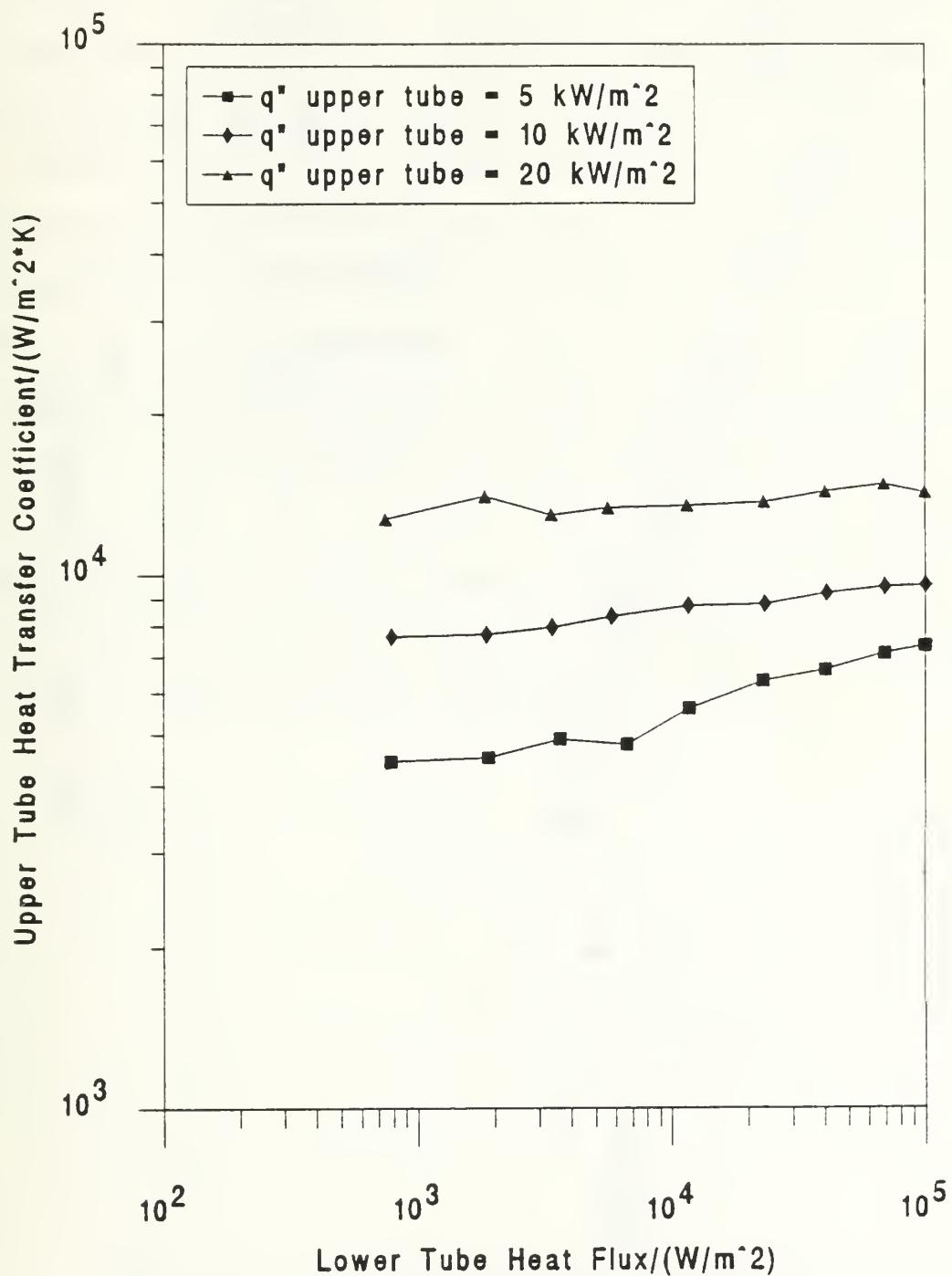
Figure 5.49   Heat Transfer Performance of a TURBO-B Upper
Tube at a Constant Heat Flux for a P/D of 1.2 (Rotated 30°)

125
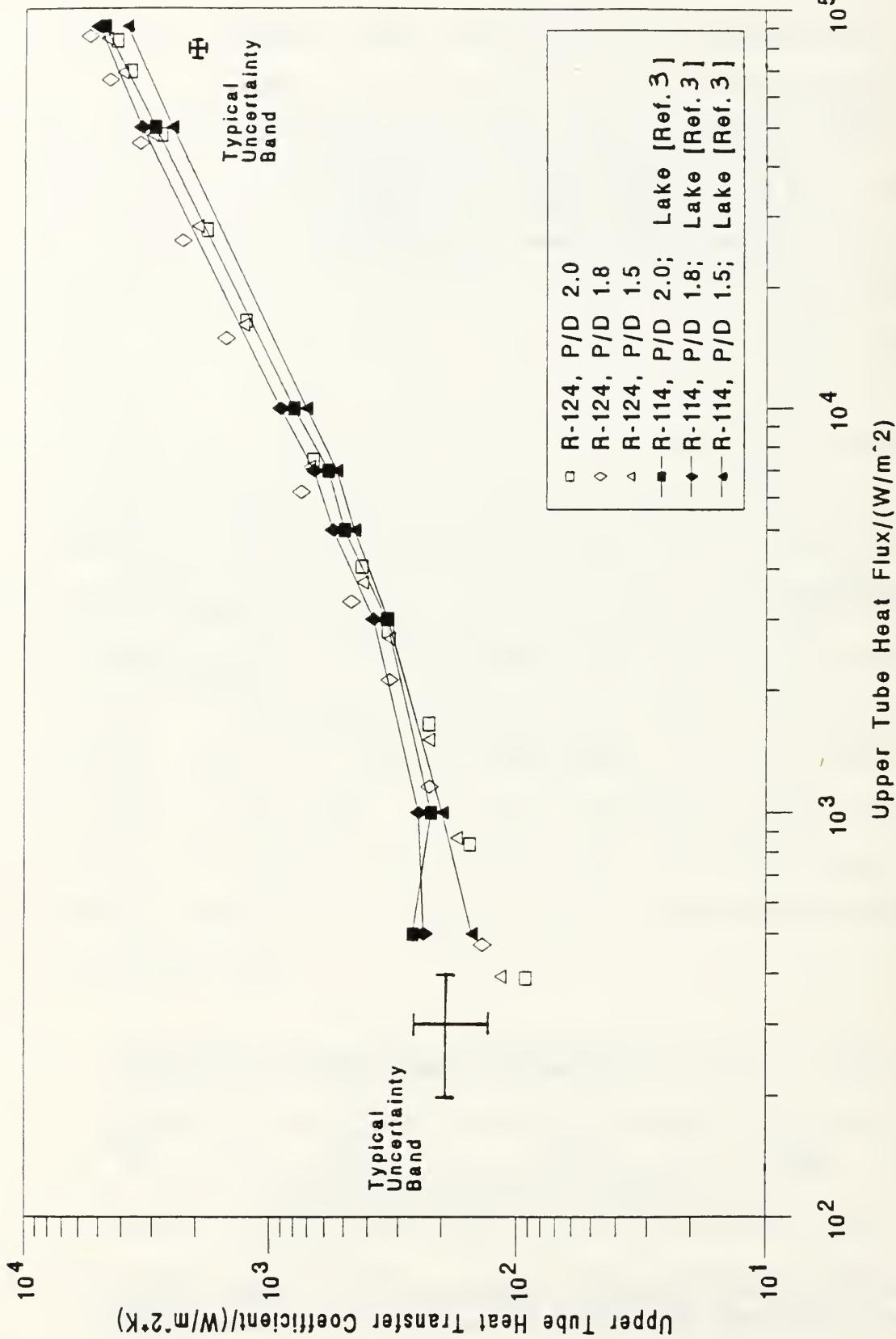
Figure 5.50 Comparison of R-124 to R-114 for Smooth Tubes
with Decreasing Heat Flux and the Lower Tube Unheated

126

regions, the P/D ratios of 1.8 and 1.5 demonstrated improved performance with the R-124, but with a P/D of 2.0, little or no improvement was found. In the low heat flux region, the uncertainty is too large to make any definitive conclusions.

Figure 5.51 compares the decreasing heat flux data for R-124 with the R-114 data of Lake [Ref. 3] for the smooth tube configurations listed in the plot legend, with 10 kW/m^2 on the lower tube. In the high heat flux region, a P/D of 1.8 and 1.5 again provided better performance using R-124, but for R-114, a P/D of 2.0 displayed slightly better performance. In the mid-range heat fluxes, R-114 exhibited improved performance in each of the three configurations. Again, in the low heat flux region, there was too much uncertainty in the data to draw any viable conclusions.
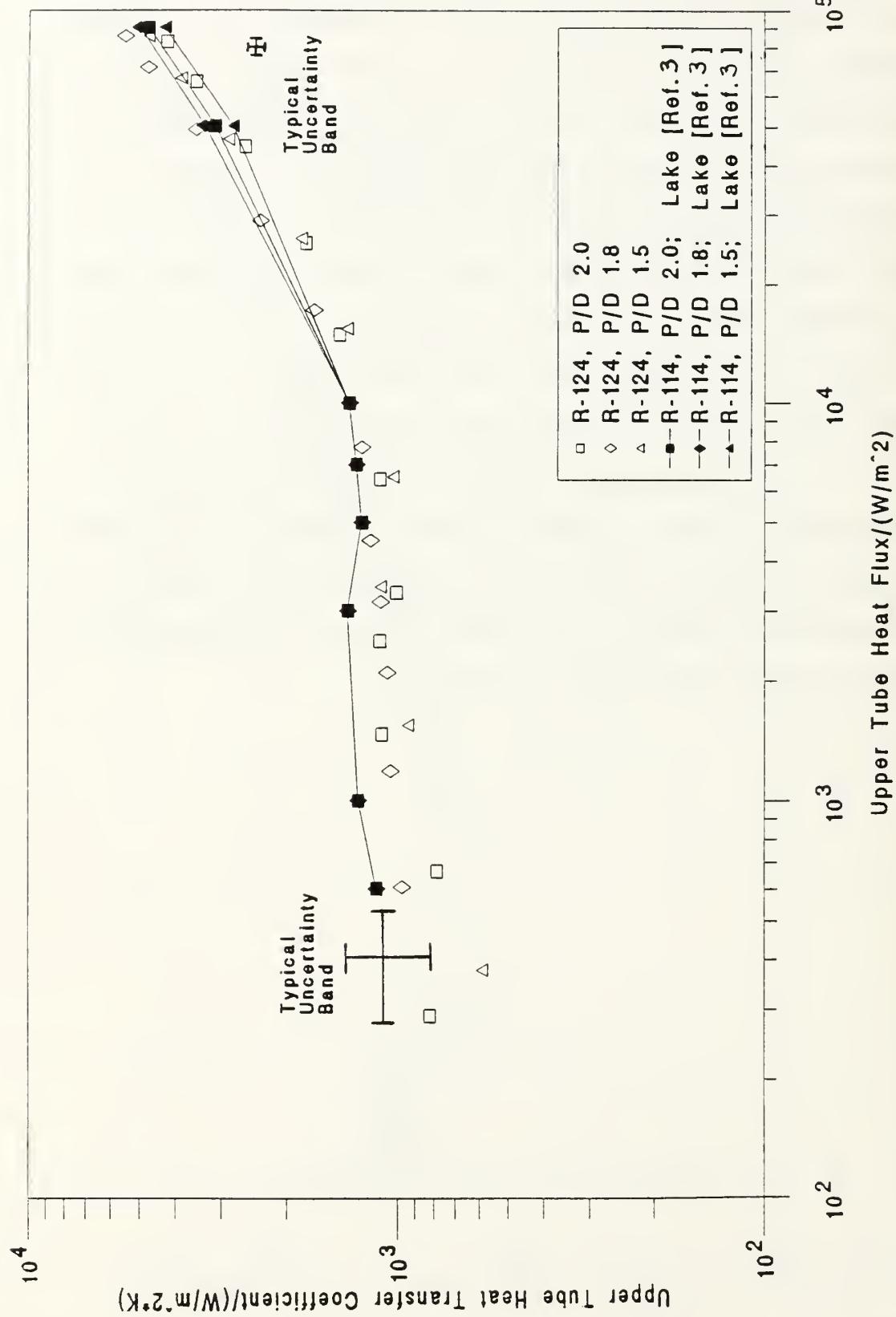
Figure 5.51 Comparison of R-124 to R-114 for Smooth Tubes with Decreasing Heat Flux and a LTHFS of 10 kW/m²

128

VI. CONCLUSIONS

The interaction effects of a lower heated tube on pool boiling of R-124 from an upper horizontal tube has been studied for tube two types: smooth and TURBO-B. Based on the data obtained, the following conclusions are made:

1. In natural convection, the effect of a lower heated tube on the heat transfer from an upper tube was small.

2. For a smooth tube array, a vigorously nucleating lower tube eliminated upper tube hysteresis.

3. For a smooth tube array in nucleate boiling, P/D of 1.8 gave the best upper tube heat transfer performance. No optimal P/D was found for the TURBO-B tube array.

4. For both arrays with upper tube heat fluxes < 5 kW/m^2, the enhancing effect of bubbles from a lower tube was dramatic. This enhancement increased as lower tube heat flux increased. When upper tube heat fluxes were > 20 kW/m^2, all enhancement disappeared.

5. For a TURBO-B tube array, a 30 degree offset of the upper tube reduced the upper tube heat transfer performance (compared to the in-line configurations). This may indicate bubbles depart TURBO-B tubes differently than smooth tubes.

6. For a smooth tube array with the lower tube unheated and an upper tube heat flux of > 3 kW/m^2, the performance of R-124 compared to R-114, improved as the P/D ratio was reduced. With a nucleating lower tube (at 10 kW/m^2), again the performance of R-124 improved as the P/D ratio decreased, but only for upper tube heat fluxes of > 40 kW/m^2.

129

VII.   RECOMMENDATIONS

1. Conduct further studies using TURBO-B tubes to verify that bubbles do depart the TURBO-B tubes differently than smooth tubes.

2. Conduct similar tests using different enhanced tubes to better understand the influence of a lower heated enhanced tube on the heat transfer behavior of an upper tube.

3. Modify the existing evaporator to accept a larger number of tubes (three and four smooth or enhanced tubes) and conduct tests to study the effect of multiple heated lower tubes on the heat transfer performance of an upper tube.

4. Conduct similar tests using multiple tube configurations with R-124/oil mixtures to determine the effect of oil on the heat transfer performance of an upper tube.

APPENDIX A.   PROGRAM SETUPJY

Program SETUPJY was used to evaluate the system performance prior to commencing a data collection run. This program is written in Hewlett-Packard Basic 5.0 language and enables the operator to:

1. Monitor the coolant sump temperature.

2. Monitor the evaporator liquid pool average temperature.

3. Monitor all the thermocouple channel output temperatures.

4. Monitor the voltage, current and power supplied to the upper tube heater (main heater) as well as the heater element electrical resistance.

5. Monitor the voltage, current and power supplied to the lower tube heater (auxiliary heater) as well as the heater element electrical resistance.

```
10!     PROGRAM: SETUPJY
20!     DATE:    MAY 15, 1993
30!     PROGRAMMER: LT DEAN SUGIYAMA
40!     MODIFIED BY LANNIE LAKE JAN 22, 1992
50!     MODIFIED BY GEORGE D. PERRY 10 APR 1993
60!     MODIFIED BY JOE YUSICIAN MAY 15, 1993
70      COM /Cc/ C(7)
80      DATA 0.10086091,25727.94369,-767345.8295,78025595.81,-9247486589,6.97688E+
11,-2.66192E+13
90      DATA 3.94078E+14
100     READ C(*)
110     ON KEY 1,15 GOTO 150
120     PRINTER IS 1
150     PRINT USING "2X,""SELECT OPTION"""
160     PRINT USING "6X,""0=MONITOR SUMP"""
170     PRINT USING "6X,""1=MONITOR LIQUID"""
180     PRINT USING "6X,""2=CHECK THERMOCOUPLES"""
190     PRINT USING "6X,""3=CHECK MAIN HEATER"""
200     PRINT USING "6X,""4=CHECK AUX HEATERS"""
210     PRINT USING "6X,""5=EXIT PROGRAM"""
230     BEEP
240     INPUT Ido
250     IF Ido>5 THEN Ido=5
260     IF Ido=0 THEN 340
270     IF Ido=1 THEN 520
280     IF Ido=2 THEN 690
290     IF Ido=3 THEN 870
300     IF Ido=4 THEN 870
310     IF Ido=5 THEN 1170
340     PRINT
350     PRINT "SUMP TEMPERATURE DEG C "
360     PRINT
370     OUTPUT 709;"AR AF19 AL19 VR5"
380     OUTPUT 709;"AS SA"
390     Sum=0
400     FOR J=1 TO 5
410     ENTER 709;E
420     Sum=Sum+E
430     NEXT J
440     Eave=Sum/5
450     Temp=FNTvsv(Eave)
460     PRINT USING "4X,MDD.DD";Temp
470     BEEP
480     PRINT
490     WAIT 5
500     GOTO 340
510!
520     PRINT
530     PRINT "LIQUID TEMPERATURE DEG C"
540     PRINT
550     OUTPUT 709;"AR AF16 AL18 VR5"
560     Sum=0
570     FOR I=1 TO 2
580     OUTPUT 709;"AS SA"
590     ENTER 709;E
600     Sum=Sum+E
610     NEXT I
620     Eave=Sum/2
630     Temp=FNTvsv(Eave)
640     PRINT USING "4X,MDD.DD";Temp
650     BEEP
660     WAIT 5
670     GOTO 610
```

132

```
680!
690    PRINT
700    PRINT "TEMPERATURE          DEG C"
710    OUTPUT 709;"AR AF00 AL19 VR5"
720    FOR I=1 TO 20
730    OUTPUT 709;"AS SA"
740    Sum=0
750    FOR J=1 TO 5
760    ENTER 709;E
770    Sum=Sum+E
780    NEXT J
790    Eave=Sum/5
800    Temp=FNTvsv(Eave)
810    PRINT TAB(3);I;TAB(15);Temp
820    NEXT I
830    BEEP
840    WAIT 5
850    GOTO 690
860!
870    PRINT
880    OUTPUT 709;"AR AF20 AL22 VR5"
890    FOR I=1 TO 3
900    OUTPUT 709;"AS SA"
910    Sum=0
920    FOR J=1 TO 5
930    ENTER 709;E
940    Sum=Sum+E
950    NEXT J
960    IF I=1 THEN Volt=Sum/5
970    IF I=2 AND Ido=3 THEN
980    PRINT "MAKE SURE VOLTAGE BOX IS SET TO MAIN HEATERS"
990    Amp=Sum/5
1000   END IF
1010   IF I=3 AND Ido=4 THEN
1020   PRINT "MAKE SURE VOLTAGE BOX IS SET TO AUX HEATERS"
1030   Amp=Sum/5
1040   END IF
1050   NEXT I
1060   Amp=ABS(Amp*1.9182)
1070   Volt=ABS(Volt*25)
1080   Power=Volt*Amp
1090   Resistance=Volt/Amp
1100   PRINT
1110   BEEP
1120   PRINT "VOLTAGE(V) CURRENT(A) RESISTENCE(ohms) POWER(W)"
1130   PRINT
1140   PRINT USING "1X,5(MDDDD.DD,4X)";Volt,Amp,Resistance,Power
1150   WAIT 5
1160   GOTO 870
1170   BEEP
1180   PRINT
1190   PRINT "SETUP COMPLETE"
1200   END
1210   DEF FNTvsv(V)
1220   COM /Cc/ C(7)
1230   T=C(0)
1240   FOR I=1 TO 7
1250   T=T+C(I)*V^I
1260   NEXT I
1270   T=T+8.626897E-2+T*(3.761199E-3-T*5.0689259E-5)
1280   RETURN T
1290   FNEND
```

133

APPENDIX B. PROGRAM DRPJY

This data acquisition/reduction program is written in Hewlett-Packard Basic 5.0 language and is listed on the following pages.

134

```
10    ! FILE NAME: DRPJY
20    ! DATE:        MAY 15, 1993
30    ! REVISED VERSION OF DRP72 FOR R-124 (2 INSTRUMENTED TUBES)
40    ! REVISED BY LT. GEORGE PERRY & LT. JOE YUSICIAN
50      COM /Idp/ Idp
60      PRINTER IS 1
70      CALL Select
80      BEEP
90      PRINT
100     PRINT "DATA COLLECTION COMPLETE"
110     END
120   !
130     SUB Main
140     COM /Iprop/ Ift
150     COM /Idp/ Idp
160     COM /Cc/ C(7),Ical
170     COM /Wil/ D2,Di,Do,L,Lu,Kcu
180     DIM Emf(20),T(20),D1a(13),D2a(13),Dia(13),Doa(13),La(13),Lua(13),Kcua(13),
Et(19),Tn$(4)[15]
190     DATA 0.10086091,25727.94369,-767345.8295,78025595.81
200     DATA -9247486589,6.97688E+11,-2.66192E+13,3.94078E+14
210     READ C(*)
220     DATA Smooth,High Flux,Turbo-B,High Flux Mod,Turbo-B Mod
230     READ Tn$(*)
240     PRINTER IS 701
250     PRINT
260     PRINT "            Date :",DATE$(TIMEDATE)
270     PRINT
280     PRINT USING "10X,""NOTE: Program name : DRPJY"""
290     BEEP
300   ! INPUT "ENTER INPUT MODE (0=3054A,1=FILE)",Im
310     Im=0
320   ! INPUT "SELECT FLUID (0=R-114,1=R-124)",Ift
330     Ift=1
340   ! INPUT "1 OR 2 TUBE OPERATION (ENTER 1 OR 2)",Hwmntu
350     Hwmntu=2
360   ! INPUT "SELECT HEATING MODE (0=ELEC; 1=WATER)",Ihm
370     Ihm=0
380   ! INPUT "ENTER THERMOCOUPLE TYPE (0=NEW,1=OLD)",Ical
390     Ical=0
400     INPUT "GIVE A NAME FOR THE RAW DATA FILE",D2_file$
410     PRINT USING "16X,""New file name: "",15A";D2_file$
420     Size1=20
430     CREATE BDAT D2_file$,Size1
440     ASSIGN @File2 TO D2_file$
450   !
460   ! DUMMY FILE UNTIL Nrun KNOWN
470     D1_file$="DUMMY"
480     CREATE BDAT D1_file$,Size1
490     ASSIGN @File1 TO D1_file$
500     OUTPUT @File1;Date$
510     BEEP
520     INPUT "ENTER NR OF DEFECTIVE UPPER TUBE TCS (0=DEFAULT, 2 MAX.)",Idtc
530     IF Idtc=0 THEN
540     Ldtc1=0
550     Ldtc2=0
560     PRINT USING "16X,""No defective UPPER TUBE TCs exist"""
570     END IF
580     IF Idtc=1 THEN
590     BEEP
600     INPUT "ENTER DEFECTIVE UPPER TUBE TC LOCATION (TEMP 1-8)",Ldtc1
610     PRINT USING "16X,""UPPER TUBE TC is defective at LOCATION:"",DD";Ldtc1
620     Ldtc2=0
630     END IF
640     IF Idtc=2 THEN
650     BEEP
660     INPUT "ENTER DEFECTIVE UPPER TUBE TC LOCATIONS (TEMP 1-8)",Ldtc1,Ldtc2
670     PRINT USING "16X,""UPPER TUBE TC are defective at LOCATIONS:"",DD,4X,DD";L
dtc1,Ldtc2
```

135

```
680     END IF
690     IF Idtc>2 THEN
700     BEEP
710     PRINTER IS 1
720     BEEP
730     PRINT "INVALID ENTRY"
740     PRINTER IS 701
750     GOTO 510
760     END IF
770     OUTPUT @File1;Ldtc1,Ldtc2
780     IF Hwmntu=1 THEN GOTO 1190
790     INPUT "ENTER NUMBER OF DEFECTIVE LOWER TUBE TCS (0=DEFAULT, 2 MAX)",Aidtc
800     IF Aidtc=0 THEN
810     Aldtc1=0
820     Aldtc2=0
830     PRINT USING "16X,""No defective LOWER TUBE TCs exist"""
840     END IF
850     IF Aidtc=1 THEN
860     BEEP
870     INPUT "ENTER DEFECTIVE TC LOWER TUBE LOCATIONS (TEMP 9-16)",Aldtc1
880     PRINT USING "16X,""LOWER TUBE TC is defective at LOCATION:"",DD";Aldtc1
890     Aldtc2=0
900     END IF
910     IF Aidtc=2 THEN
920     BEEP
930     INPUT "ENTER DEFECTIVE LOWER TUBE TC LOCATIONS (TEMP 9-16)",Aldtc1,Aldtc2
940     PRINT USING "16X,""LOWER TUBE TC are defective at LOCATIONS:"",DD,4X,DD";A
ldtc1,Aldtc2
950     END IF
960     IF Aidtc>2 THEN
970     BEEP
980     PRINTER IS 1
990     BEEP
1000    PRINT "INVALID ENTRY"
1010    PRINTER IS 701
1020    GOTO 790
1030    END IF
1040    OUTPUT @File1;Aldtc1,Aldtc2
1050    PRINTER IS 1
1060    BEEP
1070    PRINT USING "2X,""Select tube number"""
1080    PRINT USING "6X,""4   Wieland Hard 8 inch"""
1090    PRINT USING "6X,""5   HIGH FLUX 8 inch"""
1100!   PRINT USING "6X,""6   GEWA-K 40 Fins/in"""
1110!   PRINT USING "6X,""7   GEWA-K 26 Fins/in"""
1120!   PRINT USING "6X,""8   GEWA-T 19 Fins/in"""
1130!   PRINT USING "6X,""9   GEWA-T OR GEWA-TY 26 Fins/in"""
1140!   PRINT USING "6X,""10 THERMOEXCEL-E"""
1150!   PRINT USING "6X,""11 THERMOEXCEL-HE"""
1160    PRINT USING "6X,""12 TURBO-B"""
1170!   PRINT USING "6X,""13 GEWA-K 19 Fins/in"""
1180    INPUT Itt
1190    OUTPUT @File1;Itt
1200    PRINTER IS 701
1210    IF Itt=4 THEN PRINT USING "16X,""Tubes:  Wieland Hard 8 inch"""
1220    IF Itt=12 THEN PRINT USING "16X,""Tubes:  Turbo-B"""
1230    IF Itt=5 THEN PRINT USING "16X,""Tubes:  High Flux 8 inch"""
1240!   IF Itt<10 THEN PRINT USING "16X,""Tube Number:   "",D";Itt
1250!   IF Itt>9 THEN PRINT USING "16X,""Tube Number:   "",DD";Itt
1260!   INPUT "ENTER OUTPUT VERSION (0=LONG,1=SHORT,2=NONE)",Iov
1270    Iov=0
1280!   INPUT "SELECT (0=LIQ,1=VAP,2=(LIQ+VAP)/2)",Ilqv
1290    Ilqv=2
1300!
1310!   DIMENSIONS FOR TESTED TUBES
1320!
1330!   D1=Diameter at thermocouple positions
1340    DATA .0111125,.0111125,.0111125,.0129540,.012446,.0129540,.0100965
1350    DATA .0100965,.01157,.01157,.01157,.01157,.01157,.0100965
1360    READ D1a(*)
1370    D1=D1a(Itt)
```

136

```
1380!
1390! D2=Diameter of test section to the base of fins
1400   DATA .015875,.015875,.015875,.015824,.015875,.015824,.01270
1410   DATA .0127,.0138,.0138,.0138,.0138,.0138,.0127
1420   READ D2a(*)
1430   D2=D2a(Itt)
1440!
1450! Di=Inside diameter of unenhanced ends
1460   DATA .0127,.0127,.0127,.0132,.0127,.0132,.0111125,.0111125
1470   DATA .0118,.0118,.0118,.0118,.0118,.0111125
1480   READ Dia(*)
1490   Di=Dia(Itt)
1500!
1510! Do=Outside diameter of unenhanced ends
1520   DATA .015875,.015875,.015875,.015824,.015875,.015824,.01270,.01270
1530   DATA .01331,.01331,.01331,.01331,.0158,.0127
1540   READ Doa(*)
1550   Do=Doa(Itt)
1560!
1570! L=Length of enhanced surface
1580   DATA .1016,.1016,.1016,.1016,.2032,.2032,.2032,.2032,.2032,.2032,.2032,.20
32,.2032,.2032
1590   READ La(*)
1600   L=La(Itt)
1610!
1620! Lu=Length of unenhanced surface at the ends
1630   DATA .0254,.0254,.0254,.0254,.0762,.0762,.0762,.0762,.0762,.0762,.0762,.07
62,.0762,.0762
1640   READ Lua(*)
1650   Lu=Lua(Itt)
1660!
1670! Kcu=Thermal Conductivity of tube
1680   DATA 398,344,344,45,344,45,344,344,398,398,398,398,398,344
1690   READ Kcua(*)
1700   Kcu=Kcua(Itt)
1710!
1720   Xn=.8
1730   Fr=.3
1740   Cf=3.7037E+10
1750   A=PI*(Do^2-Di^2)/4
1760   P=PI*Do
1770   Nsub=0
1780   Ntc=20
1790   J=1
1800 Repeat: !
1810   Dtld=2.22
1820   Ido=2
1830   ON KEY 1,15 RECOVER 1800
1840   PRINTER IS 1
1850   PRINT USING "2X,""SELECT OPTION"""
1860   PRINT USING "6X,""0=TAKE DATA"""
1870   PRINT USING "6X,""1=SET UPPER TUBE HEAT FLUX (MAIN)"""
1880   PRINT USING "6X,""2=SET Tsat"""
1890   PRINT USING "6X,""3=SET LOWER TUBE HEAT FLUX (AUX)"""
1900   BEEP
1910   INPUT Ido
1920   IF Ido>3 THEN Ido=3
1930   IF Ido=0 THEN 3680
1940!
1950! LOOP TO SET UPPER TUBE HEAT FLUX
1960   IF Ido=1 THEN
1970   OUTPUT 709;"AR AF20 AL21 VR5"
1980   PRINT "SET VOLT BOX TO MAIN"
1990   BEEP
2000   INPUT "ENTER DESIRED Qdp",Dqdp
2010   PRINT USING "4X,""DESIRED Qdp  ACTUAL Qdp"""
```

137

```
2020   Err=1000
2030   FOR I=1 TO 2
2040   OUTPUT 709;"AS SA"
2050   Sum=0
2060   FOR Ji=1 TO 5
2070   ENTER 709;E
2080   Sum=Sum+E
2090   NEXT Ji
2100   IF I=1 THEN Volt=Sum/5
2110   IF I=2 THEN Amp=Sum/5
2120   NEXT I
2130   Amp=ABS(Amp*1.9182)
2140   Volt=ABS(Volt*25)
2150   Aqdp=Volt*Amp/(PI*D2*L)
2160   IF ABS(Aqdp-Dqdp)>Err THEN
2170   IF Aqdp>Dqdp THEN
2180   BEEP 4000,.2
2190   BEEP 4000,.2
2200   BEEP 4000,.2
2210   ELSE
2220   BEEP 250,.2
2230   BEEP 250,.2
2240   BEEP 250,.2
2250   END IF
2260   PRINT USING "4X,MZ.3DE,2X,MZ.3DE";Dqdp,Aqdp
2270   WAIT 2
2280   GOTO 2030
2290   ELSE
2300   BEEP
2310   PRINT USING "4X,MZ.3DE,2X,MZ.3DE";Dqdp,Aqdp
2320   Err=500
2330   WAIT 2
2340   GOTO 2030
2350   END IF
2360   END IF
2370!
2380! LOOP TO SET Tsat
2390   IF Ido=2 THEN
2400   IF Ikdt=1 THEN 2440
2410   Dtld=2.22
2420! PRINT USING "4X,"" DTsat   ATsat    Rate    Tv      Rate"""
2430   Ikdt=1
2440   Old1=0
2450   Old2=0
2460   Nn=1
2470   Nrs=Nn MOD 15
2480   Nn=Nn+1
2490   IF Nrs=1 THEN
2500   PRINT USING "4X,"" Tsat    Tld1     Tld2     Tv     Tsump"""
2510   END IF
2520   OUTPUT 709;"AR AF16 AL19 VR5"
2530   FOR I=1 TO 6
2540   IF I>4 THEN 2700
2550   Sum=0
2560   OUTPUT 709;"AS SA"
2570   FOR Ji=1 TO 20
2580   ENTER 709;Eliq
2590   Sum=Sum+Eliq
2600   NEXT Ji
2610   Eliq=Sum/20
2620   Tld=FNTvsv(Eliq)
2630   IF I=1 THEN Tld1=Tld
2640   IF I=2 THEN Tld2=Tld
2650   IF I=3 THEN Tv=Tld
2660   IF I=4 THEN Tsump=Tld
2670   IF I=5 THEN Tinlet=Tld
2680   IF I=6 THEN Tout=Tld
```

138

```
2690   NEXT I
2700   Atld=(Tld1+Tld2)*.5
2710   IF ABS(Atld-Dtld)>.2 THEN
2720   IF Atld>Dtld THEN
2730   BEEP 4000,.2
2740   BEEP 4000,.2
2750   BEEP 4000,.2
2760   ELSE
2770   BEEP 250,.2
2780   BEEP 250,.2
2790   BEEP 250,.2
2800   END IF
2810   Err1=Atld-Old1
2820   Old1=Atld
2830   Err2=Tv-Old2
2840   Old2=Tv
2850   IF Tld1>100. THEN 2880
2860   PRINT USING "4X,5(MDD.DD,2X)";Dtld,Tld1,Tld2,Tv,Tsump
2870   WAIT 2
2880   GOTO 2470
2890   ELSE
2900   IF ABS(Atld-Dtld)>.1 THEN
2910   IF Atld>Dtld THEN
2920   BEEP 3000,.2
2930   BEEP 3000,.2
2940   ELSE
2950   BEEP 800,.2
2960   BEEP 800,.2
2970   END IF
2980   Err1=Atld-Old1
2990   Old1=Atld
3000   Err2=Tv-Old2
3010   Old2=Tv
3020   PRINT USING "4X,5(MDDD.DD,2X)";Dtld,Tld1,Tld2,Tv,Tsump
3030   WAIT 2
3040   GOTO 2470
3050   ELSE
3060   BEEP
3070   Err1=Atld-Old1
3080   Old1=Atld
3090   Err2=Tv-Old2
3100   Old2=Tv
3110   PRINT USING "4X,5(MDDD.DD,2X)";Dtld,Tld1,Tld2,Tv,Tsump
3120   WAIT 2
3130   GOTO 2470
3140   END IF
3150   END IF
3160   END IF
3170   !
3180!  LOOP TO SET LOWER TUBE HEAT FLUX
3190   IF Ido=3 THEN
3200   PRINT " SET VOLT BOX TO AUX"
3210   OUTPUT 709;"AR AF20 AL22 VR5"
3220   BEEP
3230   INPUT "ENTER DESIRED AuQdp",Duxqdp
3240   PRINT USING "2X,""DESIRED AuxQdp   ACTUAL AuxQdp"""
3250   Err=1000
3260   FOR I=1 TO 3
3270   OUTPUT 709;"AS SA"
3280   Sum=0
3290   FOR Ji=1 TO 5
3300   ENTER 709;E
3310   Sum=Sum+E
3320   NEXT Ji
3330   IF I=1 THEN Volt=Sum/5
3340   IF I=3 THEN Amp=Sum/5
3350   NEXT I
```

139

```
3360    Amp=ABS(Amp*1.9182)
3370    Volt=ABS(Volt*25)
3380    Auxqdp=Volt*Amp/(PI*D2*L)
3390    IF ABS(Auxqdp-Duxqdp)>Err THEN
3400    IF Auxqdp>Duxqdp THEN
3410    BEEP 4000,.2
3420    BEEP 4000,.2
3430    BEEP 4000,.2
3440    ELSE
3450    BEEP 250,.2
3460    BEEP 250,.2
3470    BEEP 250,.2
3480    END IF
3490    PRINT USING "4X,MZ.3DE,2X,MZ.3DE";Duxqdp,Auxqdp
3500    WAIT 2
3510    GOTO 3260
3520    ELSE
3530    BEEP
3540    PRINT USING "4X,MZ.3DE,2X,MZ.3DE";Duxqdp,Auxqdp
3550    Err=500
3560    WAIT 2
3570    GOTO 3260
3580    END IF
3590    GOTO 1850
3600    END IF
3610!   ERROR TRAP FOR Ido OUT OF BOUNDS
3620    IF Ido>3 THEN
3630    BEEP
3640    GOTO 1850
3650    END IF
3660!
3670!   TAKE DATA LOOP
3680    IF Ikol=1 THEN 3730
3690    BEEP
3700    Ikol=1
3710    INPUT "ENTER BULK OIL %",Bop
3720    Ikol=1
3730    OUTPUT 709;"AR AF00 AL19 VR5"
3740    Ntc=20
3750    FOR I=1 TO Ntc
3760    OUTPUT 709;"AS SA"
3770    Sum=0
3780    FOR Ji=1 TO 20
3790    ENTER 709;E
3800    Sum=Sum+E
3810    IF I=(17-Nsub) OR I=(18-Nsub) THEN Et(Ji-1)=E
3820    NEXT Ji
3830    Kdl=0
3840    IF I=(17-Nsub) OR I=(18-Nsub) THEN
3850    Eave=Sum/20
3860    Sum=0.
3870    FOR Jk=0 TO 19
3880    IF ABS(Et(Jk)-Eave)<5.0E-6 THEN
3890    Sum=Sum+Et(Jk)
3900    ELSE
3910    Kdl=Kdl+1
3920    END IF
3930    NEXT Jk
3940    IF I=(17-Nsub) OR I=(18-Nsub) THEN PRINT USING "4X,""Kdl = "",DD";Kdl
3950    IF Kdl>20 THEN
3960    BEEP
3970    BEEP
3980    PRINT USING "4X,""Too much scattering in data - repeat data set"""
3990    GOTO 1840
4000    END IF
4010    END IF
4020    Emf(I)=Sum/(20-Kdl)
```

140

```
4030    NEXT I
4040    Coun=0.
4050    OUTPUT 709;"AR AF20 AL22 VR5"
4060    FOR I=1 TO 3
4070    OUTPUT 709;"AS SA"
4080    Sum=0
4090    FOR J1=1 TO 5
4100    ENTER 709;E
4110    Sum=Sum+E
4120    NEXT J1
4130    IF Coun=0. THEN
4140    IF I=1 THEN Vr=Sum/5
4150    IF I=2 THEN Ir=Sum/5
4160    ELSE
4170    IF I=1 THEN Avr=Sum/5
4180    IF I=3 THEN Air=Sum/5
4190    END IF
4200    NEXT I
4210    IF Coun=0 THEN
4220    PRINT "SHIFT VOLT BOX TO AUX"
4230    END IF
4240    IF Coun=1 THEN GOTO 4290
4250    INPUT "TAKE AUX READINGS(1=YES)?",Ccon
4260    IF Ccon>1 THEN GOTO 4250
4270    Coun=Coun+Ccon
4280    GOTO 4060
4290!
4300!   CONVERT emf'S TO TEMP,VOLT,CURRENT
4310    Twa=0
4320    Atwa=0
4330    FOR I=1 TO Ntc
4340    IF Idtc>0 THEN
4350    IF I=Ldtc1 OR I=Ldtc2 THEN
4360    T(I)=-99.99
4370    GOTO 4470
4380    END IF
4390    END IF
4400    IF Aidtc>0 THEN
4410    IF I=Aldtc1 OR I=Aldtc2 THEN
4420    T(I)=-99.99
4430    GOTO 4470
4440    END IF
4450    END IF
4460    T(I)=FNTvsv(Emf(I))
4470    NEXT I
4480    Twa=Twa/(4-Idtc)
4490    FOR I=1 TO 8
4500    IF I=Ldtc1 OR I=Ldtc2 THEN
4510    Twa=Twa
4520    ELSE
4530    Twa=Twa+T(I)
4540    END IF
4550    NEXT I
4560    Tw=Twa/(8-Idtc)
4570    FOR I=9 TO 16
4580    IF I=Aldtc1 OR I=Aldtc2 THEN
4590    Atwa=Atwa
4600    ELSE
4610    Atwa=Atwa+T(I)
4620    END IF
4630    NEXT I
4640    Atw=Atwa/(8-Aidtc)
4650    Tld=T(17-Nsub)
4660    Tld2=T(18-Nsub)
4670    Tlda=(Tld+Tld2)*.5
4680    Tv=T(19-Nsub)
4690    Tsump=T(20-Nsub)
```

141

```
4700    Amp=ABS(Ir*1.9182)
4710    Volt=ABS(Vr)*25
4720    Q=Volt*Amp
4730    Auamp=ABS(Air*1.9182)
4740    Auvolt=ABS(Avr)*25
4750    Auq=Auvolt*Auamp
4760    Kcu=Kcua(Itt)
4770!
4780!   FOURIER CONDUCTION EQUATION WITH CONTACT RESISTANCE NEGLECTED
4790    Tw=Tw-Q*LOG(D2/D1)/(2*PI*Kcu*L)
4800    Atw=Atw-Auq*LOG(D2/D1)/(2*PI*Kcu*L)
4810    Tsat=(Tlda+Tv)*.5
4820!
4830!   COMPUTE THETHAB
4840    Thetab=Tw-Tsat
4850    Athetab=Atw-Tsat
4860    IF Thetab<0 THEN
4870    BEEP
4880    INPUT "UPPER TWALL<TSAT (0=CONTINUE, 1=END)",Iev
4890    IF Iev=0 THEN GOTO 3150
4900    IF Iev=1 THEN 1850
4910    END IF
4920    IF Athetab<0 THEN
4930    BEEP
4940    INPUT "LOWER TWALL<TSAT (0=CONTINUE, 1=END)",Aiev
4950    IF Aiev=0 THEN GOTO 3150
4960    IF Aiev=1 THEN 1850
4970    END IF
4980!
4990!   COMPUTE VARIOUS PROPERTIES
5000    Tfilm=(Tw+Tsat)*.5
5010    Rho=FNRho(Tfilm)
5020    Mu=FNMu(Tfilm)
5030    K=FNK(Tfilm)
5040    Cp=FNCp(Tfilm)
5050    Beta=FNBeta(Tfilm)
5060    Hfg=FNHfg(Tsat)
5070    Ni=Mu/Rho
5080    Alpha=K/(Rho*Cp)
5090    Pr=Ni/Alpha
5100    Psat=FNPsat(Tsat)
5110!
5120!   COMPUTE VARIOUS PROPERTIES FOR AUX TUBE
5130    Atfilm=(Atw+Tsat)*.5
5140    Arho=FNRho(Atfilm)
5150    Amu=FNMu(Atfilm)
5160    Ak=FNK(Atfilm)
5170    Acp=FNCp(Atfilm)
5180    Abeta=FNBeta(Atfilm)
5190    Ani=Amu/Arho
5200    Aalpha=Ak/(Arho*Acp)
5210    Apr=Ani/Aalpha
5220!
5230!   COMPUTE NATURAL-CONVECTIVE HEAT-TRANSFER COEFFICIENT
5240!   FOR UNENHANCED END(S)
5250    Hbar=190
5260    Fe=(Hbar*P/(Kcu*A))^.5*Lu
5270    Tanh=FNTanh(Fe)
5280    Theta=Thetab*Tanh/Fe
5290    Xx=(9.81*Beta*Thetab*Do^3*Tanh/(Fe*Ni*Alpha))^.166667
5300    Yy=(1+(.559/Pr)^(9/16))^(8/27)
5310    Hbarc=K/Do*(.6+.387*Xx/Yy)^2
5320    IF ABS((Hbar-Hbarc)/Hbarc)>.001 THEN
5330    Hbar=(Hbar+Hbarc)*.5
5340    GOTO 5260
5350    END IF
5360!
5370!   COMPUTE NATURAL-CONVECTIVE HEAT-TRANSFER COEFFICIENT
5380!   FOR UNENHANCED END(S) FOR AUX TUBE
5390    Ahbar=190
5400    Fe=(Ahbar*P/(Kcu*A))^.5*Lu
5410    Atanh=FNTanh(Fe)
```

142

```
5420    Atheta=Athetab*Atanh/Fe
5430    Axx=(9.81*Abeta*Athetab*Do^3*Atanh/(Fe*Ani*Aalpha))^.166667
5440    Ayy=(1+(.559/Apr)^(9/16))^(8/27)
5450    Ahbarc=Ak/Do*(.6+.387*Axx/Ayy)^2
5460    IF ABS((Ahbar-Ahbarc)/Ahbarc)>.001 THEN
5470    Ahbar=(Ahbar+Ahbarc)*.5
5480    GOTO 5400
5490    END IF
5500!
5510! COMPUTE HEAT LOSS RATE THROUGH UNENHANCED END(S)
5520    Q1=(Hbar*P*Kcu*A)^.5*Thetab*Tanh
5530    Qc=Q-2*Q1
5540    As=PI*D2*L
5550    !
5560    !COMPUTE HEAT LOSS RATE THROUGH UNENHANCED END(S) OF AUX TUBE
5570    Aq1=(Ahbar*P*Kcu*A)^.5*Athetab*Atanh
5580    Aqc=Auq-2*Aq1
5590!
5600! COMPUTE ACTUAL HEAT FLUX AND BOILING COEFFICIENT
5610    Qdp=Qc/As
5620    Htube=Qdp/Thetab
5630    Csf=(Cp*Thetab/Hfg)/(Qdp/(Mu*Hfg)*(.014/(9.81*Rho)^.5)^(1/3.)*Pr^1.7)
5640!
5650! COMPUTE ACTUAL HEAT FLUX AND BOILING COEFFICIENT FOR AUX TUBE
5660    Auqdp=Aqc/As
5670    Ahtube=Auqdp/Athetab
5680    Acsf=(Acp*Athetab/Hfg)/(Auqdp/(Amu*Hfg)*(.014/(9.81*Arho)^.5)^(1/3.)*Apr^1
.7)
5690!
5700! COMPUTE CHURCHILL-CHU CORRELATION FOR UPPER TUBE
5710    Cc=Hbar*Thetab
5720!
5730! RECORD TIME OF DATA TAKING
5740    OUTPUT 709;"TD"
5750    ENTER 709;Told$
5760!
5770! OUTPUT DATA TO PRINTER
5780    PRINTER IS 701
5790    PRINT
5800    PRINT USING "10X,""Data Set Number = "",DDD,2X,""Bulk Oil % = "",DD.D";J,B
op
5810    PRINT "            TIME:",TIME$(TIMEDATE)
5820    PRINT
5830    PRINT USING "10X,""TC No:    1      2      3      4      5      6      7
    8"""
5840    PRINT USING "10X,""Temp :"",8(1X,MDD.DD)";T(1),T(2),T(3),T(4),T(5),T(6),T(
7),T(8)
5850    PRINT USING "10X,""TC No:    9      10     11     12     13     14     15
    16"""
5860    PRINT USING "10X,""Temp :"",8(1X,MDD.DD)";T(9),T(10),T(11),T(12),T(13),T(1
4),T(15),T(16)
5870    PRINT
5880    PRINT USING "10X,""  Twa    ATwa   Tliqd  Tliqd2 Tvapr  Psat   Tsat   Tsu
mp"""
5890    PRINT USING "10X,3(MDD.DD,1X),1X,MDD.DD,1X,3(1X,MDD.DD),2X,MDD.D";Tw,Atw,T
ld,Tld2,Tv,Psat,Tsat,Tsump
5900    PRINT USING "10X,""     Vr      Ir      Cc"""
5910    PRINT USING "10X,2(MDDD.DD,3X),1X,MZ.3DE";Vr,Ir,Cc
5920    PRINT USING "10X,"" Thetab    Htube     Qdp    Athetab Ahtube    AuQd
p"""
5930    PRINT USING "10X,MDD.3D,1X,MZ.3DE,1X,MZ.3DE,1X,MDD.3D,1X,MZ.3DE,1X,MZ.3DE"
;Thetab,Htube,Qdp,Athetab,Ahtube,Auqdp
5940    PRINT
5950    BEEP
5960    INPUT "OK TO STORE THIS DATA SET (1=Y,0=N)?",Ok
5970    IF Ok=1 THEN J=J+1
5980    IF Ok=1 AND Im=0 THEN
5990    OUTPUT @File1;Bop,Told$,Emf(*),Vr,Ir,Avr,Air
6000    END IF
6010    IF Iuf=1 THEN OUTPUT @Ufile;Vw,Uo
6020    IF Ire=1 THEN OUTPUT @Refile;Fms,Rew
6030    BEEP
```

```
6040    INPUT "WILL THERE BE ANOTHER RUN (1=Y,0=N)?",Go_on
6050    Nrun=J
6060    IF Go_on=0 THEN 6080
6070    IF Go_on<>0 THEN Repeat
6080    BEEP
6090    PRINT
6100    PRINT USING "10X,""NOTE: "",ZZ,"" data runs were stored in file "",15A";J-
1,D2_file$
6110    ASSIGN @File1 TO *
6120    OUTPUT @File2;Nrun-1
6130    ASSIGN @File1 TO D1_file$
6140    ENTER @File1;Date$,Ldtc1,Ldtc2,Itt
6150    ENTER @File1;Aldtc1,Aldtc2
6160    OUTPUT @File2;Date$,Ldtc1,Ldtc2,Itt
6170    OUTPUT @File2;Aldtc1,Aldtc2
6180    FOR I=1 TO Nrun-1
6190    ENTER @File1;Bop,Told$,Emf(*),Vr,Ir
6200    ENTER @File1;Avr,Air
6210    OUTPUT @File2;Bop,Told$,Emf(*),Vr,Ir
6220    OUTPUT @File2;Avr,Air
6230    NEXT I
6240    ASSIGN @File1 TO *
6250    PRINTER IS 1
6260    PURGE "DUMMY"
6270    PRINT
6280    PRINT "DUMMY FILE PURGED"
6290    SUBEND
6300 !
6310 ! CURVE FITS OF PROPERTY FUNCTIONS
6320 !
6330    DEF FNKcu(T)
6340 ! OFHC COPPER 250 TO 300 K
6350    Tk=T+273.15      !C TO K
6360    K=434-.112*Tk
6370    RETURN K
6380    FNEND
6390 !
6400    DEF FNMu(T)
6410    COM /Iprop/ Ift
6420    IF Ift=1 THEN
6430    !223 TO 373 K
6440 ! 170 TO 360 K CURVE FIT OF VISCOUSITY
6450    Tk=T+273.15      !C TO K
6460    Mu=EXP(-4.4636+(1011.47/Tk))*1.0E-3
6470    END IF
6480    IF Ift=1 THEN
6490 ! 223 TO 373 K
6500    Mu=3.4593-4.26E-2*T+3.9485E-4*T^2-4.193E-6*T^3+2.0709E-8*T^4
6510    Mu=Mu*1.0E-4
6520    END IF
6530    RETURN Mu
6540    FNEND
6550 !
6560    DEF FNCp(T)
6570    COM /Iprop/ Ift
6580    IF Ift=0 THEN
6590 ! 180 TO 400 K CURVE FIT OF Cp
6600    Tk=T+273.15      !C TO K
6610    Cp=.40188+1.65007E-3*Tk+1.51494E-6*Tk^2-6.67853E-10*Tk^3
6620    Cp=Cp*1000
6630    END IF
6640    IF Ift=1 THEN
6650 ! 223 TO 373 K CURVE FIT Cp(R124)
6660    Cp=1.0542+2.1405E-3*T+1.0709E-5*T^2-6.4721E-8*T^3-1.4324E-9*T^4+4.136E-11*
T^5
6670    Cp=Cp*1000
6680    END IF
6690    RETURN Cp
6700    FNEND
```

144

```
6710!
6720  DEF FNRho(T)
6730  COM /Iprop/ Ift
6740  IF Ift=0 THEN
6750  Tk=T+273.15        !C TO K
6760  X=1-(1.8*Tk/753.95)   !K TO R
6770  Ro=36.32+61.146414*X^(1/3)+16.418015*X+17.476838*X^.5+1.119828*X^2
6780  Ro=Ro/.062428
6790  END IF
6800  IF Ift=1 THEN
6810! 223 TO 373 K (R124)
6820  Ro=1434.8-2.8619*T-6.7267E-3*T^2-7.2852E-5*T^3
6830  END IF
6840  RETURN Ro
6850  FNEND
6860!
6870  DEF FNK(T)
6880  COM /Iprop/ Ift
6890  IF Ift=0 THEN
6900! T<360 K WITH T IN C
6910  K=.071-.000261*T
6920  END IF
6930! RETURN K
6940  IF Ift=1 THEN
6950! 223 TO 373 K (R-124)
6960  K=7.5191E-2-3.5436E-4*T-1.9545E-7*T^2+3.1835E-9*T^3
6970  END IF
6980  RETURN K
6990  FNEND
7000!
7010  DEF FNTanh(X)
7020  P=EXP(X)
7030  Q=1/P
7040  Tanh=(P-Q)/(P+Q)
7050  RETURN Tanh
7060  FNEND
7070!
7080  DEF FNTvsv(V)
7090  COM /Cc/ C(7),Ical
7100  T=C(0)
7110  FOR I=1 TO 7
7120  T=T+C(I)*V^I
7130  NEXT I
7140  IF Ical=1 THEN
7150  T=T-6.7422934E-2+T*(9.0277043E-3-T*(-9.3259917E-5))
7160  ELSE
7170  T=T+8.626897E-2+T*(3.76199E-3-T*5.0689259E-5)
7180  END IF
7190  RETURN T
7200  FNEND
7210!
7220  DEF FNBeta(T)
7230  Rop=FNRho(T+.1)
7240  Rom=FNRho(T-.1)
7250  Beta=-2/(Rop+Rom)*(Rop-Rom)/.2
7260  RETURN Beta
7270  FNEND
7280!
7290  DEF FNHfg(T)
7300  COM /Iprop/ Ift
7310  IF Ift=0 THEN
7320  Hfg=1.3741344E+5-T*(3.3094361E+2+T*1.2165143)
7330  END IF
7340  IF Ift=1 THEN
7350! 223 TO 373 K CURVE FIT (R124)
7360  Hfg=159.93-.4609*T-1.458E-3*T^2-1.3715E-5*T^3
7370  Hfg=Hfg*1000
```

```
7380   END IF
7390   RETURN Hfg
7400   FNEND
7410!
7420   DEF FNPsat(Tc)
7430   COM /Iprop/ Ift
7440   IF Ift=0 THEN
7450! 0 TO 80 deg F CURVE FIT OF Psat
7460   Tf=1.8*Tc+32
7470   Pa=5.945525+Tf*(.15352082+Tf*(1.4840963E-3+Tf*9.6150671E-6))
7480   Pg=Pa-14.7
7490   END IF
7500   IF Ift=1 THEN
7510! 223 TO 373 K CURVE FIT (R-124)
7520   Pa=(162.68+5.946*Tc+9.2081E-2*Tc^2+6.9359E-4*Tc^3)*.14504
7530   Pg=Pa-14.7
7540   END IF
7550   IF Pg>0 THEN       ! +=PSIG,-=in Hg
7560   Psat=Pg
7570   ELSE
7580   Psat=Pg*29.92/14.7
7590   END IF
7600   RETURN Psat
7610   FNEND
7620 :
7630 :
7640   SUB Purg
7650   BEEP
7660   INPUT "ENTER FILE NAME TO BE DELETED",File$
7670   PURGE File$
7680   GOTO 7650
7690   SUBEND
7700 :
7710 :
7720   SUB Select
7730   COM /Idp/ Idp
7740   BEEP
7750   PRINTER IS 1
7760   PRINT USING "2X,""Select option:"""
7770   PRINT USING "6X,"" 0 TAKE DATA"""
7780   PRINT USING "6X,"" 1 PURGE FILES"""
7790   INPUT Idp
7800   IF Idp=0 THEN CALL Main
7810   IF Idp=1 THEN CALL Purg
7820   SUBEND
```

146

APPENDIX C. REPRESENTATIVE DATA SET

Date :   7 Sep 1993

NOTE: Program name : DRPJY
      New file name: O0907SC2
      UPPER TUBE TC are defective at LOCATIONS: 7   8
      LOWER TUBE TC is defective at LOCATION: 9
      Tubes: Wieland Hard 8 inch

Data Set Number =   1 Bulk Oil % = 0.0
TIME: 13:13:35

```
TC No:     1      2      3      4      5      6      7      8
Temp :   3.85   3.73   3.75   3.66   3.37   3.89 -99.99 -99.99
TC No:     9     10     11     12     13     14     15     16
Temp : -99.99  20.20  18.36  20.46  19.64  20.49  18.53  17.30

   Twa   ATwa   Tliqd  Tliqd2  Tvapr  Psat   Tsat   Tsump
   3.79  19.36   2.20   2.22    2.11  10.82   2.16  -10.3
      Vr          Ir          Cc
     .34         .17      2.388E+02
   Thetab    Htube       Qdp       Athetab  Ahtube     AuQdp
   1.525  3.408E+02  5.542E+02   17.194  1.332E+02  3.150E+03
```

Data Set Number =   2 Bulk Oil % = 0.0
TIME: 13:14:38

```
TC No:     1      2      3      4      5      6      7      8
Temp :   4.37   4.31   4.32   4.32   4.96   5.10 -99.99 -99.99
TC No:     9     10     11     12     13     14     15     16
Temp : -99.99  20.49  19.22  20.57  20.07  20.32  18.38  17.68

   Twa   ATwa   Tliqd  Tliqd2  Tvapr  Psat   Tsat   Tsump
   4.94  19.55   2.29   2.36    2.18  10.90   2.25  -10.8
      Vr          Ir          Cc
    1.13         .23      4.530E+02
   Thetab    Htube       Qdp       Athetab  Ahtube     AuQdp
   2.588  3.368E+02  1.040E+03   17.397  1.793E+02  3.120E+03
```

Data Set Number =   3 Bulk Oil % = 0.0
TIME: 13:16:14

```
TC No:     1      2      3      4      5      6      7      8
Temp :   7.38   7.12   7.12   6.82   7.19   7.43 -99.99 -99.99
TC No:     9     10     11     12     13     14     15     16
Temp : -99.99  20.08  18.76  20.32  19.41  20.16  18.35  16.96

   Twa   ATwa   Tliqd  Tliqd2  Tvapr  Psat   Tsat   Tsump
   7.17  19.12   2.07   2.13    2.02  10.73   2.06  -10.3
      Vr          Ir          Cc
    1.49         .31      1.025E+03
   Thetab    Htube       Qdp       Athetab  Ahtube     AuQdp
   5.104  3.410E+02  1.740E+03   17.057  1.860E+02  3.172E+03
```

Data Set Number = 4 Bulk Oil % = 0.0
TIME: 13:17:49

TC No: 1   2   3   4   5   6   7   8
Temp : 10.40 10.10 10.12   9.64 10.01 10.50 -99.99 -99.99
TC No: 9   10   11   12   13   14   15   16
Temp : -99.99 20.02 18.77 20.12 19.61 20.29 18.32 17.29

  Twa   ATwa   Tliqd   Tliqd2 Tvapr Psat   Tsat   Tsump
 10.11 19.18   1.95   2.15   1.92 10.66   1.99   -10.7
    Vr   Ir   Cc
  1.87   .39   1.855E+03
 Thetao   Htube   Qdp   Athetao Ahtube   AuQdp
  9.121   3.319E+02 2.695E+03 17.189 1.334E+02 3.152E+03

Data Set Number = 5 Bulk Oil % = 0.0
TIME: 13:18:54

TC No: 1   2   3   4   5   6   7   8
Temp : 14.37 14.17 14.12 13.47 13.75 14.60 -99.99 -99.99
TC No: 9   10   11   12   13   14   15   16
Temp : -99.99 20.49 19.23 20.42 20.02 20.52 18.47 17.67

  Twa   ATwa   Tliqd   Tliqd2 Tvapr Psat   Tsat   Tsump
 14.05 19.52   2.01   2.25   2.04 10.76   2.09   -10.6
    Vr   Ir   Cc
  2.36   .50   3.046E+03
 Thetao   Htube   Qdp   Athetao Ahtube   AuQdp
 11.960   3.630E+02 4.342E+03 17.429 1.790E+02 3.102E+03

Data Set Number = 6 Bulk Oil % = 0.0
TIME: 13:20:03

TC No: 1   2   3   4   5   6   7   8
Temp : 17.69 17.40 17.30 16.61 16.64 17.63 -99.99 -99.99
TC No: 9   10   11   12   13   14   15   16
Temp : -99.99 20.21 18.86 20.32 19.69 20.48 18.47 17.08

  Twa   ATwa   Tliqd   Tliqd2 Tvapr Psat   Tsat   Tsump
 17.16 19.27   2.04   2.32   2.09 10.80   2.13   -10.7
    Vr   Ir   Cc
  2.58   .55   4.084E+03
 Thetao   Htube   Qdp   Athetao Ahtube   AuQdp
 15.024   3.379E+02 5.077E+03 17.139 1.834E+02 3.143E+03

148

```
Data Set Number =   7  Bulk Oil % =  0.0
TIME:    13:21:13

TC No:    1       2       3       4       5       6       7       8
Temp :  19.40   19.10   18.35   18.05   19.12   19.37  -99.99  -99.99
TC No:    9      10      11      12      13      14      15      16
Temp :  -99.99  19.99   18.74   19.34   19.50   20.11   18.08   17.07

  Twa    ATwa    Tliqd   Tliqd2  Tvapr   Psat    Tsat    Tsump
 18.79   19.03    1.89    2.21    1.96   10.68    2.00   -10.7
    Vr            Ir       Cc
  2.80          .60    4.707E+03
 Thetab    Htube      Qdp       Athetab  Ahtube     AuQdp
 16.783   3.612E+02  6.061E+03  17.027  1.848E+02  3.146E+03


Data Set Number =   8  Bulk Oil % =  0.0
TIME:    13:22:11

TC No:    1       2       3       4       5       6       7       8
Temp :  22.76   22.21   21.96   20.36   21.04   22.51  -99.99  -99.99
TC No:    9      10      11      12      13      14      15      16
Temp :  -99.99  19.75   18.48   19.79   19.35   20.05   18.04   16.85

  Twa    ATwa    Tliqd   Tliqd2  Tvapr   Psat    Tsat    Tsump
 21.84   18.87    1.81    2.19    1.90   10.63    1.95   -10.7
    Vr            Ir       Cc
  3.07          .65    5.353E+03
 Thetab    Htube      Qdp       Athetab  Ahtube     AuQdp
 19.389   3.552E+02  7.263E+03  16.325  1.364E+02  3.153E+03


Data Set Number =   9  Bulk Oil % =  0.0
TIME:    13:23:55

TC No:    1       2       3       4       5       6       7       8
Temp :  26.91   26.51   26.32   25.12   24.95   26.71  -99.99  -99.99
TC No:    9      10      11      12      13      14      15      16
Temp :  -99.99  20.53   19.25   20.45   20.10   20.75   18.59   17.71

  Twa    ATwa    Tliqd   Tliqd2  Tvapr   Psat    Tsat    Tsump
 26.03   19.60    2.14    2.47    2.23   10.32    2.27   -10.7
    Vr            Ir       Cc
  3.29          .70    7.369E+03
 Thetab    Htube      Qdp       Athetab  Ahtube     AuQdp
 23.757   3.391E+02  8.056E+03  17.329  1.785E+02  3.094E+03
```

149

```
Data Set Number =  10  Bulk Oil % =  0.0
TIME:     13:27:26

TC No:    1      2      3      4      5      6      7      8
Temp :  10.92  11.50  11.27  11.74  11.29  10.35 -99.99 -99.99
TC No:    9     10     11     12     13     14     15     16
Temp : -99.99  17.36  15.38  17.50  17.07  18.05  16.48  14.36

  Twa   ATwa   Tliqd  Tliqd2 Tvapr  Psat   Tsat   Tsump
 11.16  16.64   2.26    2.25   2.09  10.33   2.17  -10.6
    Vr      Ir      Cc
  3.79     .81   2.114E+03
 Thetab   Htube      Qdp       Athetab  Ahtube    AuQdp
 8.991  1.510E+03  1.357E+04  14.471  2.456E+02  3.553E+03


Data Set Number =  11  Bulk Oil % =  0.0
TIME:     13:29:22

TC No:    1      2      3      4      5      6      7      8
Temp :  11.77  12.52  12.23  12.73  12.40  11.31 -99.99 -99.99
TC No:    9     10     11     12     13     14     15     16
Temp : -99.99  16.90  15.33  16.98  16.60  17.31  16.36  13.76

  Twa   ATwa   Tliqd  Tliqd2 Tvapr  Psat   Tsat   Tsump
 12.14  16.21   2.23    2.22   2.01  10.78   2.12  -10.6
    Vr      Ir      Cc
  4.48     .96   2.430E+03
 Thetab   Htube      Qdp       Athetab  Ahtube    AuQdp
 10.027  1.924E+03  1.929E+04  14.092  4.218E+02  5.944E+03


Data Set Number =  12  Bulk Oil % =  0.0
TIME:     13:30:20

TC No:    1      2      3      4      5      6      7    _ 8
Temp :  13.30  14.46  14.14  14.73  14.52  13.94 -99.99 -99.99
TC No:    9     10     11     12     13     14     15     16
Temp : -99.99  16.21  14.70  16.26  15.95  17.07  15.51  13.21

  Twa   ATwa   Tliqd  Tliqd2 Tvapr  Psat   Tsat   Tsump
 14.07  15.53   2.11    2.14   1.93  10.70   2.03  -10.6
    Vr      Ir      Cc
  5.38    1.25   3.072E+03
 Thetab   Htube      Qdp       Athetab  Ahtube    AuQdp
 12.039  2.792E+03  3.361E+04  13.502  2.755E+02  3.720E+03
```

```
Data Set Number = 13  Bulk Oil % =  0.0
TIME:    13:31:43

TC No:    1      2      3      4      5      6      7      8
Temp :  16.12  16.75  16.45  17.02  16.97  16.17 -99.99 -99.99
TC No:    9     10     11     12     13     14     15     16
Temp : -99.99  15.79  14.44  15.97  15.71  16.93  15.49  13.23

   Twa    ATwa   Tliqd   Tliqd2  Tvapr   Psat    Tsat    Tsump
  16.24  15.34   2.21    2.32    2.16   10.37    2.21   -10.6
      Vr        Ir        Cc
     7.71      1.64     3.739E+03
  Thetab    Htube      Qdp      Athetab  Ahtube    AuQdp
  14.030  4.162E+03  5.339E-04  13.125  2.369E+02  3.766E+03


Data Set Number = 14  Bulk Oil % =  0.0
TIME:    13:32:48

TC No:    1      2      3      4      5      6      7      8
Temp :  17.77  18.27  17.93  18.48  18.53  17.70 -99.99 -99.99
TC No:    9     10     11     12     13     14     15     16
Temp : -99.99  15.53  14.22  15.66  15.59  15.51  14.99  12.90

   Twa    ATwa   Tliqd   Tliqd2  Tvapr   Psat    Tsat    Tsump
  17.64  15.03   2.29    2.36    2.21   10.92    2.27   -10.6
      Vr        Ir        Cc
     3.23      1.96     4.207E+03
  Thetab    Htube      Qdp      Athetab  Ahtube    AuQdp
  15.375  5.453E+03  3.384E-04  12.760  2.372E+02  3.792E+03


Data Set Number = 15  Bulk Oil % =  0.0
TIME:    13:34:20

TC No:    1      2      3      4      5      6      7    - 8
Temp :  16.96  17.52  17.20  17.74  17.69  16.30 -99.99 -99.99
TC No:    9     10     11     12     13     14     15     16
Temp : -99.99  15.59  14.13  15.58  15.59  16.64  15.18  12.94

   Twa    ATwa   Tliqd   Tliqd2  Tvapr   Psat    Tsat    Tsump
  16.95  15.05   2.40    2.54    2.31   11.03    2.39   -10.4
      Vr        Ir        Cc
     3.23      1.75     3.925E+03
  Thetab    Htube      Qdp      Athetab  Ahtube    AuQdp
  14.563  4.572E+03  6.658E+04  12.562  2.387E+02  3.782E+03
```

```
Data Set Number = 16  Bulk Oil % =  0.0
TIME:    13:35:45

TC No:    1      2      3      4      5      6      7      8
Temp :  15.61  16.29  15.38  16.59  16.32  15.60 -99.99 -99.99
TC No:    9     10     11     12     13     14     15     16
Temp : -99.99  15.49  14.01  15.51  15.51  16.33  14.36  12.72

  Twa   ATwa   Tliqd  Tliqd2  Tvapr  Psat   Tsat   Tsump
 15.30  14.36   2.33    2.35   2.25  10.34   2.29  -10.4
    Vr        Ir        Cc
   5.38      1.47     3.560E+03
  Thetab    Htube       Qdp       Athetab  Ahtube     AuQdp
 13.503  3.431E+03  4.634E+04  12.568  3.038E+02  3.318E+03


Data Set Number = 17  Bulk Oil % =  0.0
TIME:    13:36:51

TC No:    1      2      3      4      5      6      7      8
Temp :  13.76  14.46  14.18  14.31  14.21  13.65 -99.99 -99.99
TC No:    9     10     11     12     13     14     15     16
Temp : -99.99  15.21  13.75  15.17  15.10  16.15  14.60  12.42

  Twa   ATwa   Tliqd  Tliqd2  Tvapr  Psat   Tsat   Tsump
 14.02  14.60   2.25    2.29   2.08  10.33   2.17  -10.2
    Vr        Ir        Cc
   5.28      1.13     3.010E+03
  Thetab    Htube       Qdp       Athetab  Ahtube     AuQdp
 11.348  2.271E+03  2.690E+04  12.427  3.095E+02  3.347E+03


Data Set Number = 18  Bulk Oil % =  0.0
TIME:    13:38:09

TC No:    1      2      3      4      5      6      7      8
Temp :  11.36  12.64  12.42  12.38  12.20  11.69 -99.99 -99.99
TC No:    9     10     11     12     13     14     15     16
Temp : -99.99  15.29  13.82  15.29  15.25  16.45  15.07  12.61

  Twa   ATwa   Tliqd  Tliqd2  Tvapr  Psat   Tsat   Tsump
 12.21  14.30   2.28    2.24   2.06  10.32   2.16  -10.1
    Vr        Ir        Cc
   4.06       .87     2.437E+03
  Thetab    Htube       Qdp       Athetab  Ahtube     AuQdp
 10.048  1.556E+03  1.563E+04  12.838  3.305E+02  3.797E+03
```

152

Data Set Number = 19 Bulk Oil % = 0.0
TIME: 13:39:29

TC No: 1   2   3   4   5   6   7   8
Temp :   9.20   9.58   9.45   9.30   9.35   9.39 -99.99 -99.99
TC No: 9   10   11   12   13   14   15   16
Temp : -99.99   15.63   14.21   15.46   15.56   16.68   15.32   13.16

  Twa   ATwa   Tliqd   Tliqd2 Tvapr   Psat   Tsat   Tsump
  9.50   15.13   2.28   2.35   2.17   10.90   2.24   -10.1
     Vr   Ir   Cc
  2.72   .58   1.609E+03
 Thetab   Htube   Qdp   Athetab   Ahtube   AuQdp
  7.291   9.245E+02 6.712E+03 12.990   2.368E+02   3.696E+03

Data Set Number = 20 Bulk Oil % = 0.0
TIME: 13:40:18

TC No: 1   2   3   4   5   6   7   8
Temp :   7.12   7.13   7.03   7.10   7.79   7.23 -99.99 -99.99
TC No: 9   10   11   12   13   14   15   16
Temp : -99.99   15.65   14.29   15.45   15.68   16.67   15.31   13.21

  Twa   ATwa   Tliqd   Tliqd2 Tvapr   Psat   Tsat   Tsump
  7.21   15.15   2.25   2.32   2.22   10.91   2.25   -10.1
     Vr   Ir   Cc
  2.04   .43   9.373E+02
 Thetab   Htube   Qdp   Athetab   Ahtube   AuQdp
  4.956   7.498E+02 3.717E+03 12.900   2.322E+02   3.769E+03

Data Set Number = 21 Bulk Oil % = 0.0
TIME: 13:41:00

TC No: 1   2   3   4   5   6   7   8
Temp :   6.17   6.12   6.04   6.02   6.77   6.33 -99.99 -99.99
TC No: 9   10   11   12   13   14   15   16
Temp : -99.99   15.78   14.52   15.68   15.39   16.76   15.50   13.48

  Twa   ATwa   Tliqd   Tliqd2 Tvapr   Psat   Tsat   Tsump
  6.23   15.34   2.29   2.36   2.25   10.94   2.29   -10.0
     Vr   Ir   Cc
  1.74   .37   7.367E+02
 Thetab   Htube   Qdp   Athetab   Ahtube   AuQdp
  3.936   6.901E+02 2.577E+03 13.053   2.368E+02   3.744E+03

153

```
Data Set Number = 22  Bulk Oil % =  0.0
TIME:     13:42:13

TC No:     1        2        3        4        5        6        7        8
Temp :   4.38     4.40     4.39     4.37     4.33     4.51  -99.99  -99.99
TC No:     9       10       11       12       13       14       15       16
Temp : -99.99    15.38    14.70    15.33    16.07    16.36    15.58    13.55

   Twa    ATwa    Tliqd    Tliqd2   Tvapr    Psat     Tsat     Tsump
   4.47   15.51    2.45     2.51     2.35    11.06     2.41     -10.1
      Vr       Ir        Cc
    1.33       .27     3.225E+02
   Thetap    Htube       Qdp        Athetap   Ahtube      AuQdp
   2.058   7.640E+02  1.572E+03    13.095   2.868E+02   3.755E+03


Data Set Number = 23  Bulk Oil % =  0.0
TIME:     13:43:07

TC No:     1        2        3        4        5        6        7        8
Temp :   3.58     3.53     3.52     3.47     3.83     3.50  -99.99  -99.99
TC No:     9       10       11       12       13       14       15       16
Temp : -99.99    15.38    14.54    15.38    15.98    16.39    15.54    13.42

   Twa    ATwa    Tliqd    Tliqd2   Tvapr    Psat     Tsat     Tsump
   3.58   15.42    2.31     2.37     2.19    10.92     2.27     -10.0
      Vr       Ir        Cc
     .99       .20     1.825E+02
   Thetap    Htube       Qdp        Athetap   Ahtube      AuQdp
   1.317   6.529E+02  3.597E+02    13.153   2.808E+02   3.593E+03


Data Set Number = 24  Bulk Oil % =  0.0
TIME:     13:44:32

TC No:     1        2        3        4        5        5        7     _  8
Temp :   2.36     2.34     2.95     2.33     3.12     2.99  -99.99  -99.99
TC No:     9       10       11       12       13       14       15       16
Temp : -99.99    15.99    14.63    15.37    16.08    17.01    15.58    13.50

   Twa    ATwa    Tliqd    Tliqd2   Tvapr    Psat     Tsat     Tsump
   2.38   15.52    2.46     2.48     2.34    11.05     2.40     -10.0
      Vr       Ir        Cc
     .70       .14     6.344E+01
   Thetap    Htube       Qdp        Athetap   Ahtube      AuQdp
    .574   7.393E+02  4.241E+02    13.120   2.847E+02   3.735E+03


NOTE: 24 data runs were stored in file 00907SC2
```

154

APPENDIX D.   SAMPLE CALCULATIONS[3]

Data file D0921ASC4 was used for sample calculations. The saturation temperature was 2.2 °C with a heat flux of 59,130 W/m^2 on the smooth upper test tube.

A.   SMOOTH TEST TUBE DIMENSIONS

Do = 0.015875 m

Di = 0.0127 m

D1 = 0.012446 m

L = 0.2032 m

Lu = 0.0762 m

B.   MEASURED PARAMETERS

$V = Vr \cdot 25 = (7.76 \text{ V})(25) = 194.0$ V

$I = Ir \cdot 1.9182 = (1.66 \text{ A})(1.9182) = 3.18$ A

T1 = 19.44 °C   T2 = 20.03 °C

T3 = 19.75 °C   T4 = 19.63 °C

T5 = 19.46 °C   T6 = 19.38 °C

T7 and T8 not used, defective

---

[3]This analysis is essentially identical to the analysis done by Perry [Ref. 2] and therefore his procedure is largely reproduced.

155

Tsat = 2.20 °C

kc = 344 W/m·K

C. OUTER WALL TEMPERATURE OF THE UPPER TEST TUBE

1. Surface Area of Smooth Tube

$P = \pi \cdot Do = \pi(0.015875 \text{ m}) = 0.04987 \text{ m}$

$Ac = \pi(Do^2-Di^2)/4 = \pi((0.015875 \text{ m})^2-(0.0127)^2)/4$

$Ac = 7.13 \times 10^{-5} \text{ m}^2$

2. Heater Power

$Qh = V \cdot I = (194.0 \text{ V})(3.18 \text{ A}) = 616.92 \text{ W}$

3. Average Inside Tube Temperature

$Tavg = \Sigma_1^m \ Tn/m = \Sigma_1^6 \ Tn/6 = (T1+T2+T3+T4+T5+T6)/6$

$Tavg = (19.44+20.03+19.75+19.63+19.46+19.38)/6$

$= 19.62 \text{ °C}$

4. Outside Wall Tube Temperature

Two is calculated using Fourier's Conduction Law, assuming uniform radial conduction and using a known Tavg:

$Two = Tavg - \{Qh(\ln(Do/Di))/(2\pi \cdot L \cdot kc)\}$

$Two = 19.62-\{616.92(\ln(0.015875/0.01245))/$

$(2\pi \cdot 0.203 \cdot 344 \ )\}$

$Two = 19.28 \text{ °C}$

5. Tube Wall Superheat

$\theta = Two - Tsat = 19.28 - 2.20 = 17.08 \text{ °C}$

D. R-124 PROPERTIES AT FILM TEMPERATURE

The thermophysical properties of R-124 were computed at the film temperature using the REFPROP equations provided by Bertsch [Ref. 1]:

1. Film Temperature

$Tf = (Two + Tsat)/2 = (19.28 + 2.20)/2 = 10.74$ °C

2. Dynamic Viscosity

$\mu = 3.4593 - (0.0426)Tf + (3.9485 \times 10^{-4})Tf^2 - (4.193 \times 10^{-6})Tf^3 + (2.0709 \times 10^{-8})Tf^4$

$\mu = \{3.4593 - (0.0426)10.74 + (3.9485 \times 10^{-4})(10.74)^2 - (4.193 \times 10^{-6})(10.74)^3 + (2.0709 \times 10^{-8})(10.74)^4\} \times 10^{-4}$

$\mu = 3.0424 \times 10^{-4}$ N·s/m²

3. Density

$\rho = 1434.8 - (2.8619)Tf - (6.7267 \times 10^{-3})Tf^2 - (7.2852 \times 10^{-5})Tf^3$

$\rho = 1434.8 - (2.8619)10.74 - (6.7267 \times 10^{-3})(10.74)^2 - (7.2852 \times 10^{-5})(10.74)^3$

$\rho = 1403.2$ kg/m³

4. Kinematic Viscosity

$\nu = \mu/\rho = 3.0422 \times 10^{-4}/1403.2 = 2.17 \times 10^{-7}$ m/s

5. Thermal Conductivity

$k = 7.5191 \times 10^{-2} - (3.5436 \times 10^{-4})Tf - (1.9545 \times 10^{-7})Tf^2 + (3.1835 \times 10^{-9})Tf^3$

$k = 7.5191 \times 10^{-2} - (3.5436 \times 10^{-4})(10.74) - (1.9545 \times 10^{-7})(10.74)^2 + (3.1835 \times 10^{-9})(10.74)^3$

$k = 7.137 \times 10^{-2}$ W/m·K

6. **Specific Heat**

$$Cp = 1.0542 + (2.1405 \times 10^{-3})\,Tf + (1.0709 \times 10^{-5})\,Tf^2 -$$

$$(6.4721 \times 10^{-8}) \cdot Tf^3 - (1.4324 \times 10^{-9})\,Tf^4 + (4.136 \times 10^{-11})\,Tf^5$$

$$Cp = \{1.0542 + (2.1405 \times 10^{-3})(10.74) + (1.0709 \times 10^{-5})(10.74)^2 -$$

$$(6.4721 \times 10^{-8})(10.74)^3 - (1.4324 \times 10^{-9})(10.74)^4 +$$

$$(4.136 \times 10^{-11})(10.74)^5\} \times 10^3$$

$$Cp = 1078.35 \ J/kg \cdot K$$

7. **Thermal Diffusivity**

$$\alpha = k/(\rho \cdot Cp) = 7.137 \times 10^{-2}/(1403.2 \cdot 1078.35)$$

$$\alpha = 4.717 \times 10^{-8} \ m^2/s$$

8. **Volumetric Thermal Expansion Coefficient**

$$\beta = -\Delta\rho/(\rho \cdot \Delta Tf) = -(1402.89 - 1403.50)/(1403.2 \cdot 0.2)$$

$$\beta = 2.174 \times 10^{-3} \quad (1/K)$$

9. **Prandtl Number**

$$Pr = \nu/\alpha = 2.17 \times 10^{-7}/4.717 \times 10^{-8} = 4.60$$

E. HEAT FLUX THROUGH NON-BOILING TUBE LENGTHS

Using the Churchill-Chu correlation [Ref. 9] for a smooth cylinder in natural convection, the average natural convection heat transfer coefficient of one non-boiling tube length is:

$$h = k/Do\{0.6 + 0.387[\Gamma/(1+(0.559/Pr)^{9/16})^{8/27}]\}^2$$

where $\Gamma = \{[g \cdot \beta \cdot Do^3 \cdot \theta \cdot \tanh(m \cdot Lu)]/(\nu \cdot \alpha \cdot Lu \cdot m)\}^{1/6}$

$\quad\quad\quad m = \{(h \cdot P)/(kc \cdot Ac)\}^{1/2}$

The program DRPJY computes the value of h by assuming a starting value of 190 $W/m^2 \cdot K$ and iterating to the final value. The resulting values of h and m are:

$h = 281.93 \ W/m^2 \cdot K$

$m = 23.94 \ (1/m)$

therefore,

$Qf = (h \cdot p \cdot kc \cdot Ac)^{1/2} \cdot \theta \cdot \tanh(m \cdot Lu) = 9.52 \ W$

F.   HEAT FLUX THROUGH BOILING TUBE LENGTH

$Q = Qh - 2 \cdot Qf = 616.92 - 2(9.52) = 597.88 \ W$

$Ab = \pi \cdot Do \cdot L = \pi(0.015875)(.2032) = 1.013 \times 10^{-2} \ m^2$

$q" = Q/Ab = 597.88/1.013 \times 10^{-2} = 59,021 \ W/m^2$

$h = q"/\theta = 59021/17.08 = 3456 \ W/m^2 \cdot K$

The following results were calculated by the data acquisition and reduction program DRPJY:

$q" = 59,130 \ W/m^2$

$h = 3463 \ W/m^2 \cdot K$

$\theta = 17.08 \ °C$

159

APPENDIX E. UNCERTAINTY ANALYSIS[4]

The same data run used for the sample calculations (Appendix D) was used for the uncertainty analysis, thus all the measured and most of the calculated results still apply. A lower heat flux of 1561 W/m^2 was also analyzed from the same data run to show the difference between the two heat fluxes. All uncertainties are presented as a percentage of the calculated parameter, i.e. a relative uncertainty. The uncertainty analysis method suggested by Kline and McClintock [Ref. 29] was used. For example: If $R = R(x_1, x_2, x_3, \ldots \ldots x_n)$, then:

$$\delta R = \left[\left(\frac{\delta R}{\delta x_1} \delta X_1 \right)^2 + \left(\frac{\delta R}{\delta x_2} \delta X_2 \right)^2 + \ldots + \left(\frac{\delta R}{\delta x_3} \delta X_3 \right)^2 \right]^{\frac{1}{2}}$$

where:

δR = uncertainty of the desired dependent variable

x_n = measured variable

δx_n = uncertainty in the measured variable

---

[4]This analysis is essentially identical to the analysis done by Perry [Ref. 2] and therefore his procedure is largely reproduced.

A. HEAT TRANSFER RATE UNCERTAINTY

$$Ir = 1.66 \text{ amps} \qquad \delta Ir = 0.025 \text{ amps}$$
$$Vr = 7.76 \text{ volts} \qquad \delta Vr = 0.05 \text{ volts}$$

so we have:

$$\frac{\delta Qh}{Qh} = \left[\left(\frac{\delta Vr}{Vr}\right)^2 + \left(\frac{\delta Ir}{Ir}\right)^2\right]^{\frac{1}{2}}$$

$$\frac{\delta Qh}{Qh} = \left[\left(\frac{0.05}{7.76}\right)^2 + \left(\frac{0.025}{1.66}\right)^2\right]^{\frac{1}{2}} = 1.64\%$$

B. SURFACE AREA UNCERTAINTY

The following dimensions were taken from the manufacturer's data sheet, and from actual measurements:

$$Do = 15.88 \quad (mm) \qquad \delta Do = 0.1 \ (mm)$$
$$L \ = 203.2 \quad (mm) \qquad \delta L \ = 0.1 \ (mm)$$
$$Ab = Do \times L$$

$$\frac{\delta Ab}{Ab} = \left[\left(\frac{\delta Do}{Do}\right)^2 + \left(\frac{\delta L}{L}\right)^2\right]^{\frac{1}{2}}$$

$$\frac{\delta Ab}{Ab} = \left[\left(\frac{0.1}{15.88}\right)^2 + \left(\frac{0.1}{203.2}\right)^2\right]^{\frac{1}{2}} = 0.63\%$$

C.   WALL SUPERHEAT UNCERTAINTY

The following temperatures were measured:

T1 = 19.44 °C

T2 = 20.03 °C

T3 = 19.75 °C

T4 = 19.63 °C

T5 = 19.46 °C

T6 = 19.38 °C

Tavg = 19.62   °C

Standard Deviation = 0.245   °C

Tsat = 2.20 °C   and δTsat = 0.01 °C

$$Two = Tavg - Qh\left[\frac{\ln(\frac{Do}{D1})}{2\pi \cdot L \cdot kc}\right]$$

Note: The second term on the right hand side of the above equation is the Fourier heat transfer conduction term, and can be neglected for the uncertainty analysis since its value is less than the standard deviation, so:

Two = Tavg = 19.62 °C

ΔT = Two - Tsat = 19.62 °C - 2.20 °C = 17.42 °C

162

therefore,

$$\frac{\delta \Delta T}{\Delta T} = \left[\left(\frac{\delta \Delta Two}{\Delta T}\right)^2 + \left(\frac{\delta Tsat}{\Delta T}\right)^2\right]^{\frac{1}{2}}$$

$$\frac{\delta \Delta T}{\Delta T} = \left[\left(\frac{0.245}{17.42}\right)^2 + \left(\frac{0.01}{17.42}\right)^2\right]^{\frac{1}{2}} = 1.41\%$$

D. HEAT FLUX UNCERTAINTY

$$q'' = \frac{(Qh - 2 \times Qf)}{Ab}$$

where: Qh = V x I = (194 V)(3.18 A) = 616.92 W

and δQh = (616.92)(0.0164) = 10.12 W

q'' = 59130 W/m^2 (measured)

Ab = 0.010137 m^2

$Qh - 2.Qf$ = (q)(Ab) = (59130)(0.010137) = 599.40 W

solving for Qf:

Qf = (616.92 - 599.40)/2 = 8.76 W

assuming the same proportion uncertainty for Qf, we have:

δQf = (8.76)(0.0164) = 0.144 W

163

and for the uncertainty:

$$\frac{\delta q''}{q''} = \left[\left(\frac{\delta Qh}{Qh - 2Qf} \right)^2 + \left(\frac{2\delta Qf}{Qh - 2Qf} \right)^2 + \left(\frac{\delta Ab}{Ab} \right)^2 \right]^{\frac{1}{2}}$$

$$\frac{\delta q''}{q''} = \left[\left(\frac{10.12}{599.4} \right)^2 + \left(\frac{2 \times 0.144}{599.4} \right)^2 + (0.0063)^2 \right]^{\frac{1}{2}} = 1.80\%$$

E.   **HEAT TRANSFER COEFFICIENT UNCERTAINTY**

$$h = q''/\Delta T$$

therefore,

$$\frac{\delta h}{h} = \left[\left(\frac{\delta q''}{q''} \right)^2 + \left(\frac{\delta \Delta T}{\Delta T} \right)^2 \right]^{\frac{1}{2}}$$

$$\frac{\delta h}{h} = \left[(0.018)^2 + (0.0141)^2 \right]^{\frac{1}{2}} = 2.29\%$$

The above series of calculations was also conducted with a lower heat flux for the same data run and with a high and low heat flux from a TURBO-B data run (D1022FTBC4) with the results tabulated in Table 5.

TABLE 5. RESULTS OF UNCERTAINTY ANALYSIS

PARAMETER	SMOOTH 1561 W/m^2	SMOOTH 59130 W/m^2	TURBO-B 1703 W/m^2	TURBO-B 71270 W/m^2
$\delta Qh/Qh$ (%)	8.49	1.64	10.47	1.60
$\delta Ab/Ab$ (%)	0.63	0.63	0.63	0.63
$\delta \Delta T/\Delta T$ (%)	3.55	1.41	26.62	12.44
$\delta q''/q''$ (%)	13.05	1.80	9.26	1.55
$\delta h/h$ (%)	13.52	2.29	28.18	12.54

LIST OF REFERENCES

1. Bertsch, G., *Nucleate Pool Boiling Characteristics of R-124,* M.S. Thesis, Naval Postgraduate School, Monterey, CA, March 1993.

2. Perry, G., *Effect of Oil on the Onset of Nucleate Pool Boiling of R-124 from a Single Horizontal Tube,* M.S. Thesis, Naval Postgraduate School, Monterey, CA, June 1993.

3. Lake, L., *The Influence of a Lower Heated Tube on Nucleate Pool Boiling from a Horizontal Tube,* Master's Thesis, Naval Postgraduate School, Monterey, CA, June 1992.

4. Bar-Cohen, A., *Hysteresis Phenomena at Onset of Nucleate Boiling,* Proceedings of the Engineering Foundation Conference on Pool and External Flow Boiling, Santa Barbara, CA, pp. 1-13, 1992.

5. You, S.M., Bar-Cohen, A., Simon, T.W., and Tong, W., *Experimental Investigation of Nucleate Boiling Incipience with a Highly-Wetting Dielectric Fluid (R-113),* International Journal Heat Mass Transfer, Vol. 33, No. 1, pp. 105-117, 1990.

6. Bar-Cohen, A., and Simon, T.W., *Wall Superheat Excursions in the Boiling Incipience of Dielectric Fluids,* Heat Transfer Engineering, Vol. 9, No. 3, pp. 19-31, 1988.

7. Tong, W., Bar-Cohen, A., Simon, T.W., and You, S.M., *Contact Angle Effects on Boiling Incipience of Highly-Wetting Liquids,* International Journal Heat Mass Transfer, Vol. 33, No. 1, pp. 91-103, 1990.

8. Thome, J.R., *Enhanced Boiling Heat Transfer,* Hemisphere Publishing Corp, pp. 5-7, 1990.

9. Churchill, S.W., and Chu, F.H.S., *Correlating Relations from a Laminar and Turbulent Free Convection from a Horizontal Cylinder*, International Journal Heat Mass Transfer, Vol. 18, pp.1049-1070, 1975.

10. Thome, J.R., *Enhanced Boiling Heat Transfer,* Hemisphere Publishing Corp, pp. 155-157, 1990.

11. Sparrow, E.M., and Niethammer, J.E., *Effect of Vertical Separation Distance and Cylinder-to-Cylinder Temperature Imbalance on Natural Convection for a Pair of Horizontal Cylinders,* Journal of Heat Transfer, Vol. 103, pp. 638-644, 1981.

12. Al-Alusi, T.R., and Bushnell, D.J., *An Experimental Study of Free Convection Heat Transfer From an Array of Horizontal Cylinders Parallel to a Vertical Wall,* Journal of Heat Transfer, Vol. 114, pp. 394-400, 1992.

13. Tokura, I., Saito, H., Kishinami, K., and Muramoto, K., *An Experimental Study of Free Convection Heat Transfer From a Horizontal Cylinder in a Vertical Array Set in Free Space Between Parallel Walls,* Journal of Heat Transfer, Vol. 105, pp. 102-107, 1983.

14. Sparrow, E.M., and Boessneck, D.S., *Effect of Transverse Misalignment on Natural Convection from a Pair of Parallel, Vertically Stacked, Horizontal Cylinders,* Journal of Heat Transfer, Vol. 105, pp. 241-247, 1983.

15. Inagaki, T., and Komori, K., *Natural Convection Heat Transfer from Two Horizontal Cylinders in Vertical Alignment,* Transactions of JSME, Vol. 56, pp. 3050-3055, 1990 (in Japanese):   Translation in Heat Transfer - Japanese Research, Vol. 20, No. 6, pp. 549-559, 1991.

16. Cornwell, K., Duffin, N.W., and Schuller, R.B., *An Experimental Study of the Effects of Fluid Flow on Boiling Within a Kettle Reboiler Tube Bundle,* ASME Paper 80 HT-45, National Heat Transfer Conference, Orlando, 1980.

17. Cornwell, K., and Schuller, R.B., *A Study of Boiling Outside a Tube Bundle Using High Speed Photography,* International Journal Heat Mass Transfer, Vol. 25, pp. 683-690, 1982.

18. Cornwell, K., and Scoones, D.J., *Analysis of Low Quality Boiling on Plain and Low-Finned Tube Bundles,* 2nd UK National Heat Transfer Conference, Vol. 1, pp. 21-32, 1988.

19. Cornwell, K., *The Influence of Bubbly Flow on Boiling from a Tube in a Bundle,* Eurotherm Seminar No. 8, Advances in Pool Boiling Heat Transfer, FRG, pp. 177-183, 1989.

20. Fujita, Y., Ohta, H., Hidaka, S., and Nishikawa, K., *Nucleate Boiling Heat Transfer on Horizontal Tubes in*

Bundles, 8th International Heat Transfer Conference, Vol. 5, pp. 2131-2136, San Francisco, 1986.

21.   Stephan, K., and Mitrovic, J., *Heat Transfer in Natural Convection/Boiling of Refrigerants and Refrigerant/Oil Mixtures in Bundles of T-Shaped Finned Tubes,* Advances in Enhanced Heat Transfer, ASME, pp. 131-146, 1981.

22.   Hahne, E., and Muller, J., *Boiling on a Finned Tube and a Finned Tube Bundle,* International Journal Heat Mass Transfer, Vol. 26, No. 6, pp. 849-859, 1983.

23.   Windisch, R., Hahne, E., and Kiss, V., *Heat Transfer for Boiling on Finned Tube Bundles,* International Committee Heat Mass Transfer, Vol. 12, pp. 355-368, 1985.

24.   Hahne, E., Chen, Q., and Windisch, R., *Pool Boiling Heat Transfer on Finned Tubes - An Experimental and Theoretical Study,* International Journal Heat Mass Transfer, Vol. 34, No. 8, pp. 2071-2079, 1991.

25.   Karasabun, M., *An Experimental Apparatus to Study Nucleate Pool Boiling of R-114 and Oil Mixtures,* M.S. Thesis, Naval Postgraduate School, Monterey, CA, 1984.

26.   Reilley, J., *The Influence of Oil Contamination on the Nucleate Pool Boiling Behavior of R-114 from a Structured Surface,* M.S. Thesis, Naval Postgraduate School, Monterey, CA, 1985.

27.   Sugiyama, D., *Nucleate Pool Boiling of R-114 and R-114/Oil Mixtures from Single Enhanced Tubes*, M.S. Thesis, Naval Postgraduate School, Monterey, CA, 1991.

28.   Gallager, J., Mclinden, M., and Morrison, G., *NIST Thermodynamic Properties of Refrigerants and Refrigerant Mixtures Database,* RefProp Version 2.0, National Institute of Standards and Technology, Gaithersburg, MD, 1991.

29.   Kline, S.J., and McClintock, F.A., *Describing Uncertainties in Single Sample Experiments,* Mechanical Engineering, p. 3, 1953.

INITIAL DISTRIBUTION LIST

1. Defense Technical Information Center   2
   Cameron Station
   Alexandria, Va   22304-6145

2. Library, Code 052   2
   Naval Postgraduate School
   Monterey, CA   93943-5002

3. Professor Matthew D. Kelleher, Code ME/Kk   1
   Department of Mechanical Engineering
   Naval Postgraduate School
   Monterey, CA   93943-5002

4. Professor Paul J. Marto, Code ME/Mx   2
   Department of Mechanical Engineering
   Naval Postgraduate School
   Monterey, CA   93943-5002

5. Professor Stephen B. Memory   1
   Department of Mechanical Engineering
   McArthur Bldg.
   University of Miami
   Coral Gables, FL   33124-0624

6. Mr. R. Helmick, Code 2722   2
   Annapolis Detachment, C. D.
   Naval Surface Warfare Center
   Annapolis, MD   21402-5067

7. Mr. Bruce G. Unkel   1
   NAVSEA (Code 56Y15)
   Department of the Navy
   Washington, D.C.   20362-5101

8. Naval Engineering Curricular Officer, Code 34   1
   Naval Postgraduate School
   Monterey, CA   93943-5002

9. LT Joseph E. Yusician, Jr.   1
   9817 Dungan Road
   Philadelphia, PA   19115